Graduate School Form 30
(Revised 08/14)

PURDUE UNIVERSITY
GRADUATE SCHOOL
Thesis/Dissertation Acceptance

This is to certify that the thesis/dissertation prepared

By Adam Garrett Fogarty

Entitled
High Voltage Rear Electric Drivetrain Design for a Parallel-Through-the-Road Plug-in Hybrid Electric Vehicle

For the degree of Master of Science in Mechanical Engineering

Is approved by the final examining committee:

Gregory M Shaver

Peter H Meckl

Oleg Wasynczuk

To the best of my knowledge and as understood by the student in the Thesis/Dissertation Agreement, Publication Delay, and Certification/Disclaimer (Graduate School Form 32), this thesis/dissertation adheres to the provisions of Purdue University's "Policy on Integrity in Research" and the use of copyrighted material.

Approved by Major Professor(s): Gregory M Shaver
Peter H Meckl

Approved by: Anil Bajaj 12/12/2014

Head of the Department Graduate Program Date

HIGH VOLTAGE REAR ELECTRIC DRIVETRAIN DESIGN FOR A PARALLEL-THROUGH-THE-ROAD PLUG-IN HYBRID ELECTRIC VEHICLE

A Thesis

Submitted to the Faculty

of

Purdue University

by

Adam Garrett Fogarty

In Partial Fulfillment of the

Requirements for the Degree

of

Master of Science in Mechanical Engineering

December 2014

Purdue University

West Lafayette, Indiana

In dedication to the memory of Barbara Jean Fogarty

Just as energy is conserved, so must our souls be

Wherever you are mom, I will always love you

Thank you for everything

ACKNOWLEDGMENTS

I would like to thank General Motors, the U.S. Department of Energy and Argonne National Laboratory along with many more sponsors, supporters and faculty who made EcoCar2: Plugging Into the Future the amazing experience that it was. It was the most substantial learning experience of my educational career. I would like to thank the faculty members of Purdue University's EcoCar2 team, Dr. Greg Shaver, Dr. Peter Meckl, Dr. Vahid Motevalli, Dr. Oleg Wasynczuk and Dr. Haiyan Zhang for taking time from their own lives to educate, mentor and guide the many members of our team throughout the years. I would like to thank our General Motors mentor Dale Klein for his many donations of time, energy and patience. You always seemed to answer my many phone calls and emails despite what time they may have occurred. Finally, I would like to thank the many students involved in Purdue's EcoCar team, specifically Kevin Oswald, Whitney Belt, Ashish Vora, Alec Lind, Bilwa Jadhav, Jagdish Hiremath, Abhishek Saxena, Xianan Huang, Haotian Wu, Yili Qian, Nathan Smart, Jordan Butler, Jon Pazar, Chenhao Ma, Akshit Singh, Jose Viana, Joseph Maddy, Aaron Woodard and Joshua Baird. By no way was EcoCar a one-person effort. Every one of you deserves extreme credit for the hours and energy spent on the project. Just remember that your hours were well spent everyone, Desirae performed beautifully all the way to the podium.

TABLE OF CONTENTS

Page

LIST OF TABLES

LIST OF FIGURES

Figure Page

ABBREVIATIONS

A/C	Air Conditioning
AN	Aeronautical-Navy
ANL	Argonne National Labs
AVTC	Advanced Vehicle Technology Competition
AWD	All Wheel Drive
BCM	Battery Control Module
CSM	Current Shunt Module
CAD	Computer Aided Drawing
COP	Coefficient of Performance
CV	Continuous Velocity
DOE	Department of Energy
E&EC	Emissions and Energy Consumption
EDS	Electrical Distribution System
EPRV	Evaporator Pressure Regulating Valve
ESS	Energy Storage System
FEA	Finite Element Analysis
FL	Front Left
FR	Front Right
GM	General Motors
HE	Heat Exchanger
HEV	Hybrid Electric Vehicle
HV	High Voltage
HVAC Compressor	High Voltage Air Conditioning Compressor
HVDS	High Voltage Disconnect Switch
HVIL	High Voltage Interlock Loop

ID	Inner Diameter
JIC	Joint Industry Council
LV	Low Voltage
LVDS	Low Voltage Disconnect Switch
MABX	Micro Auto Box
MBB	Measurement and Balance Board
MSDS	Manual Service Disconnect Switch
NYSR	Non Year-Specific Rules
OD	Outer Diameter
PE	Petroleum Energy
PHEV	Plug-in Hybrid Electric Vehicle
PTTR	Parallel-Through-The-Road
RL	Rear Left
RR	Rear Right
SOC	State of Charge
TXV	Thermal Expansion Valve
UF	Utility Factor
VTS	Vehicle Technical Specifications

GLOSSARY

Chiller	Common term for the heat exchanger used to cool the battery pack
Framerails	Individual rails of vehicle chassis which run underneath vehicle body
Halfshaft	Single driveshaft which transfers power from one source to one wheel
Hard-Mounting	When two objects are attached such that there is little to no vibrational isolation between the two bodies
Nominal	Describes the average value of a function versus time
Peak	Describes the maximum value of a funciton versus time
Soft-Mounting	When two objects are attached such that there is significant vibrational isolation between the two bodies
Subframe	Common term for a suspension cradle
Toe Link	Forward-most link of the rear suspension assembly which adds fore/aft rigidity to the linkage assembly
Uni-body	Description of a vehicle's structure as a single, rigid structure

ABSTRACT

Fogarty, Adam Garrett MSME, Purdue University, December 2014. High Voltage Rear Electric Drivetrain Design for a Parallel-Through-the-Road Plug-in Hybrid Electric Vehicle. Major Professors: Gregory M. Shaver and Peter H. Meckl, School of Mechanical Engineering.

Purdue University was selected as one of 15 universities to participate in a three year Advanced Vehicle Technology Competition (AVTC) called EcoCar2: Plugging Into the Future. The vehicle built by the Purdue team was a Parallel-Through-The-Road Plug-in Hybrid Electric Vehicle (PTTR PHEV). The vehicle utilized a B20 diesel powertrain to power the front wheels, as well as a custom electric drivetrain to power the rear wheels. Using this vehicle during the final year of the competition, the team was successful in placing 4th overall as well as 2nd in the category of Well-To-Wheel (WTW) Greenhouse Gas Emissions.

A stock 2013 Chevrolet Malibu was given to all teams in the competition to use as a base vehicle. The Purdue team removed the stock 2.4L gasoline engine of the Malibu in order to make room for the diesel powertrain and switched the stock Malibu rear suspension assembly to that of a 2013 All-Wheel-Drive (AWD) Buick LaCrosse in order to make room for the electric drivetrain. The electric drivetrain utilized a 16.4 kWhr Lithium Ion battery pack, a 103 kW (peak) 45 kW (nominal) electric motor, and the driveline components of a 2013 AWD Buick LaCrosse in order to transfer power to the wheels.

Significant challenges concerning the custom electric drivetrain during the competition included the design, fabrication, installation and operation of a rear suspension cradle, Energy Storage System (ESS) and a Thermal Management System for the ESS. Computer Aided Drawing (CAD) and Finite Element Analysis (FEA) were used heavily during the design stages of vehicle development in order to give the Pur-

due team and AVTC competition organizers sufficient confidence to allow the team to build the designs they had proposed. This work describes the design, analysis and fabrication procedures used by the Purdue team in order to create the electric drivetrain used in their vehicle for the EcoCar2 competition.

1. INTRODUCTION

1.1 Motivation

As time passes, increasing amounts of effort across the globe are being spent towards decreasing the overall environmental impact of many industries. One industry in particular is the automotive industry. In the automotive world, it is possible to implement systems and strategies that decrease harmful environmental effects. However, these systems often come at the cost of lower performance and consumer acceptability. Therefore, it is the goal of automotive manufacturers to find ways of decreasing negative environmental impacts while still maintaining the same levels of performance and acceptability that consumers have grown to expect from a modern vehicle.

For the past 25 years, the United States Department of Energy has partnered with the North American Automotive industry in order to achieve the goals mentioned previously by sponsoring several Advanced Vehicle Technology Competitions (AVTC's) that are managed by Argonne National Laboratory. Most recently, EcoCar2: Plugging Into The Future was an AVTC that began in the fall of 2011 and ended in the summer of 2014 [1].

1.1.1 EcoCar2: Plugging Into The Future

It was the intent of EcoCar2: Plugging into the Future to allow students of varying backgrounds and educational experience to work together in order to modify a 2013 Chevrolet Malibu to reduce Well-to-Wheel (WTW) petroleum consumption, energy consumption, Greenhouse Gas (GHG) emissions and criteria tailpipe emissions without sacrificing consumer acceptability, performance, utility and safety. 15 Collegiate Universities across North America were involved with EcoCar2, including Purdue

University which was one of six first-time competitors. Since EcoCar2 was a three year program, it was divided into three stages of vehicle development which reflected the vehicle design procedure (VDP) used by General Motors.

Year 1

During year 1, no teams had a physical vehicle to work with. Instead, the focus of this phase was mainly on software design and simulation. It was up to each team to undergo a Powertrain and Architecture selection procedure using software such as MATLAB and Autonomie in order to determine what hardware components were desired. Additionally, teams were required to show thorough design strategies via CAD drawings and assemblies that proved they were capable of successfully implementing each piece of hardware within their vehicle. Hardware aside, teams were also expected to create control models and conduct simulations that proved they were capable of successfully controlling all hardware in the form of one cohesive vehicle. From these simulations, teams were required to determine what theoretical performance parameters their vehicles would achieve. Once achieved, this data would be compared to a list of Vehicle Technical Specifications (VTS) that were determined by the competition organizers in order to ensure that all team vehicles would be capable of meeting the minimum performance standards set by the competition [2].

Year 2

During year 2, all teams that demonstrated valid software design and simulation were given a 2013 Chevrolet Malibu to use as their base vehicle. The focus during this year was to achieve approximately 60 percent operating status of their intended vehicle's design by the end of the year. At the end of year 2, teams were gathered at the GM Desert Proving Grounds in Yuma, AZ in order to demonstrate that their vehicles operated successfully using their custom designs and powertrains. However, before any vehicle was allowed to operate, it was first necessary for each vehicle to pass

both a static and dynamic safety inspection via Argonne National Laboratory (ANL) inspectors prior to vehicle operation. Once done, the inspected vehicle was allowed to compete in dynamic events such as braking, acceleration and gradability. If a vehicle did not operate as was intended on software and simulation, the team responsible would have received either a "Run as intended" or "Run as designed" penalty based on the circumstances. For example, if a team used a combustion engine on the front wheels and an electric drivetrain on the rear wheels of their vehicle, yet experienced a malfunction with their combustion engine, the team would still be allowed to compete in dynamic events using only their electric drivetrain while incurring a penalty to their overall score since the vehicle was not designed to run on one drivetrain. Therefore, it was the intention of all teams to have their vehicles safely operate as intended on all powertrains in order to compete in as many scored events as possible without penalty. It should be noted that at this stage, it was not imperative to have a clean and polished look to their vehicle since the focus was mainly on safety and powertrain operation [3].

Year 3

During year 3, the focus was mainly on polishing each vehicle such that powertrain and control algorithm efficiencies were increased, as well as polishing the look and comfort of each vehicle using materials such as carpeting, sound insulation and interior trim. At the end of year 3, teams were expected to have all powertrains running successfully without control errors so that they may participate in dynamic events at a final competition in Milford, MI. The goal of year 3 was to have all vehicles achieve a 99 percent completion status when compared to a show-room quality vehicle. Metrics such as noise, ride harshness, ease of access and comfort became more important than previous years. Once all vehicles had performed as many events as possible as best they could in the time given, the scores of all events were summed together and added to each team's overall yearly score [4].

1.1.2 Vehicle Technical Specifications

The Vehicle Technical Specifications given to all teams were exactly the same values. Included in the specifications were values from a stock 2013 Malibu, values determined to be the minimum that a vehicle must achieve and values determined to be the "goal" of a team's vehicle [5]. The values can be seen in Table 1.1.

Table 1.1. Vehicle Technical Specifications.

Specification	Production 2013 Malibu	Competition Design Target	Competition Requirement
Acceleration 0–60 mph	8.2 sec	9.5 sec	11.5 sec
Acceleration 50–70 mph (Passing)	8.0 sec	8.0 sec	10 sec
Braking 60–0 mph	143.4 ft. (43.7 m)	143.4 ft. (43.7 m)	180 ft. (54.8 m)
Highway Gradeability @ 20 min	10+% @ 60 mph	3.5% @ 60 mph	3.5% @ 60 mph
Cargo Capacity	16.3 ft^3	16.3 ft^3	7 ft^3
Passenger Capacity	5	>=4	2
Mass	1,589.6 kg	<2,250 kg	<2,250 kg
Starting Time	<2 sec	<2 sec	<15 sec
Ground Clearance	155 mm	155 mm	>127 mm
Vehicle Range	736 km [457 mi] (CAFE)	322 km [200 mi]*	322 km [200 mi]*
Charge-Depleting Range*	N/A	**	N/A
Charge-Depleting Fuel Consumption*	N/A	**	N/A
Charge-Sustaining Fuel Consumption*	N/A	**	N/A
UF-Weighted Fuel Energy Consumption*	8.83 (lge/100 km) [787 Wh/km]	7.12 (lge/100 km) [634 Wh/km]	N/A
UF-Weighted AC Electric Energy Consumption*	N/A	**	N/A
UF-Weighted Total Energy Consumption*	787 (Wh/km)	634 (Wh/km)	N/A
UF-Weighted WTW Petroleum Energy (PE) Use*	774 (Wh PE/km)	624 (Wh PE/km)	N/A
UF-Weighted WTW GHG Emissions*	253 (g GHG/km)	204 (g GHG/km)	N/A
Criteria Emissions	Tier 2 Bin 5	Tier 2 Bin 5	N/A

1.2 Vehicle Architecture

Given the VTS goals of the competition, it was the task of each team to perform simulations of several different vehicle architectures as part of the powertrain and vehicle architecture selection process. The Purdue team used Autonomie to perform its vehicle simulations, which required the team to determine how power would flow from an energy source on the vehicle to the wheels of the vehicle. During this stage,

the Purdue team assumed that it would be constructing a combustion/electric hybrid vehicle. Given this, there would be two sources of energy onboard the vehicle: a combustible fuel and an electric battery pack. Typically, Hybrid Electric Vehicles (HEV's) are constructed as one of three types: Series, Parallel or Split [6].

1.2.1 Architecture Selection

Series HEV

In a series HEV architecture, the power begins with a combustion engine that converts fuel into mechanical work to be used by an electric generator. From the generator, electric current is sent to a battery pack, which powers the electric traction motor. Therefore, the driving power of the vehicle is determined by the electric traction motor, since it is the sole mover of the vehicle's wheels.

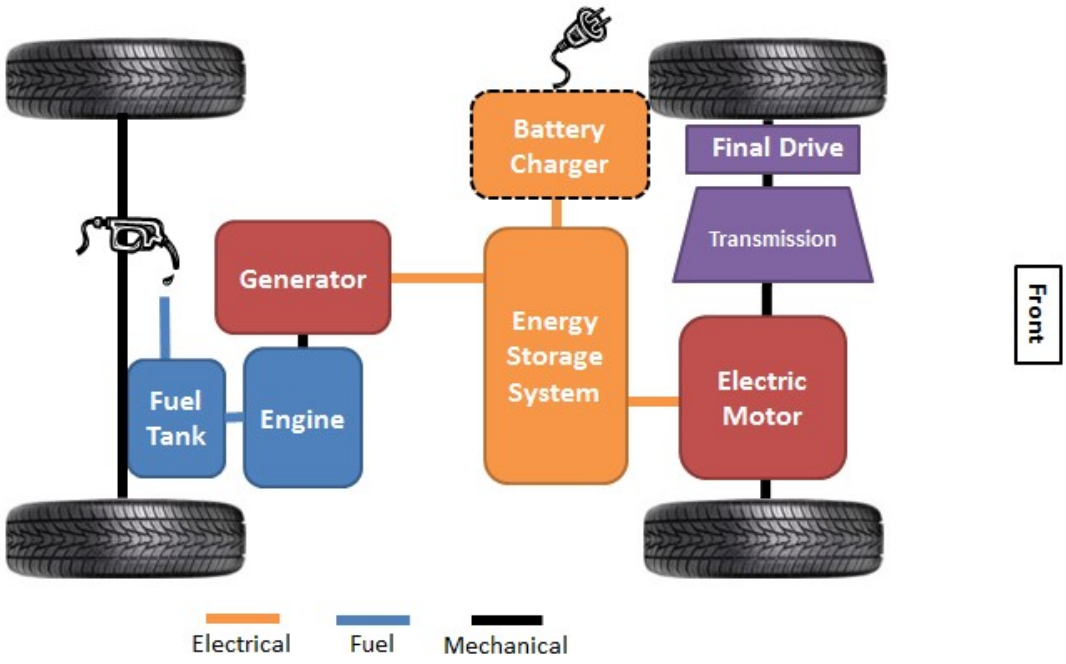

Figure 1.1. Block Diagram of a Series HEV.

The main benefit to a series HEV is that the combustion engine is allowed to operate continuously at its most fuel efficient speed. Therefore, a relatively small combustion engine may serve as the power generation source of a comparatively larger vehicle. With a smaller combustion engine, weight is reduced and packaging challenges are lightened.

Parallel HEV

In a parallel HEV architecture, power can be sent from a fuel source to one or more moving components via two separate pathways. This allows for more total driving power output than a series architecture if given the same powertrain components since there are two power units acting as the moving components that are used to drive the vehicle. For the Purdue team, the parallel architecture explored is known as Parallel-Through-The-Road.

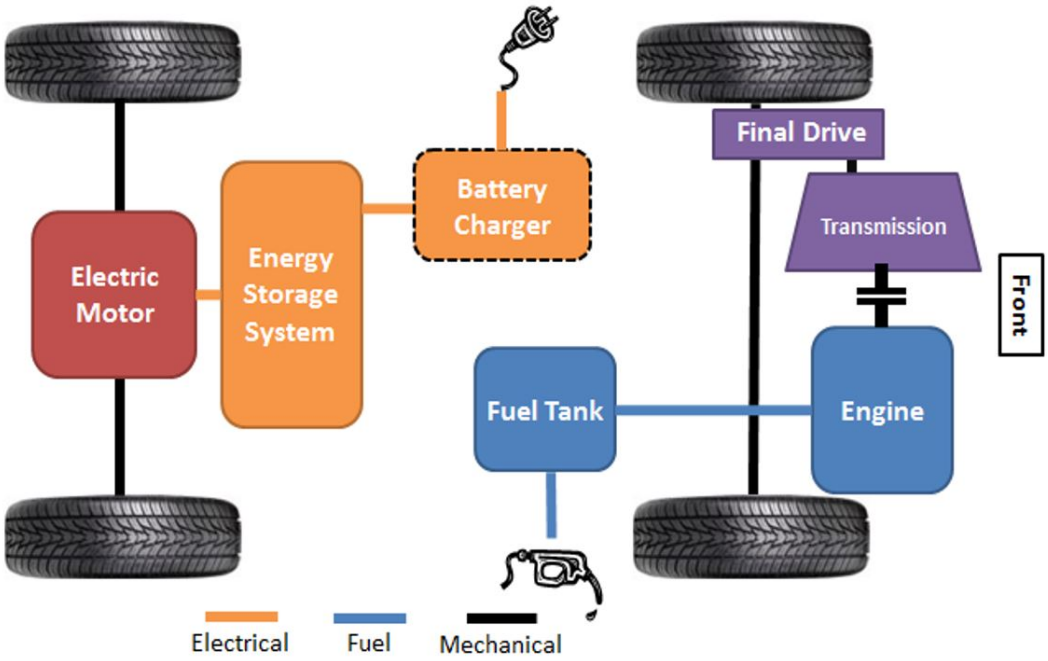

Figure 1.2. Block Diagram of a Parallel HEV.

In this case, one powertrain acts upon one axle while the other powertrain acts upon the other. For the Purdue vehicle, as seen in Figure 1.2, an electric drivetrain was placed on the rear wheels, while a combustion powered drivetrain acted upon the front wheels. Since the two powertrains are acting upon different sets of wheels at the same time, it is imperative that the controls algorithms used allows them to work in sync with each other in order to prevent dynamic instabilities of the vehicle.

Split HEV

In a split HEV architecture, power is sent from two sources into a mechanism that has two degrees of freedom, resulting in one output that is used to drive the vehicle. In the parallel architecture, each drivetrain can operate the vehicle independently of the other. This is beneficial in case one of the powertrains malfunctions, or if the control algorithm determines it to be preferable.

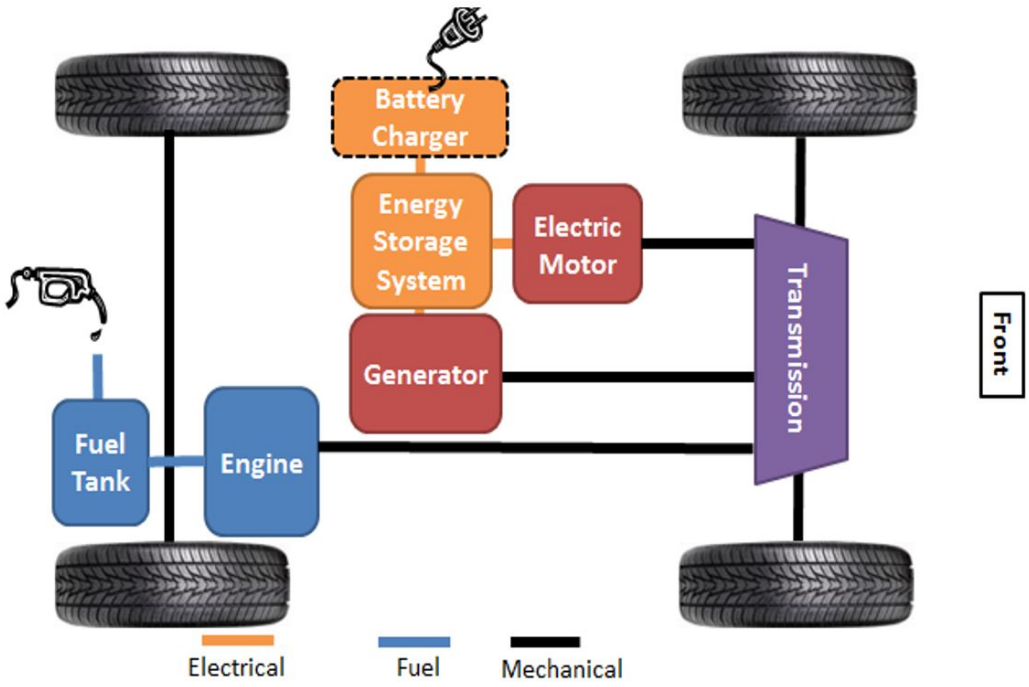

Figure 1.3. Block Diagram of a Split HEV.

However, in the split architecture, both powertrains must be operational in order to power the moving unit that drives the vehicle unless the power split mechanism has the ability of eliminating one degree of freedom, such as the addition of a locking mechanism on the electric drivetrain.

HEV vs PHEV

When dealing with hybrid vehicles, they can have the capability of being a Plug-in HEV. This means that there are two modes of driving operation: Charge Depleting (CD) and Charge Sustaining (CS). Charge Sustaining mode implies that the vehicle operates such that the energy stored within the battery pack fluctuates near a nominal value within a given range, thus sustaining the charge value it began with. If a battery pack State of Charge (SOC) drops too low, irreversible damage can be caused to the battery cells. Logically, the lower bound of the battery pack SOC range in Charge Sustaining mode would be set near the battery pack's minimum SOC value within a predetermined buffer range.

Charge Depleting mode implies that the battery pack SOC is much higher than its minimum value such that the vehicle may operate more aggressively on the electric drivetrain, causing the battery pack SOC to decrease over time. Once the battery pack SOC reaches its minimum value, the car may switch to Charge Sustaining mode such that the SOC does not decrease to harmful values. Typically, HEV's operate solely in Charge Sustaining mode, while PHEV's operate both in Charge Depleting mode and Charge Sustaining mode.

Utility Factor

When considering Charge Depleting range, it is important to note the frequency of short vehicle trips in North America. If a PHEV begins with 100% SOC and is used over a short distance, it is possible that the vehicle will operate solely in Electric only mode, resulting in zero fuel consumption over the course of the trip. Therefore,

having a larger battery pack is desirable for this effect. However, there is a trend of diminishing return when considering the value of a vehicle's Charge Depleting range since the frequency of longer vehicle trips is lower. Therefore, the EcoCar2 competition used a metric known as "Utility Factor" to take this into consideration as seen in Figure 1.4. This factor is used to benefit teams with large CD ranges when calculating their WTW GHG emissions and overall energy consumption.

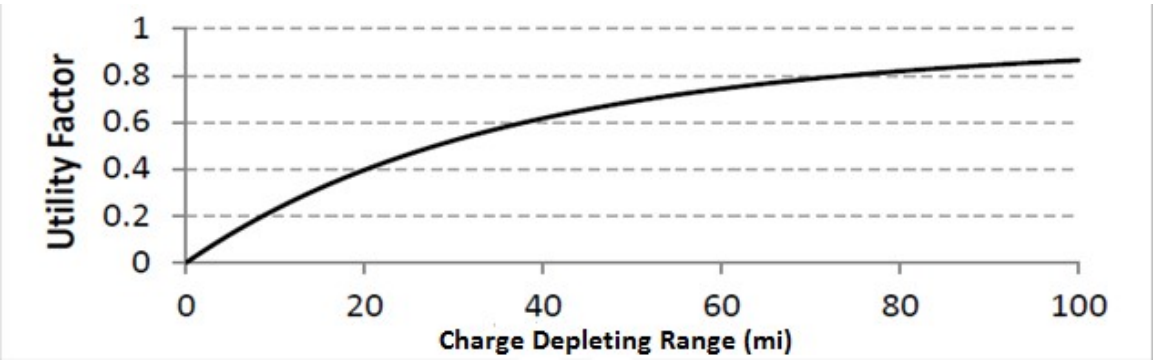

Figure 1.4. Utility Factor versus Charge Depleting range.

Well-To-Wheel

When considering what the overall impact of a certain energy source is, a Well-To-Wheel cycle analysis is used. In this scenario, the total emissions caused by extraction, refinement, distribution and use of an energy source are all considered as the emission of that energy source. For example, when using electrical energy, the emissions caused by a typical electrical power plant (mining fuel, shipping fuel, converting fuel into electricity) will be factored into the emission data and score of the competition [7].

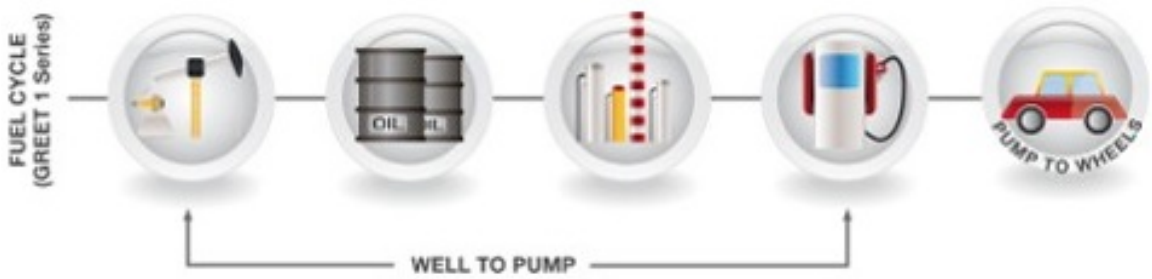

Figure 1.5. Diagram of Well-To-Wheel cycle analysis.

Component Comparison

Since the competition included scoring metrics such as Utility Factor and Well-To-Wheel emissions, choosing the type and size of each powertrain component and fuel source was not a trivial procedure. When choosing what fuel source(s) to use, three combustible fuels were allowed by the competition: Gasoline, E85 (85% Ethanol, 15% Gasoline) and B20 (20% Biodiesel, 80% Diesel). To make use of the fuels available, several powertrain options were available for donation via General Motors as seen in Table 1.2. Similarly, other sponsors of the competition made several Electric Motors available for donation as seen in Table 1.3.

Table 1.2. Engines available for donation.

Maker	**Size**	**Fuel Source**	**Ignition Source**
General Motors	1.4 Liter	Gasoline	Spark Ignition
General Motors	2.4 Liter	E 85	Spark Ignition
General Motors	1.7 Liter	B20	Compression Ignition

When sizing battery packs, several A123 Lithium Ion battery packs were available for donation. The ID's of each battery arrangement reflected the number and sequence in which individual cells were arranged. Several cells would be connected in series,

Table 1.3. Electric motors available for donation.

Maker	Nominal Power (kW)	Peak Power (kW)
Camry	35	70
Magna	45	90
UQM	55	105

then several of these series would be connected in parallel to create a single battery module. Therefore, each battery pack ID indicated the number of cells in series, the number of series in parallel, and the number of modules in the arrangement. All ID's followed the syntax: (Number of modules)xS(Number of cells in series)P(Number of series in parallel). Since the volume of a single battery cell remained fixed, the total amount of cells in a battery pack were directly proportional to the overall volume and mass of the battery pack. The battery packs available can be seen in Table 1.4.

Table 1.4. Battery Packs available for donation

Pack ID	Max Energy (kWhr)	Cont. Power (kW)	Peak Power (kW)
6xS15P2	10.8	34	101
7xS15P2	12.6	40	118
6xS15P3	16.2	51	152
7xS15P3	18.9	60	177

Knowing the powertrain and battery pack options available, vehicle architectures using combinations of each item were simulated to determine an estimate of the performance of each combination [8]. Additionally, each combination was simulated when performing both as a PHEV and an HEV. Shown in Figure 1.6 is the simulation result concerning Well-To-Wheel Greenhouse-Gas (WTWGHG) emissions. Once the

results of these simulations were interpreted, it was clear that a PHEV architecture was preferable for lower emissions.

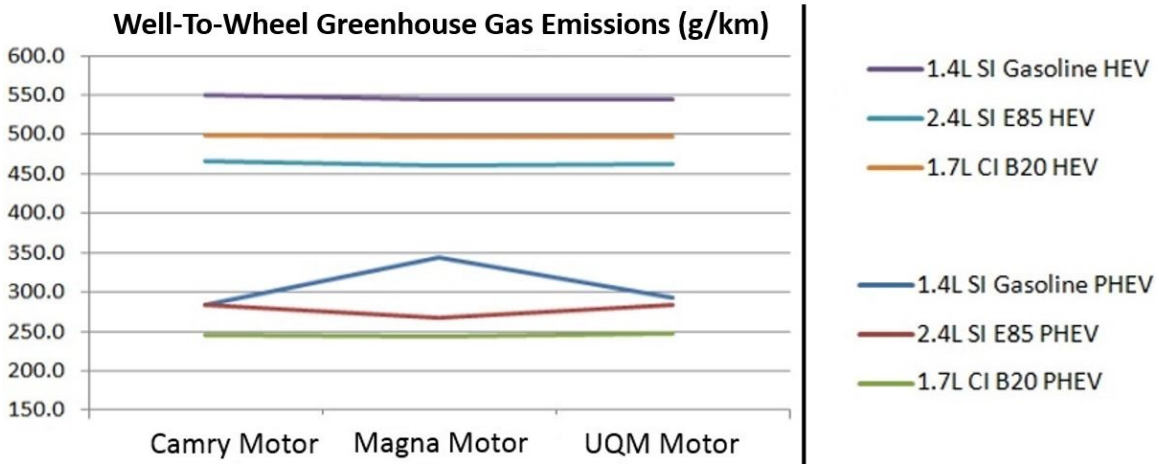

Figure 1.6. Simulation results of both PHEV and HEV architectures using various powertrain components.

Once WTW and UF effects were considered, more simulation results were performed. Additionally, types of fuel were varied as both B20 biodiesel and E85 Ethanol were considered. Shown in Figure 1.7 is the emissions results comparison and shown in Figure 1.8 is the dynamic performance results comparison. Both figures show examples of how for both the parallel and split architectures, when the engine and motor remained fixed, a battery pack with seven modules performed better than a battery pack with six modules. Therefore, a battery pack with 7 modules was preferred.

	Engine	Motor	Battery
Series	1.7L B20	45/90	7x15s3p
	2.4L E85	45/90	7x15s3p
Parallel-through-the-road	1.7L B20	45/90	7x15s3p
	1.7L B20	45/90	6x15s3p
Power-Split	1.7L B20	45/90	7x15s3p
	1.7L B20	45/90	6x15s3p

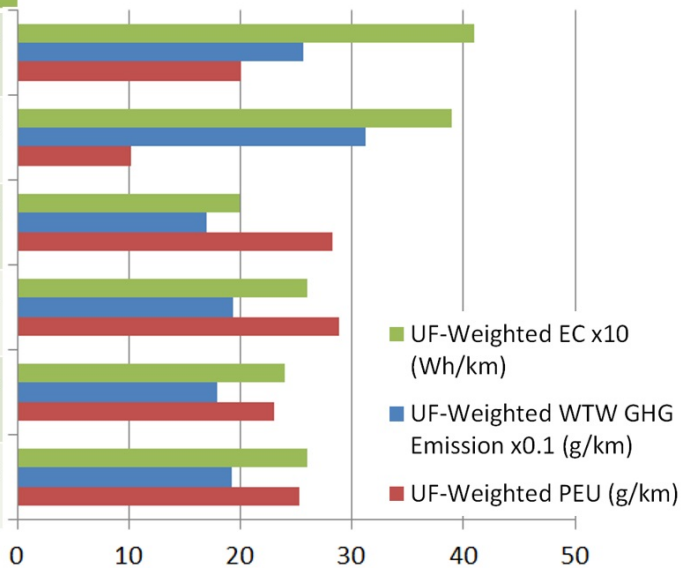

Figure 1.7. WTW E&EC simulation results of various vehicle architectures.

	Engine	Motor	Battery
Series	1.7L B20	45/90	7x15s3p
	2.4L E85	45/90	7x15s3p
Parallel-through-the-road	1.7L B20	45/90	7x15s3p
	1.7L B20	45/90	6x15s3p
Power-Split	1.7L B20	45/90	7x15s3p
	1.7L B20	45/90	6x15s3p

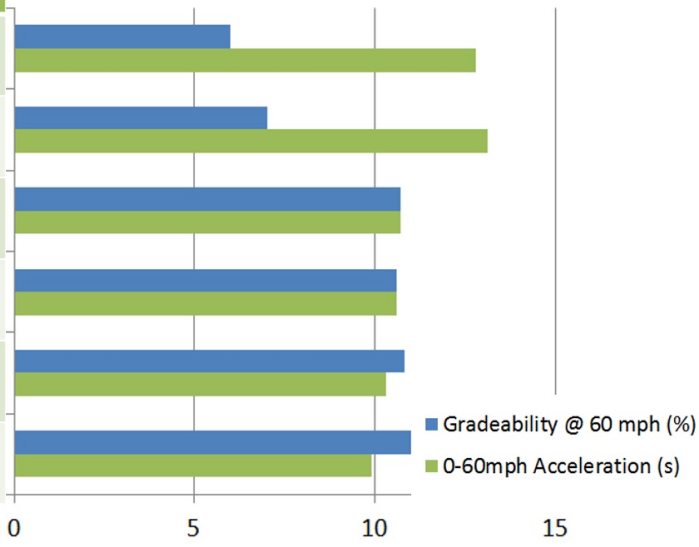

Figure 1.8. Performance simulation results of various vehicle architectures.

Parallel-Through-The-Road

After reviewing the simulation results shown in Figures 1.7 and 1.8, some conclusions were made concerning which architecture would be the most likely candidate for success. For example, in Table 1.1, it is shown that the minimum 0-60 mph acceleration time of each vehicle must have been less than 11.5 seconds. However, Figure 1.8 shows that the series architecture was the slowest of the three choices with acceleration times between 12.5 and 13 seconds. Additionally, Figure 1.7 shows that the series architecture had the highest overall energy consumption and greenhouse gas emissions. With this in mind, the team ruled the series architecture out of candidacy.

Once the team ruled out the series architecture, there were many discussions concerning whether to use a split or parallel architecture. Figures 1.7 and 1.8 show that these two archietectures performed similarly well, although the split architecture had better performance and lower petroleum energy conumption. In order to implement the split architecture, a power split mechanism was required in order to distribute power between the engine, wheels and motor simultaneously. However, the mechanism available to the team to perform this task required specific information concerning what signals would be output by the mechanism as well as what signals were required to be input to the mechanism. Without this information, the Purdue team was not convinced that the benefits of a split architecture were worth the time required to investigate the required signals of the power split mechanism.

In a Parallel-Through-The-Road architecture, the engine and motor work independently of each other. Therefore, the vehicle would have two independant drivetrains capable of moving the vehicle. This would be beneficial in the event of a malfunction, since the malfunction would most likely only affect one drivetrain, thus allowing the vehicle to continue operating using the other drivetrain. Additionally, since both drivetrains are isolated from one another, the packaging challenges of mating the two powertrains together were non existent. The Purdue team reasoned that without this packaging challenge, they would have more time with a working vehicle in order

to test their control algorithms on a physical vehicle. Therefore, since the Parallel-Through-The-Road arhcitecture demonstrated sufficient performance and emissions capabilities and the team was confident they had all the information and components to implement it successfully, the team chose this as its desired vehicle architecture.

Figure 1.9 depicts the vehicle structure, while emphasizing the packaging constraints of the structure. For instance, subsystems such as the Exhaust and Fuel system were required to remain outside the vehicle such that they do not invade the cabin of the vehicle. Additionally, the fuel system was required to be in front of the rear suspension as well as behind the front suspension so that it was well protected in the event of a collision. Therefore, the engine bay contained the engine and transmission, the exhaust tunnel contained the exhaust system, underneath the rear seats contained the fuel system and the rear suspension contained the electric motor, thus leaving the rear of the vehicle to be the only remaining place to package the Energy Storage System. Additionally, all of the high voltage components were placed in the rear of the vehicle such that no high voltage wiring was required to be routed across the vehicle, thus increasing the safety of accessing components during maintenence and vehicle operation.

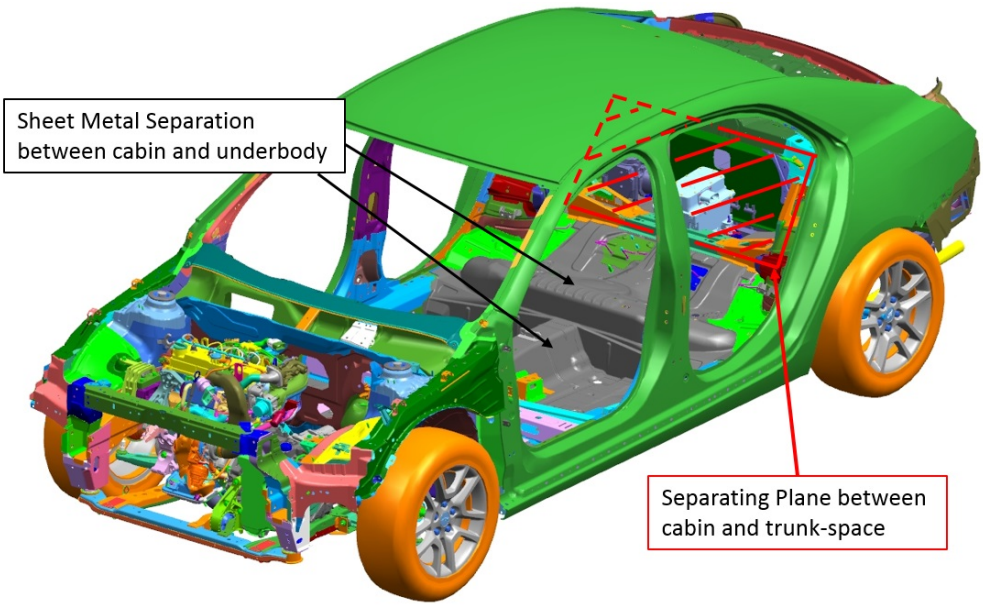

Figure 1.9. Vehicle Structure with structural constraints emphasized.

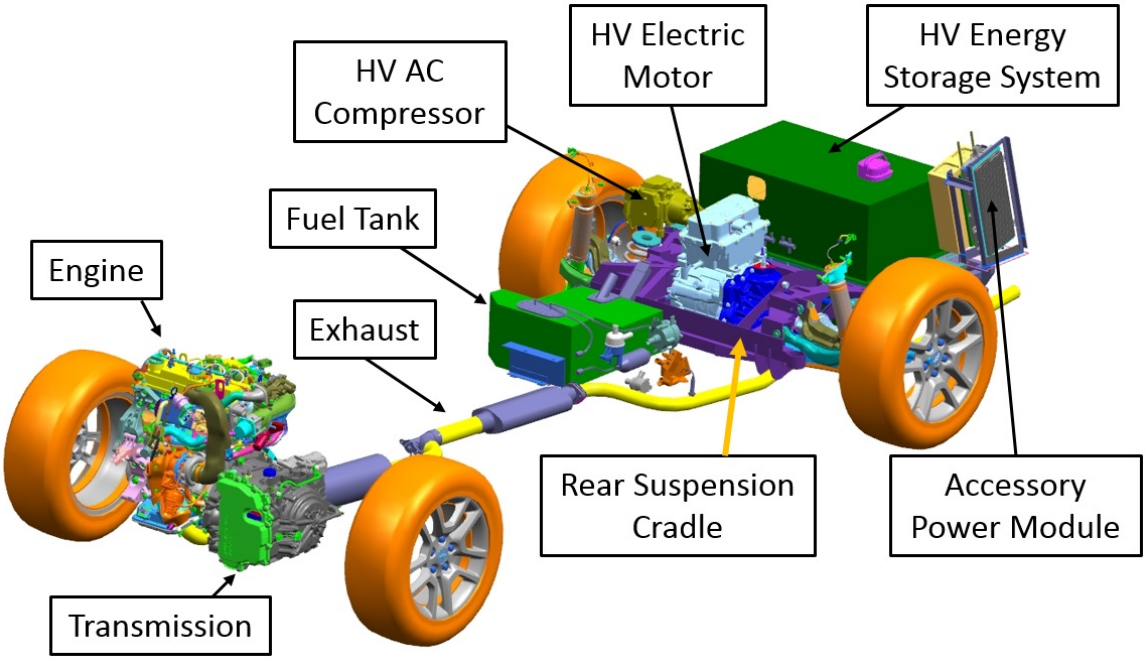

Figure 1.10. Parallel-Through-The-Road subsystem Packaging Assembly.

Battery Sizing

Although the simulation results shown in Figures 1.7 and 1.8 indicated that 7 battery modules were preferable over 6 modules, it was very difficult during the early stages of CAD design and subsystem placement to ensure that the Purdue team would be capable of successfully implementing 7 battery modules. For example, the rules of the competition stated that each team vehicle was required to have a Class II trailer hitch similar to the one shown in Figure 1.11. Additionally, it was stated that the exhaust tip of each vehicle must be located in the same area as the stock vehicle, approximately 19.5" to the left of the trailer hitch tip as seen in Figure 1.12.

Figure 1.11. Class II trailer hitch recommended to be used by each team.

Because of the requirements seen in Figure 1.12, there was a feeling that the area underneath the chassis frame rails of the rear structure would become crowded due to the existence of a trailer hitch as well as the necessary routing of an exhaust tube. These requirements had implications when sizing the battery pack since it was desired that the battery modules be placed in the rear of the vehicle's structure. Figure 1.14 depicts a battery box arrangement with seven modules which includes an area through which the exhaust tube may pass through.

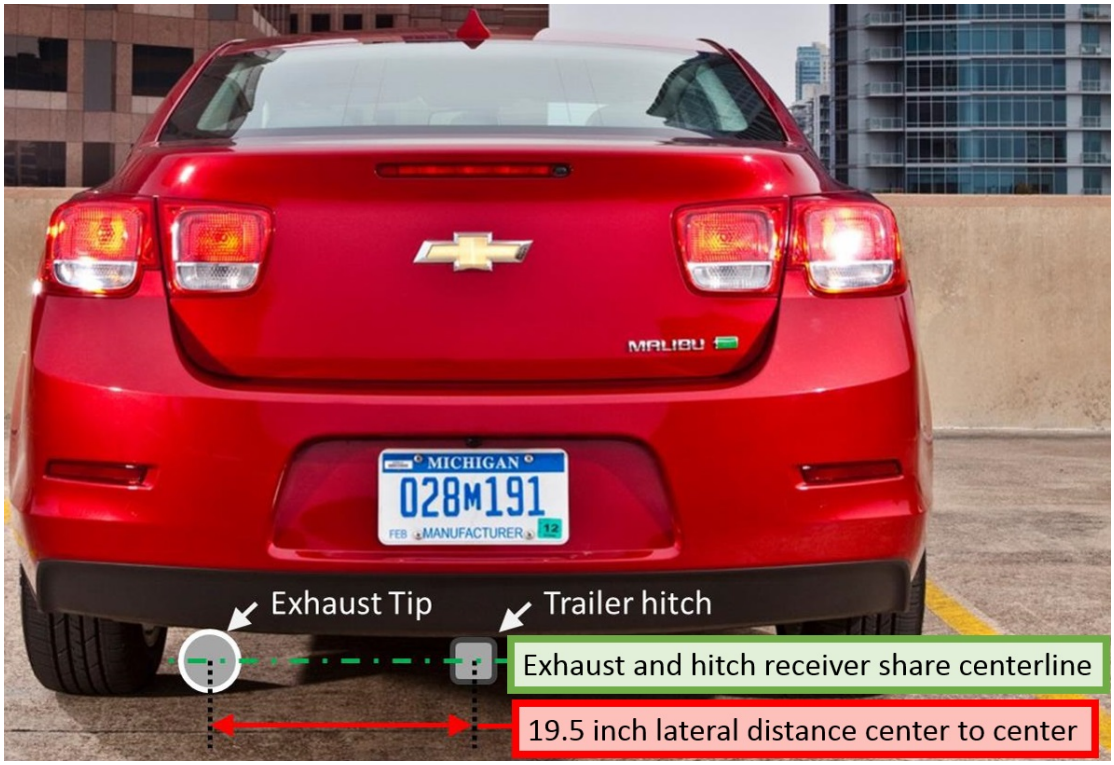

Figure 1.12. Exhaust and trailer hitch tip locations required by competition.

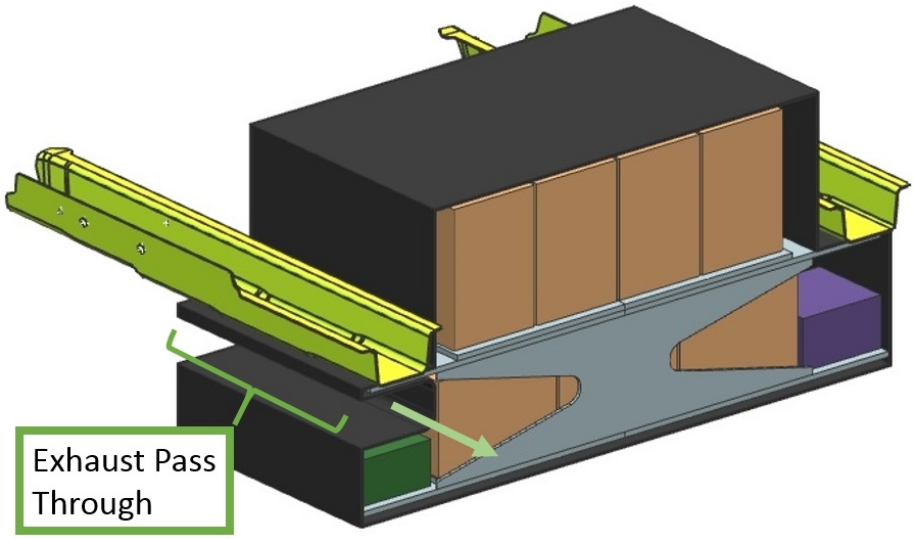

Figure 1.13. ESS Arrangement with 7 battery modules and an exhaust pass-through.

Although this design allowed room for the exhaust tube, there was no room to add a trailer hitch to the chassis. Additionally, the top of this ESS arrangement is substantially higher than the top of the framerails which represents the floor of the trunkspace. Therefore, it was reasoned that this ESS would not allow the vehicle to fit all of the cargo modules needed by the compeition. Similarly, Figure 1.14 shows an ESS arrangement which contains seven battery modules which remains lower within the trunkspace than the arrangement in Figure 1.13. However, there is no room underneath the framerails for an exhaust tube or a trailer hitch as depicted in Figure 1.15.

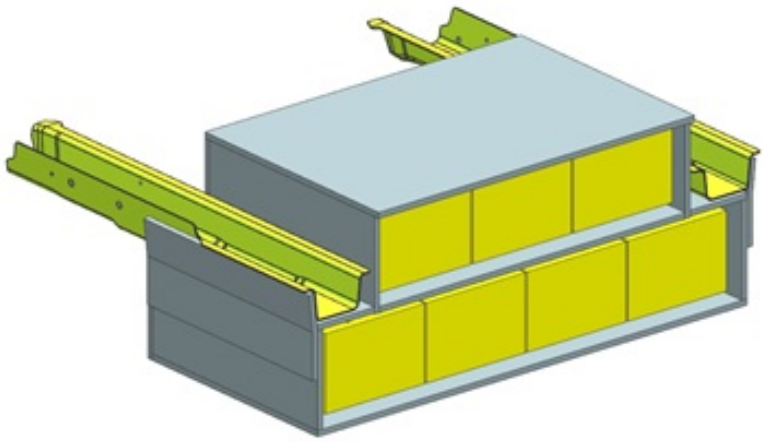

Figure 1.14. ESS Arrangement with 7 battery modules - Isometric view.

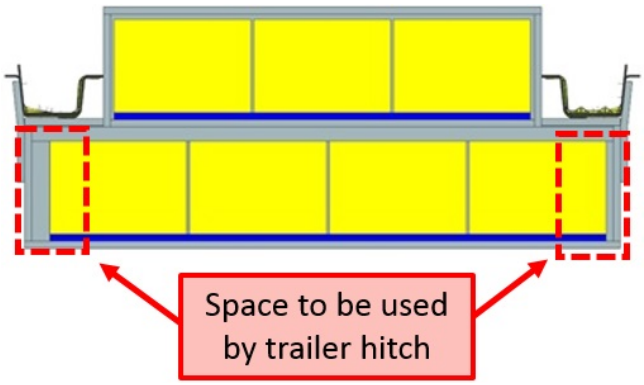

Figure 1.15. ESS Arrangement with 7 battery modules - Rear view.

Difficulties such as these convinced the Purdue team to explore ESS arrangements using only 6 battery modules such as the one shown in Figure 1.16 which allowed for packaging of both a trailer hitch and exhaust tubing. Additionally, since the battery modules above and below the middle of the plate were symmetrical, threaded rods (shown in green in Figure 1.16) were passed vertically through the entire ESS such that they could mount two battery modules with one set of four rods.

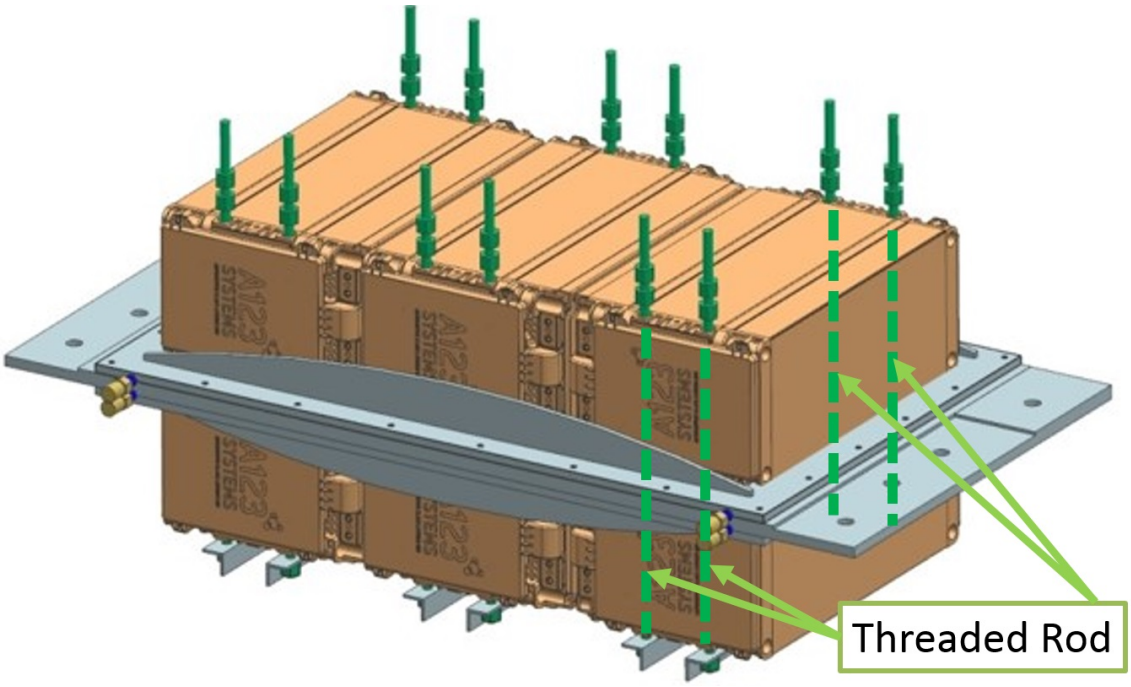

Figure 1.16. ESS Arrangement with 6 battery modules.

Overall, the Purdue team was very confident that they could incorporate the ESS depicted in Figure 1.16 quickly and robustly. Therefore, this arrangement was pursued.

Final Architecture

Based upon the simulation results and initial CAD packaging of components, the architecture that the Purdue team chose to pursue was a Parallel-Through-The-Road Plug-in Hybrid-Electric Vehicle with B20 as its combustion fuel as seen in Figure 1.17.

Table 1.5. Architecture Components.

Component Type	Component Name
Engine	GM 1.7L CI B20
Electric Motor	Magna E-Drive 45kW nom 90kW peak
Energy Storage	A123 6x15sx3p 16.2 kWh
Transmission	6-Speed Automatic Gearbox

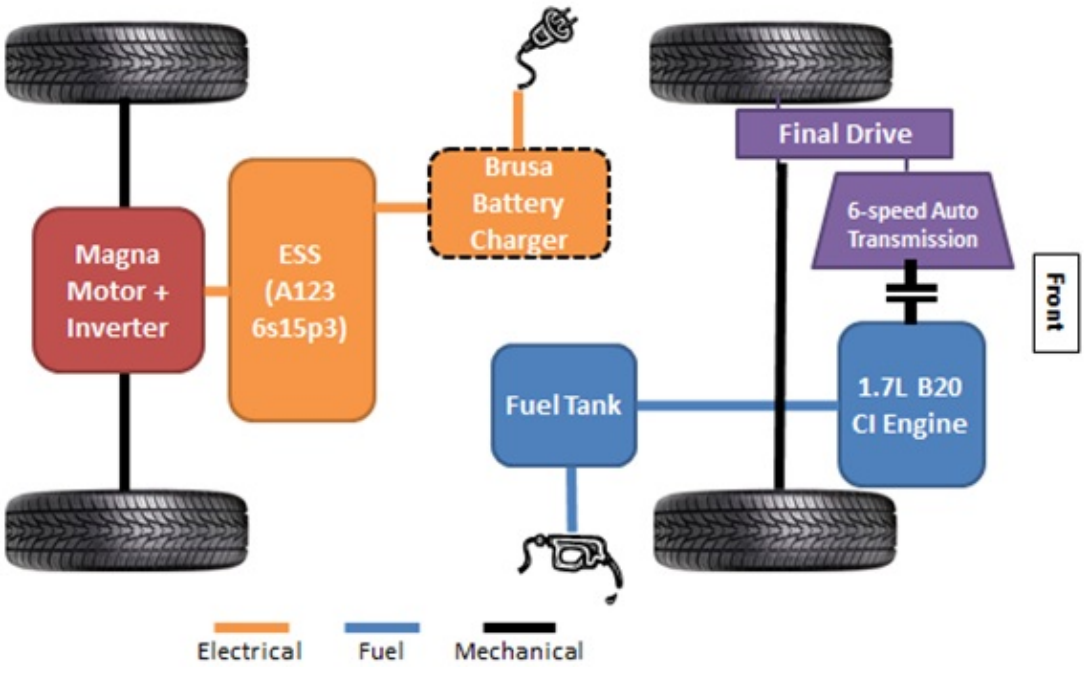

Figure 1.17. Final Purdue Vehicle Architecture.

1.2.2 Powertrain Placement

Once a block diagram was created that detailed how the vehicle would ideally fit together, the next step was to place the main powertrain components to determine what interferences would occur.

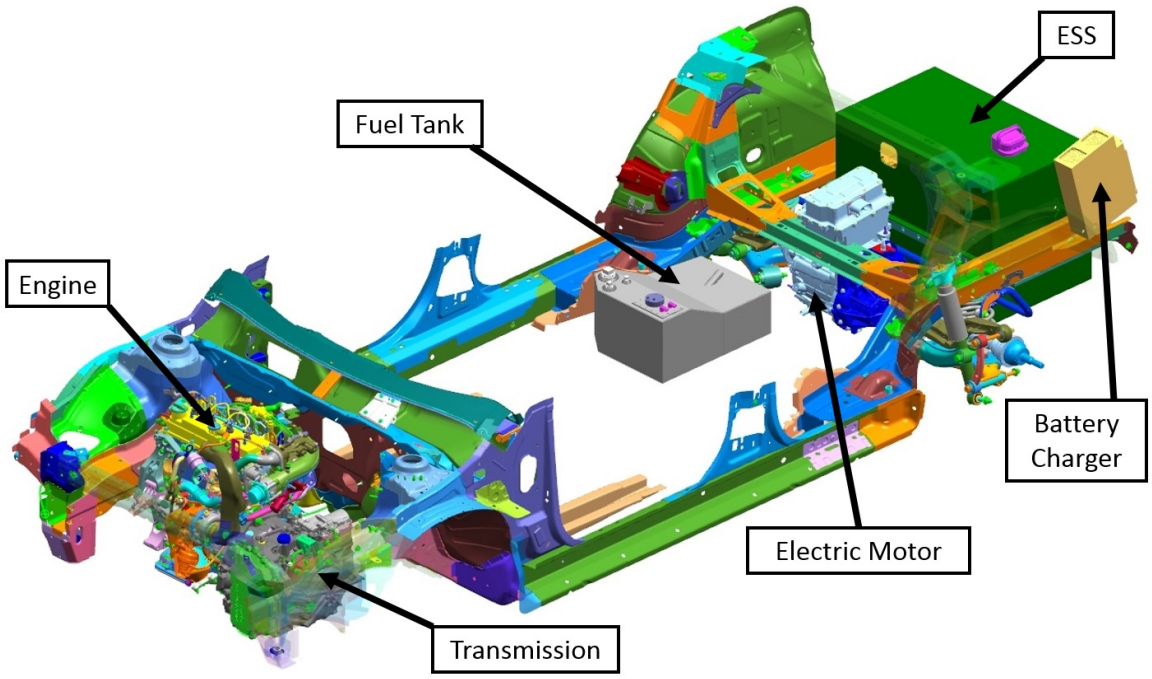

Figure 1.18. Vehicle lower structure with main powertrain components.

As seen in Figure 1.18, the rear traction motor, front engine, front transmission, fuel tank, Battery Charger and Energy Storage System have been placed within the vehicle's safety cage similar to the diagram in Figure 1.17 in order to determine the severity of any necessary structural changes.

1.2.3 Structural Constraints

When placing components, there were specific rules to be followed concerning what parts of the base vehicle may be modified. Shown in Figure 1.19 is the safety cage of the vehicle, which was unmodifiable for any reason.

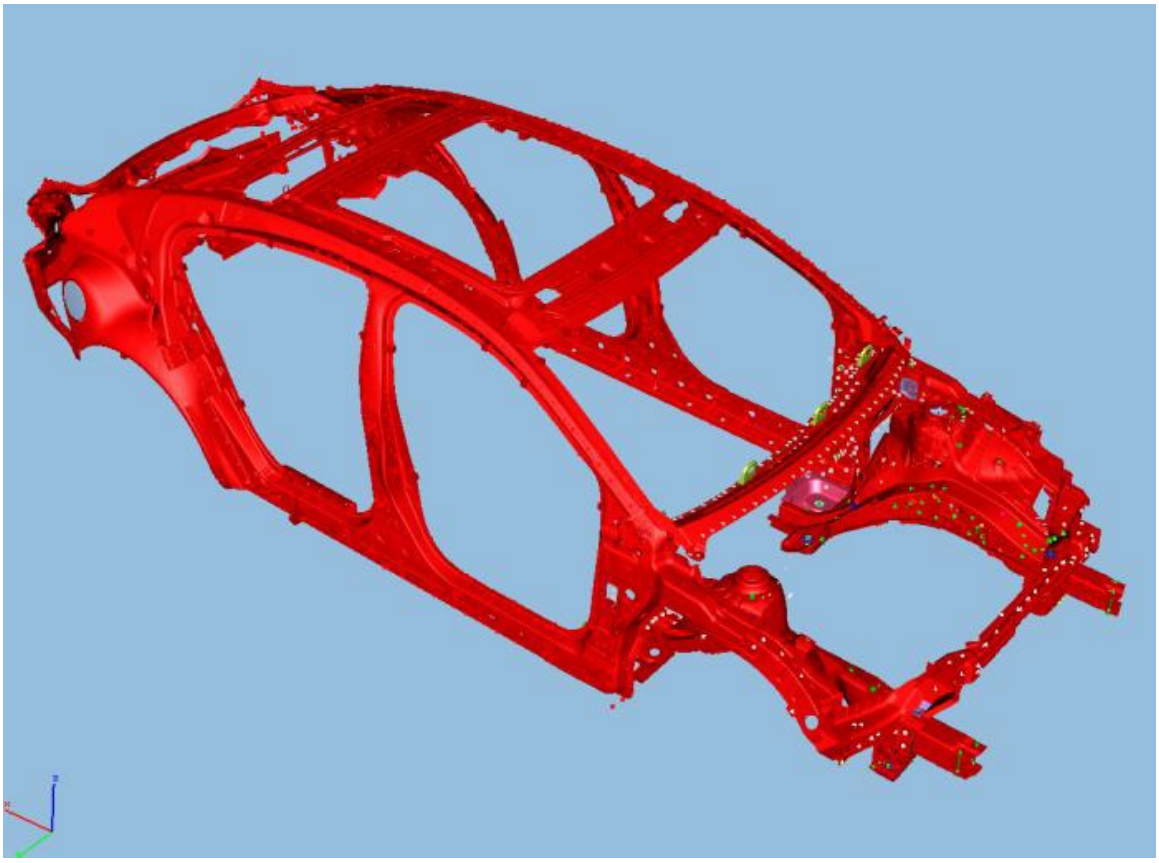

Figure 1.19. Safety Cage of the Base Vehicle - Unmodifiable.

With this constraint set, it was inferred that any component that was not part of the safety cage was capable of being modified. However, as seen in Figure 1.20, there are green zones and yellow zones as well. Any green component could have been modified at will, however any modifications that affected yellow components must have first passed an extensive and in-depth waiver review process given by a waiver review committee consisting of members of both ANL and GM.

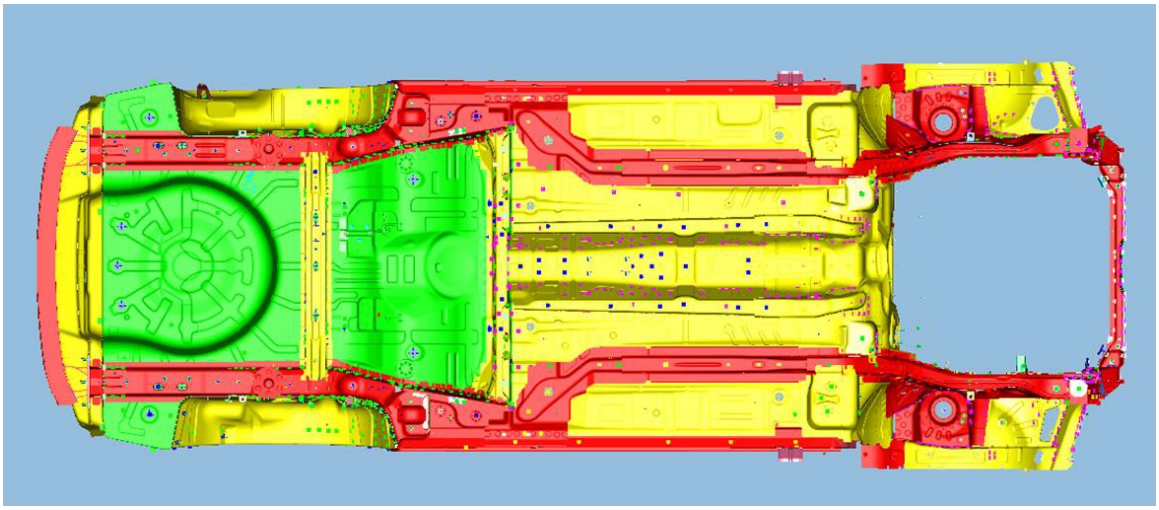

Figure 1.20. Modifiability template of the Base Vehicle - Underneath view of vehicle.

Additionally, when packaging both the fuel and energy storage systems, it was required that neither system sit below two distinct planes of the vehicle's structure. As seen in Figure 1.21, all fuel components must sit above the yellow line, while all ESS components were required to sit above the black line.

When considering how to package the ESS, it was proposed that the most plausible area to package a battery pack was the rear of the vehicle - the lower volume of the trunk space as well as the spare tire well. However, this volume came with its own packaging constraints. Specifically, it was required that the vehicle have a departure angle of approximately 13 degrees so that the battery box would not scrape the ground when the vehicle begins ascending a hill. Additionally, no part of the ESS was allowed to extend behind the rear end of the chassis framerails. This is due to the fact that this rear bumper area is known as a "crumple zone", which is intended to absorb energy during a rear end collisions. Therefore, by remaining outside the rear crumple zone, all ESS components would have stood a better chance of remaining intact during a rear end collision.

Other than safety zones, there was also a cargo requirement for the trunk space. As specified by Table 1.1, approximately 7 cubic feet were the minimum trunk space of the vehicle. Additionally, it was required that the cargo space be accessible via the trunk opening. Seen in Figure 1.22 are representations of all the volumetric constraints concerning the trunk space packaging specified by the competition.

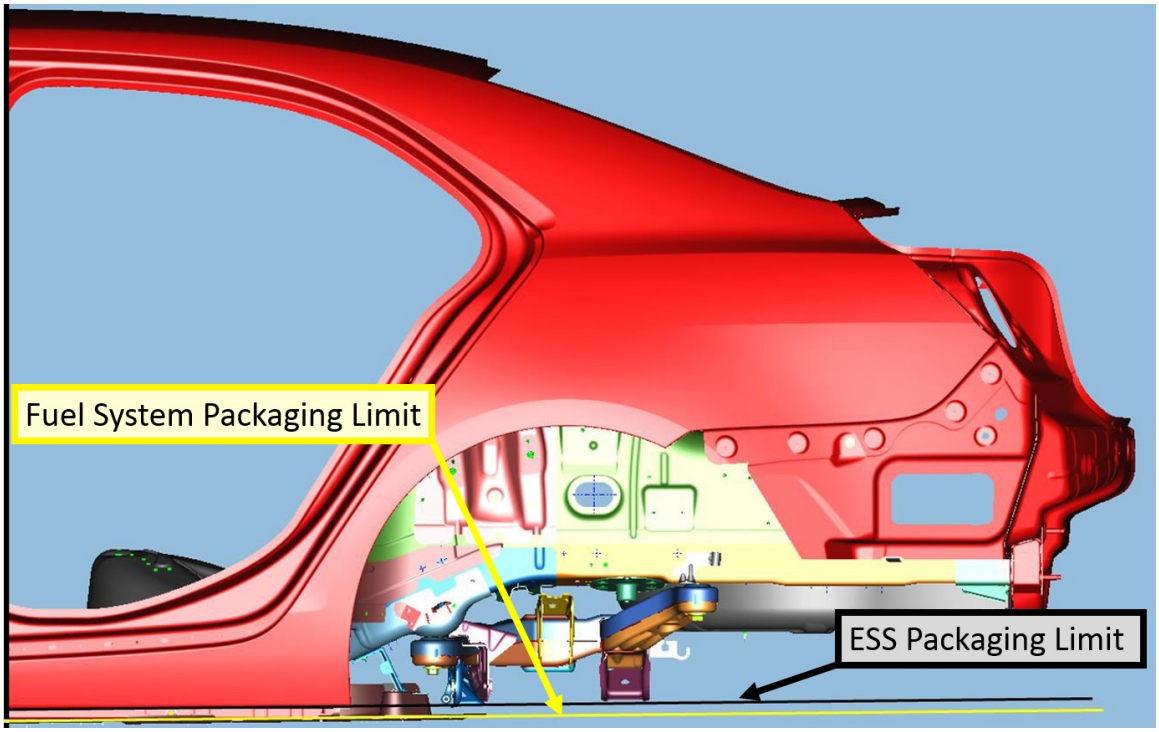

Figure 1.21. Required ground clearance for fuel and ESS components - Rear Side view of vehicle.

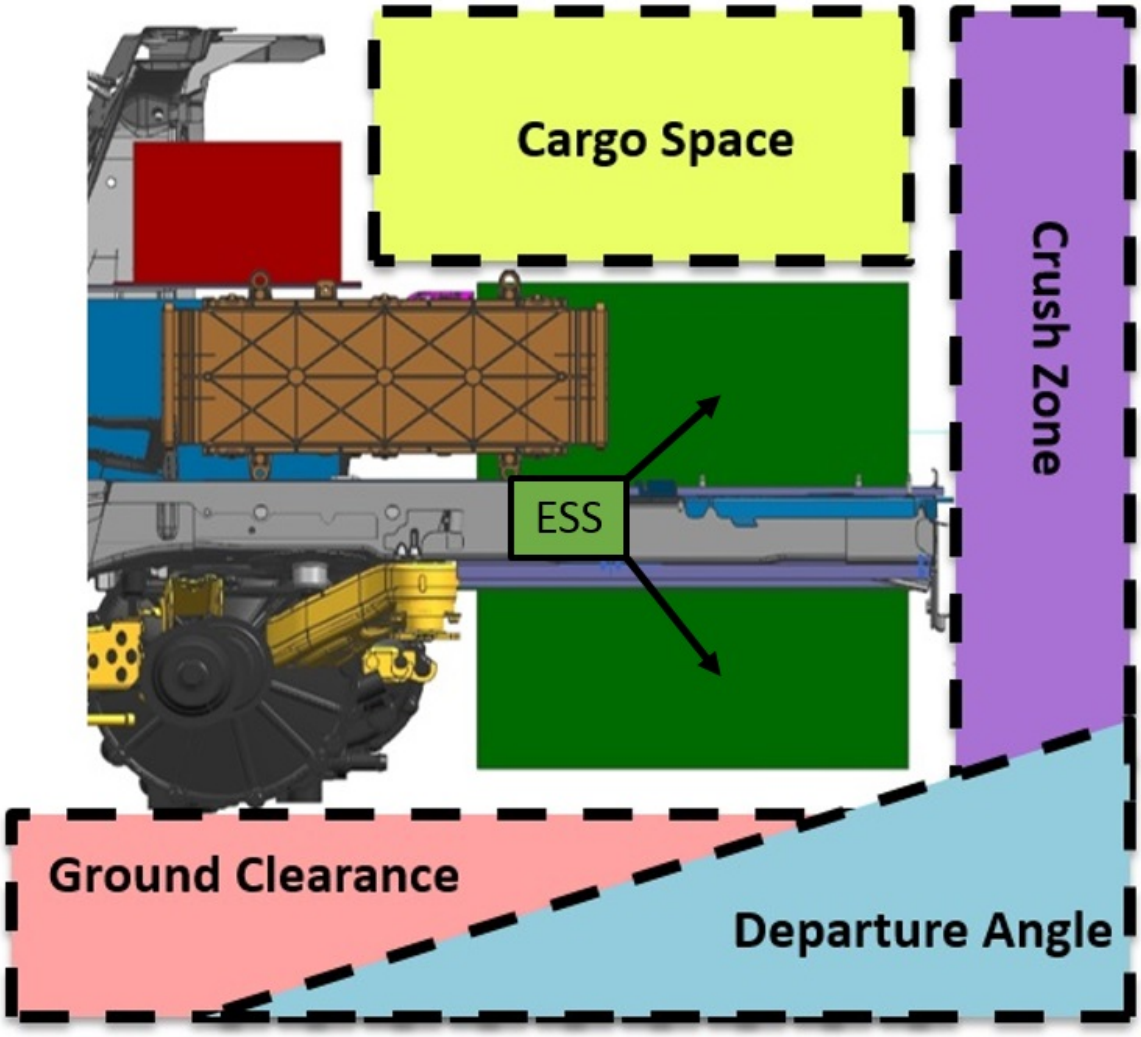

Figure 1.22. Required buffer zones for ESS placement - Rear Side view of vehicle.

1.2.4 Subsystem Placement

Once spatial constraints were set and necessary powertrain components were placed, it was possible to begin adding important substructures of the vehicle such as suspension components, drive shafts, and cooling systems as depicted in Figure 1.23. If there were interferences with these vehicle substructures, it was important to consider the tradeoffs between modifying a vehicle subsystem versus attempting to modify the vehicle structure, which required substantial analysis and justification via the waiver review process.

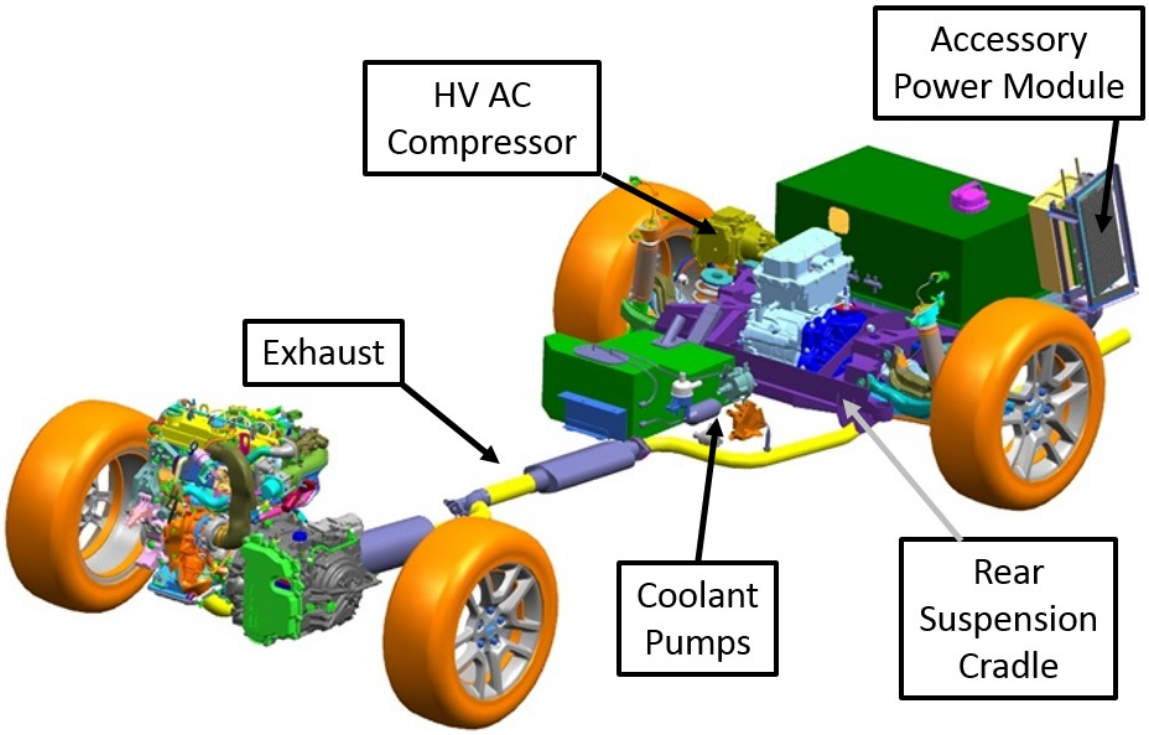

Figure 1.23. Vehicle subsystem components.

After all powertrain components were placed, and discussions were held concerning the severity of structural modifications, it was decided that several subsystems would require custom-built structures to hold components in place. For example, a custom rear suspension cradle, a five-bar support brace and a support and cooling system

for the ESS were required to be custom made by the Purdue team in order to ensure proper vehicle operation.

1.3 Significant subsystems

During the vehicle development process, three subsystems in particular required significant attention and effort: the rear suspension cradle, the Energy Storage System, and the thermal management system.

1.3.1 Rear Suspension Cradle

With the addition of the electric rear traction motor, it was determined exceedingly difficult to adjust the stock Malibu suspension in order to allow for the motor. Because of this, the Purdue team elected to create a custom rear suspension cradle to hold both the motor and the suspension linkages in place. The design of the rear suspension cradle will be discussed in detail in Chapter 2 of this thesis. Figure 1.24 depicts the rear suspension with cradle, linkages, motor and ehaust routing in place.

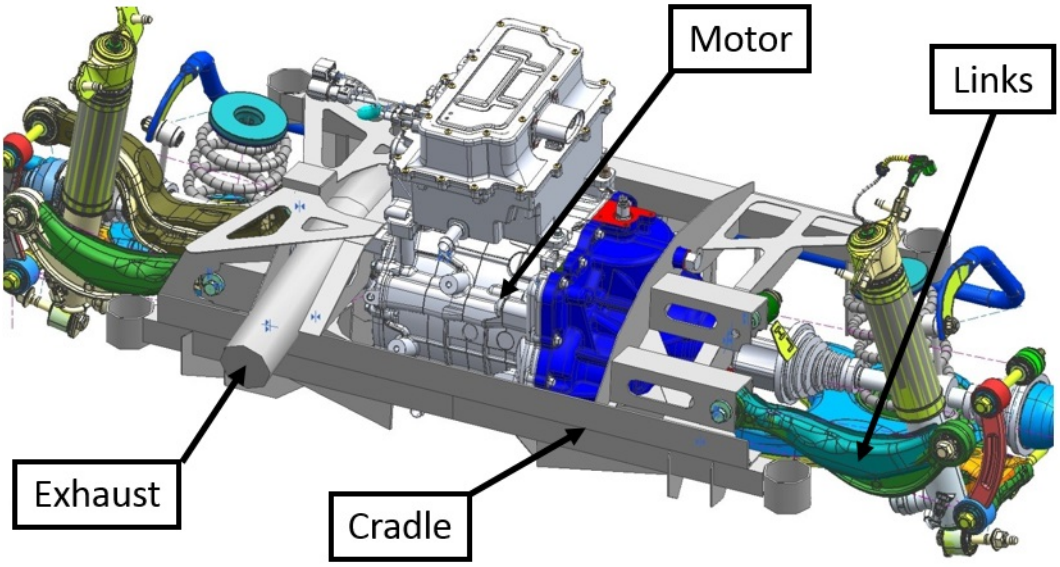

Figure 1.24. Front view of rear suspension assembly.

1.3.2 Energy Storage System

The Energy Storage System was a highly critical design project for several reasons. Since it contained materials of very high energy density, the most important requirement to meet was to assure that no catastrophic releases of energy occurred throughout the competition. This required structural support, proper battery module arrangement, robust high voltage routing as well as a capable cooling strategy. Design and analysis of the ESS will be discussed in detail in Chapter 3 of this thesis. Figure 1.25 shows a CAD assembly of the ESS.

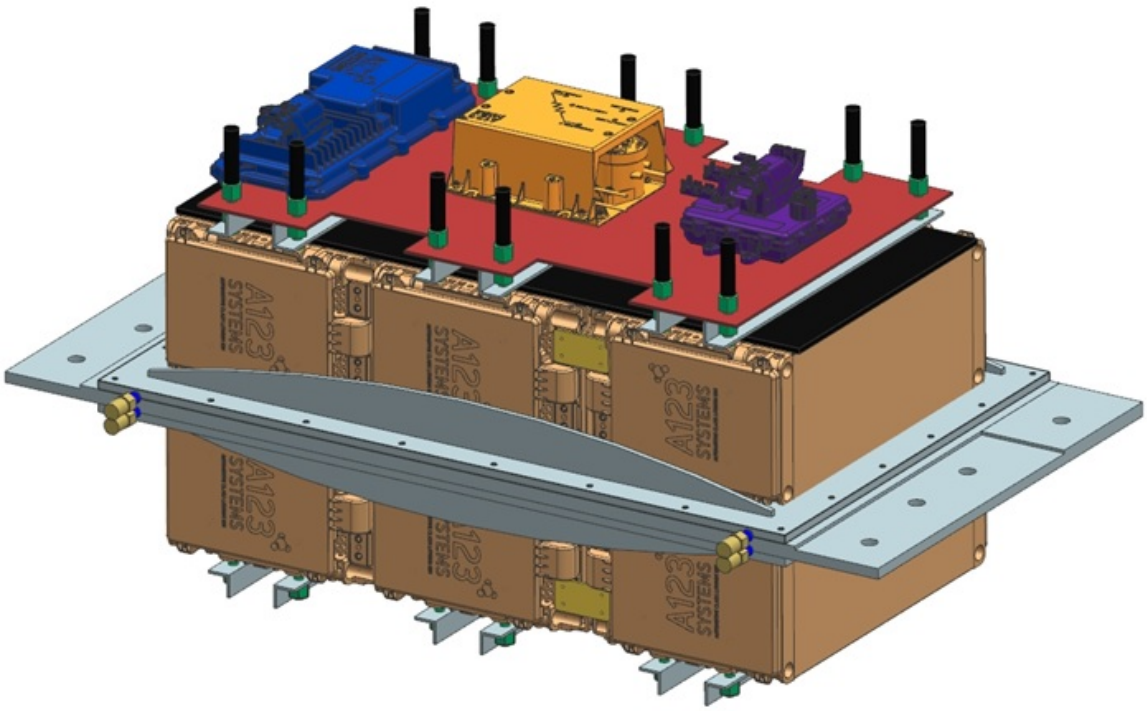

Figure 1.25. Front view of Energy Storage System.

1.3.3 Thermal Management System

Since it was determined that the Year 2 competition would take place in Yuma, AZ during a summer month, the Purdue team determined that a cooling system was desired for the Energy Storage System to ensure that all battery modules could remain under 35 degrees Celsius despite the ambient temperature. This required a refrigerant circuit since it was desired that the pack temperature be lower than the ambient temperature. Therefore, this thermal management system will be described as sub-ambient-capable in this thesis. Design and analysis of this system will be discussed in detail in Chapter 4 of this thesis.

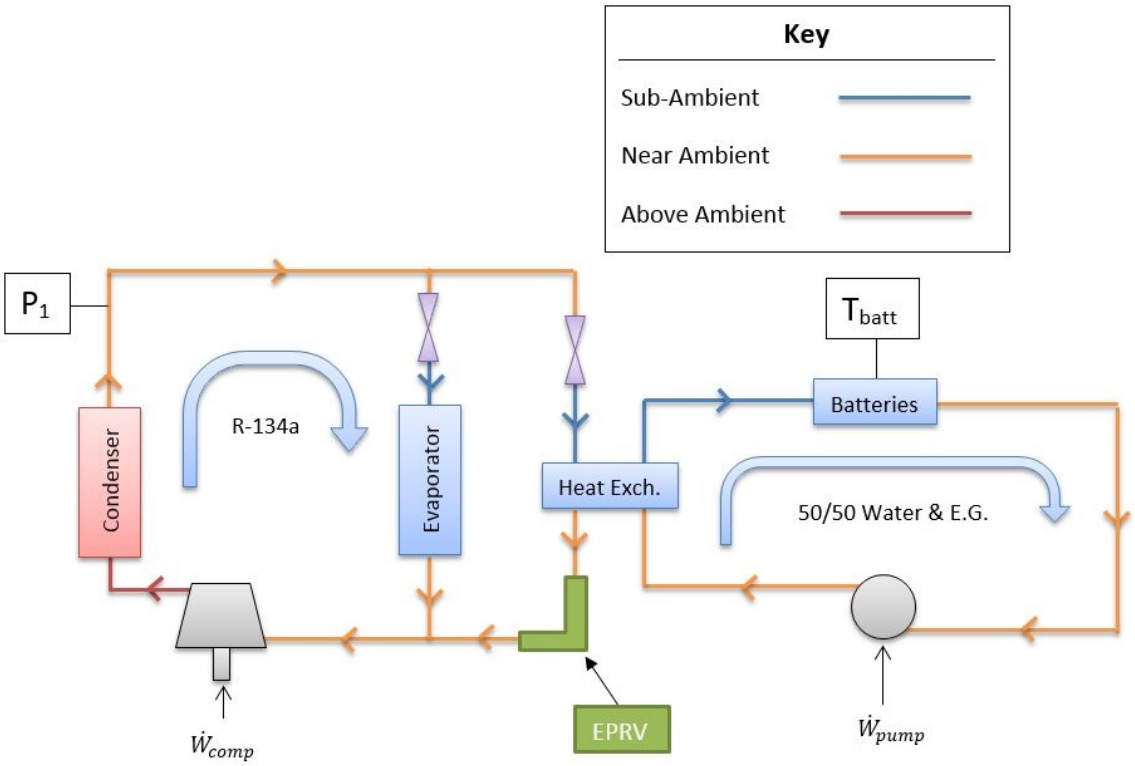

Figure 1.26. Diagram of Thermal Management System.

1.4 Personal Contributions

1.4.1 Year 1

At the beginning of the fall 2011 semester, I joined Purdues EcoCar 2 team as a senior undergraduate student in Mechanical Engineering. During the fall semester, I was the leader of a group of other undergraduate students who were tasked with performing several Autonomie simulations to determine which powertrain architectures and components would allow the Purdue vehicle to meet its desired performance goals.

During the spring 2012 semester, I volunteered to be the leader of a team of undergraduate students who were tasked with designing the high-voltage electrical energy storage system to be used on the vehicle. By the end of the semester we had created a viable design that passed the inspection of the battery sponsor of the competition, A123 systems. The design conceived during this semester became the system that was installed and used successfully for years 2 and 3 of the competition.

1.4.2 Year 2

During the summer semester of 2012, I was taking the final 2 courses required for my undergraduate degree, one of which was a technical elective which used EcoCar2 as its research focus. My goal for this elective was to design a custom rear suspension cradle to be used on the vehicle. By the end of the semester, I had created a design for the suspension cradle which was viable, yet difficult to manufacture. Additionally, the Finite Element Analysis (FEA) performed on the design was insufficient.

During the fall semester of 2012, I began my first year as a graduate student at Purdue University in the school of Mechanical Engineering. The mechanically-focused technical sections of Purdues EcoCar2 team were divided into two teams: the Front Drivetrain team and the Rear Drivetrain team. At the beginning of the semester, I volunteered to be the leader of the Rear Drivetrain team. Tasks to be

completed by this team included: integrating the rear electric motor, designing a thermal management system for both the cabin of the vehicle and the rear drivetrain components (electric motor and ESS), as well as fabricating and installing both the Energy Storage System and the rear suspension cradle. Of these tasks, the design and fabrication of the rear suspension cradle was my main responsibility.

During the spring semester of 2013, I was responsible for overseeing three senior design students and two additional undergraduate students in the effort of completing any remaining rear drivetrain integration challenges so that the electric drivetrain would be ready and operational for the May 2013 EcoCar2 Year 2 competition in Yuma, AZ. During this time, I was directly involved with the design, fabrication and installation of the rear suspension cradle, thermal management system, Energy Storage System, a five-bar structural brace and a custom trailer hitch. Additionally, I was responsible for switching the rear suspension linkages of the stock 2013 Malibu (the base vehicle) with those of an all-wheel drive 2013 Buick LaCrosse.

1.4.3 Year 3

During the summer semester of 2013, I volunteered to be the overall team leader of the Purdue EcoCar2 team. Technical responsibilities of this position included the management of both the rear and front drivetrains of the vehicle. Although both drivetrains were operational during the Year 2 competition in May of 2013, there were significant refinement changes to be made to the vehicle. During this semester, it was determined that the most desirable technical projects were updates to be made to the thermal management, exhaust after-treatment and fuel systems, all of which I was personally responsible for overseeing.

During the fall semester of 2013, my main focus was on successful team operation such that all involved members were contributing efficiently and successfully. Additionally, my own technical projects included: the updated fuel system, updated

thermal management system and the physical routing and component placement of the exhaust after-treatment system.

During the spring semester of 2014, my main responsibility as team leader was to ensure that all entities of the Purdue EcoCar2 team would be operational and ready for the EcoCar2 Year3 competition in Milford, MI and Washington, DC. The vehicle operated successfully at the GM facility, and all required presentations were delivered in Washington, DC. From these actions, the Purdue team placed 4th overall out of the 15 teams in the competition.

2. REAR SUSPENSION CRADLE

As was mentioned previously, a custom rear suspension cradle was required by the Purdue team to ensure robust packaging of the rear traction motor as well as the inboard bushing locations of the rear suspension linkages. The following sections detail what suspension linkages were used and why, as well as describe the overall design and analysis procedures used to create the custom cradle.

2.1 Rear Suspension Modification

One critical packaging focus that appeared quickly was the rear suspension area. This area is where the rear traction motor was placed, the exhaust tubing passed through, and was bounded on both front and rear ends by the fuel system and ESS, respectively. Since the rear traction motor being used (Magna E-Drive) had a built-in differential, it was desired to place the motor in line with the rear axle of the vehicle to avoid any driveshaft placement issues. However, due to the motor's large size, there were immediate interferences with the stock 2013 Chevy Malibu rear suspension. The most critical components affected were the inboard bearing locations of the suspension control arms, since they served as pivot points of the suspension linkages, thereby determining the motion of the wheels as they travel up and down within the wheel well.

Suspension Geometry

Figure 2.1 shows the linkages of the Stock 2013 Malibu rear suspension that came with the base vehicle of the competition. All of the linkages are held by a ground link known as the suspension cradle. Therefore, the links create a linkage similar to a four bar linkage in order for the wheel to travel up and down while still maintaining

flat contact with the road. Figure 2.2 shows the suspension with the cradle in place, and Figure 2.3 depicts the suspension geometry as a four bar linkage.

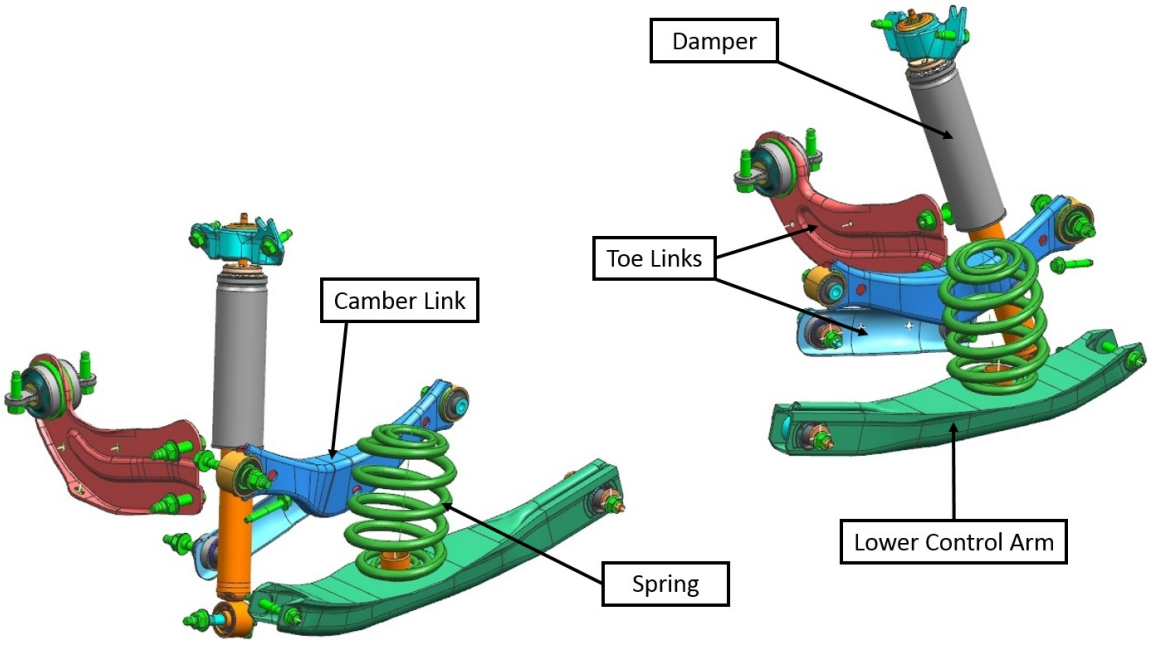

Figure 2.1. Malibu Rear suspension linkages - Rear isometric view.

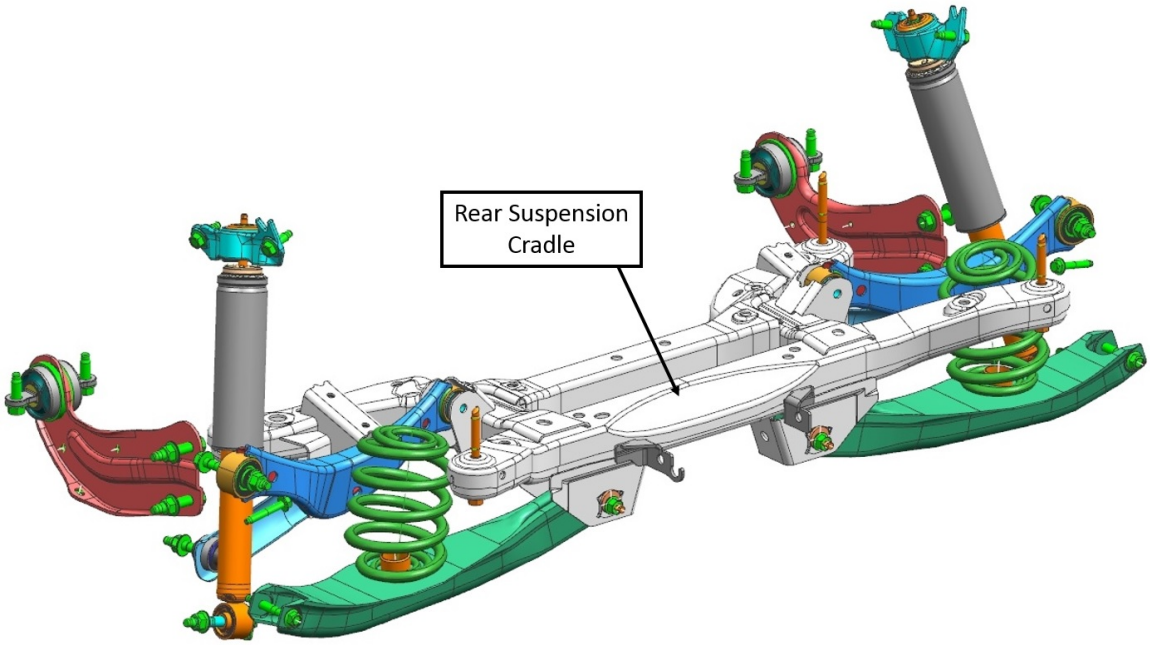

Figure 2.2. Malibu Rear suspension - Rear isometric view.

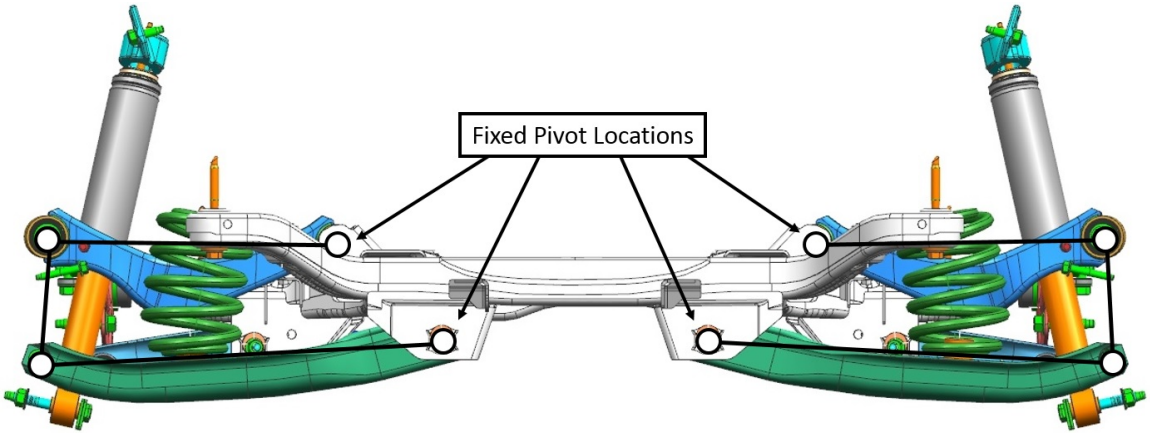

Figure 2.3. Malibu Rear suspension - Rear normal view.

2.1.1 Bushing Interference

Since the suspension systems relies on a four-bar linkage, correct motion requires specific pivot locations for the ground link. Therefore, maintaining the geometry of the ground link is critical. Figure 2.4 shows a rear-isometric view of the lower vehicle body with the motor in place. Figure 2.5 shows a rear-isometric view of the motor placement with some of the vhehicle structure removed and Figure 2.6 shows a rear-normal view of the motor placement.

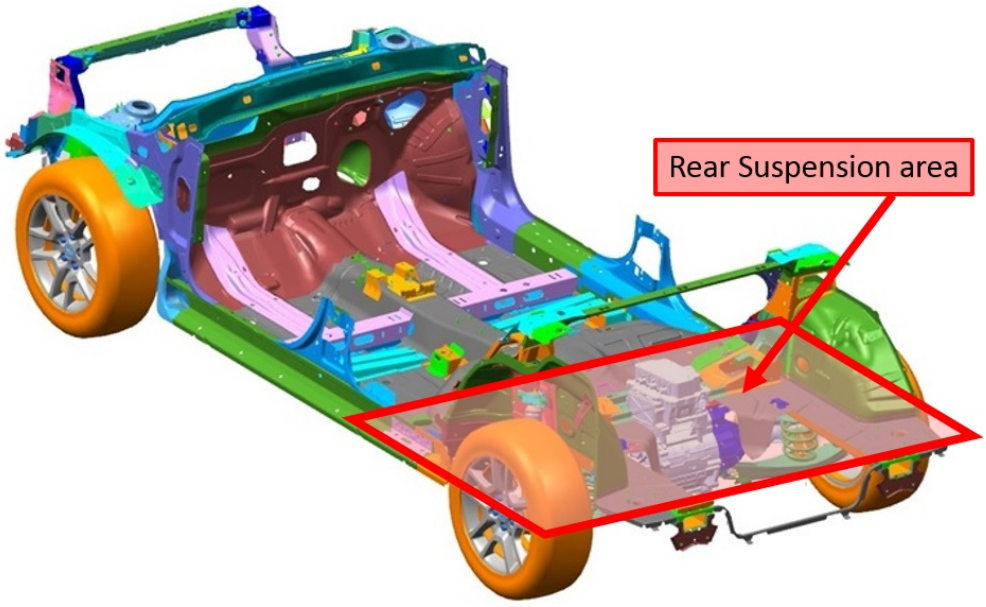

Figure 2.4. Lower Structure of Malibu with motor in place - Rear isometric view.

As can be seen in Figure 2.6, the rear traction motor interferes severely with the inboard bearing locations of the lower control arms of the suspension. Movement of these bearing locations would severely affect the geometry of the suspension linkages to the point where dynamic stability would not be ensured during vehicle operation. To avoid this interference, three options were proposed: move the motor upward, move the motor forward and change rear suspensions.

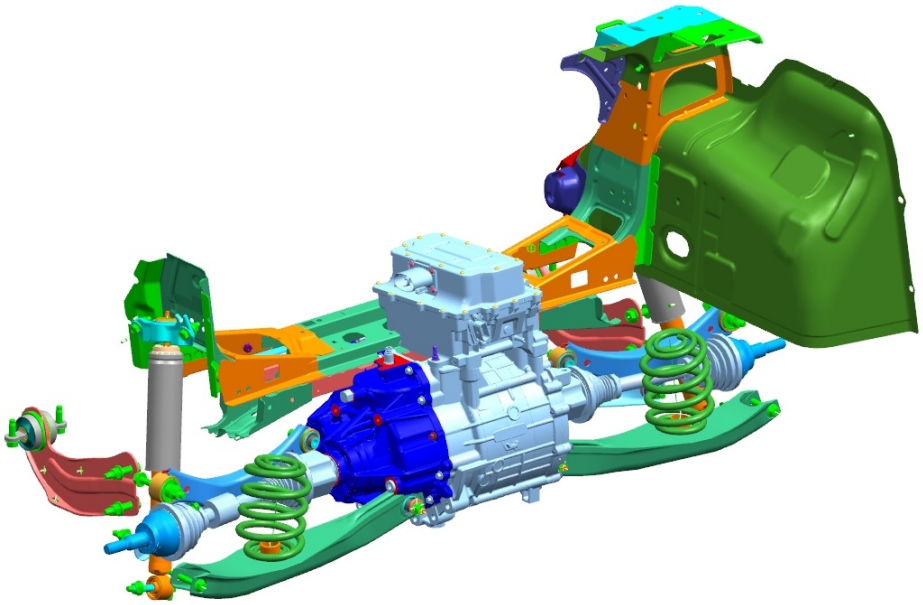

Figure 2.5. Electric motor placement within stock Malibu suspension - rear isometric view.

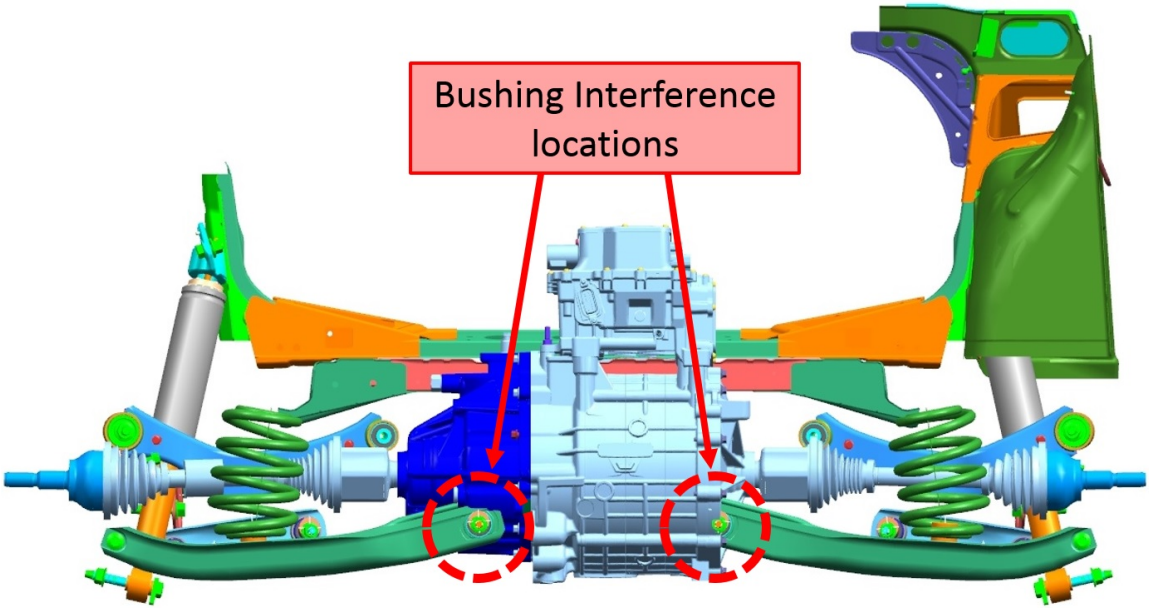

Figure 2.6. Electric motor placement within stock Malibu suspension - rear normal view.

Five Bar Interference

Within the rear suspension area of the vehicle body is a structural brace known as a "Five Bar" which is comprised of two gusset sections on each side as well as a bridge sections that connects the gussets together as shown in Figures 2.7 - 2.9.

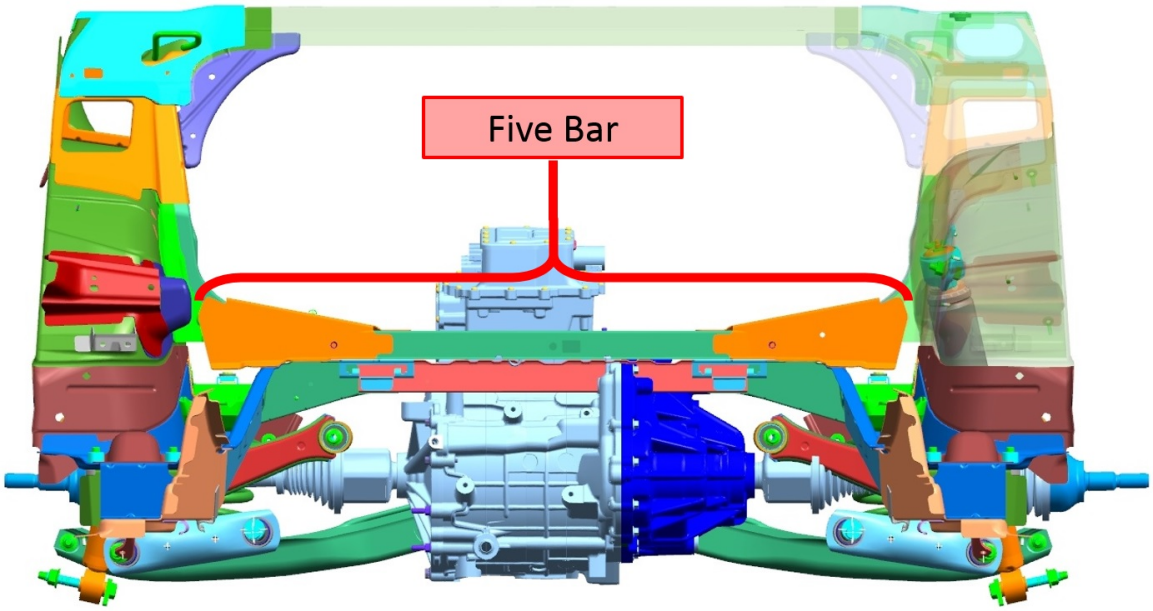

Figure 2.7. Five Bar of Vehicle Body - Front normal view.

This brace absorbs energy during collision events and is a critical safety component for the vehicle. Therefore, modification of the Five Bar required a waiver. However, only the bridge section was allowed to be modifiied. Therefore, the gusset sections were treated as an unmodifiable portion of the vehicle structure. This had implications when placing the motor since they served as spatial limitations for the motor.

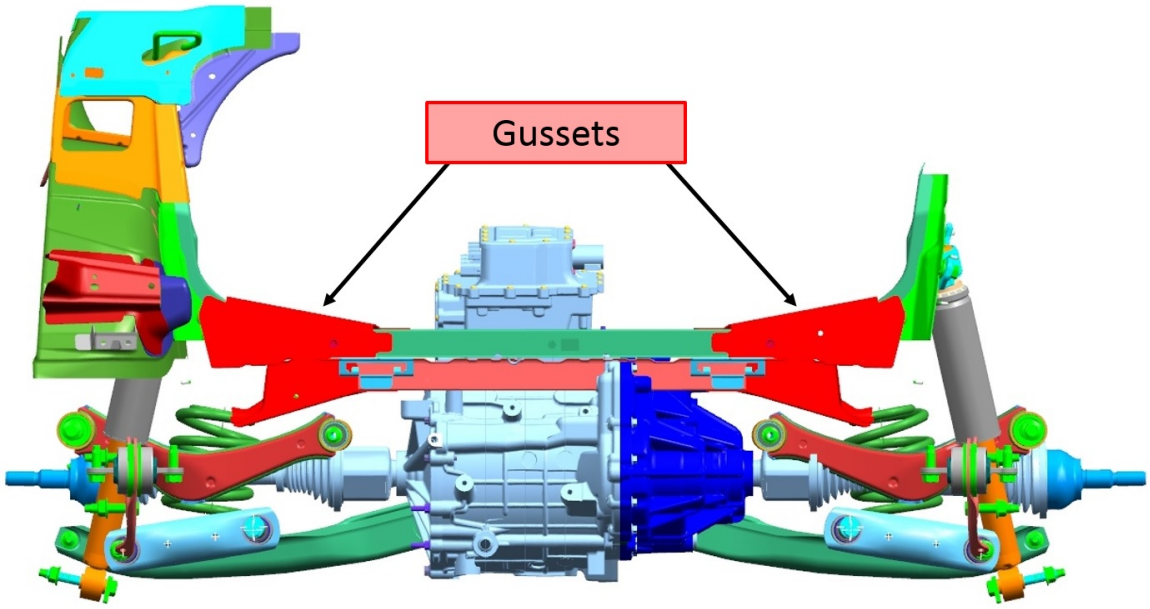

Figure 2.8. Five Bar of Vehicle Body with Gussets highlighted.

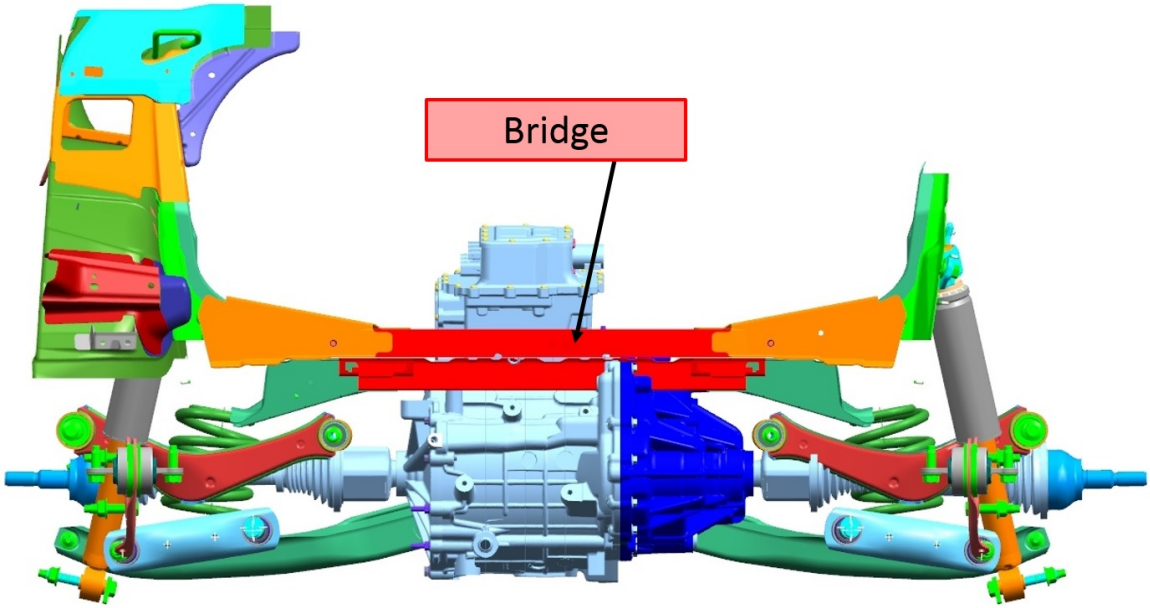

Figure 2.9. Five Bar of Vehicle Body with Bridge highlighted.

Move Motor Forward

The first option in attempting to fit the motor with the stock Malibu suspension involved moving the motor forward. However, this resulted in interference with the Five bar. Figure 2.10 shows the motor in the forward location, while Figure 2.11 shows the interference with the five bar.

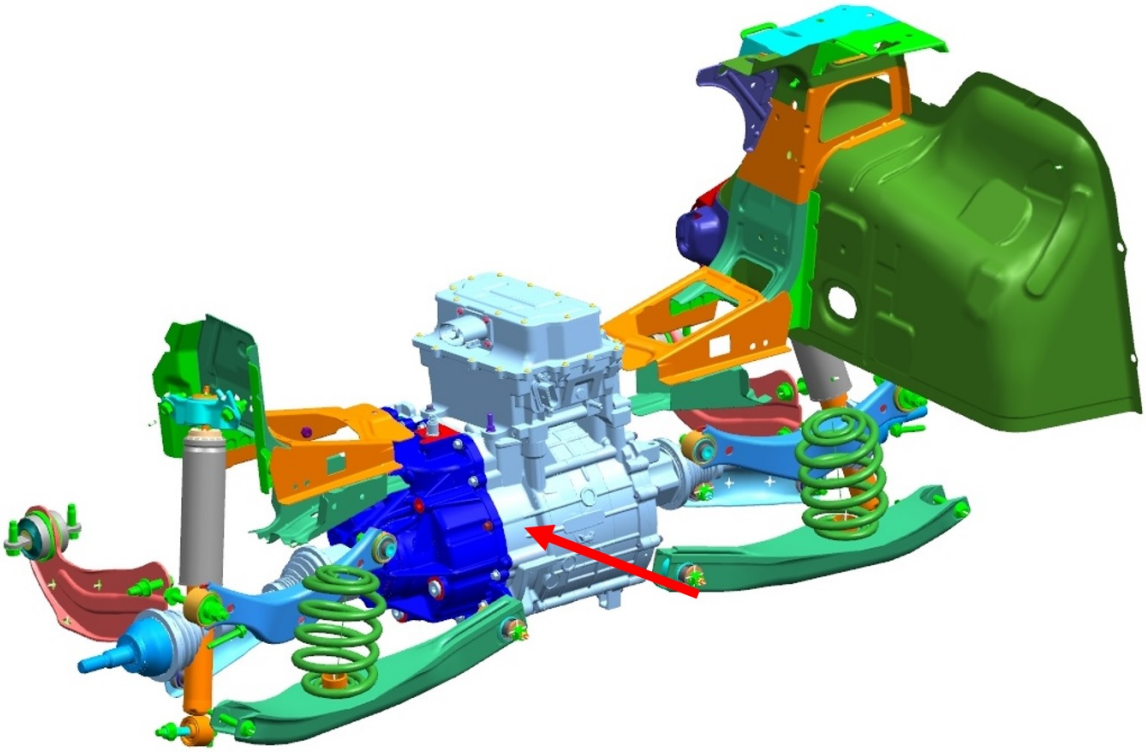

Figure 2.10. Forward motor placement within stock Malibu suspension - rear isometric view.

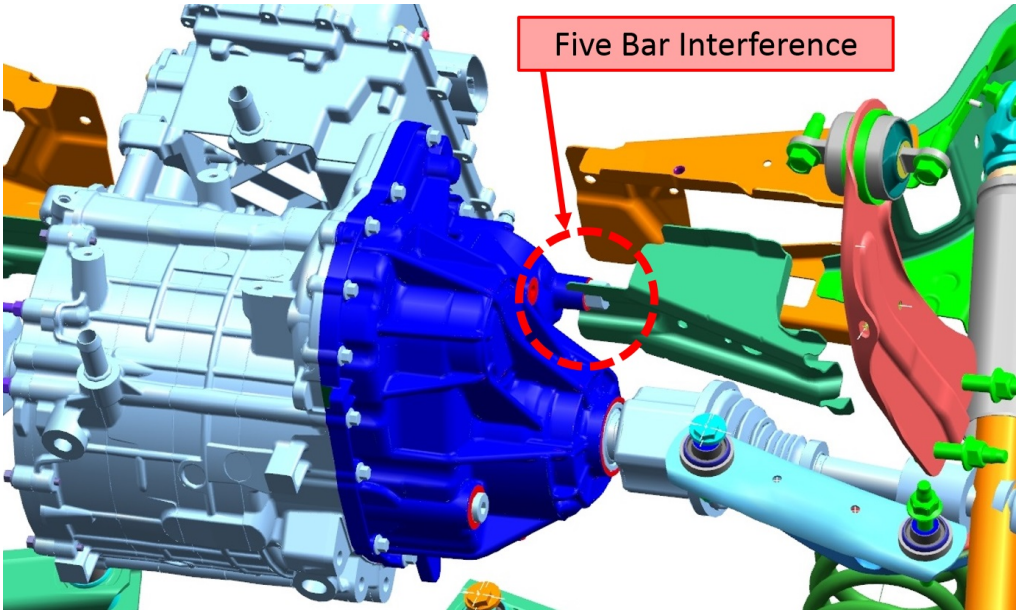

Figure 2.11. Motor interference with the Five Bar - Front isometric view.

Move Motor Upward

The second option in attempting to fit the motor with the stock Malibu suspension involved moving the motor upward. However, this also resulted in interference with the Five bar. Figure 2.12 shows the motor in the forward location, while Figure 2.13 shows the interference with the five bar. Figure 2.14 shows the interference with the five bar while highlighting the significant amount of Five Bar material (outlined in red) that would interefere with the motor.

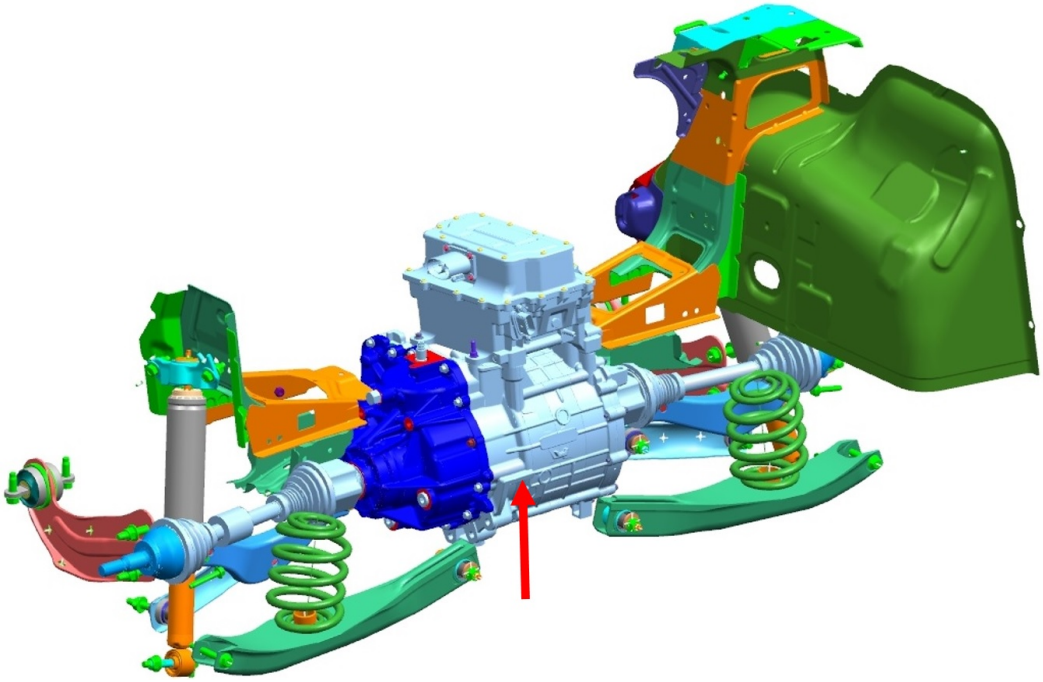

Figure 2.12. Upward motor placement within stock Malibu suspension - rear isometric view.

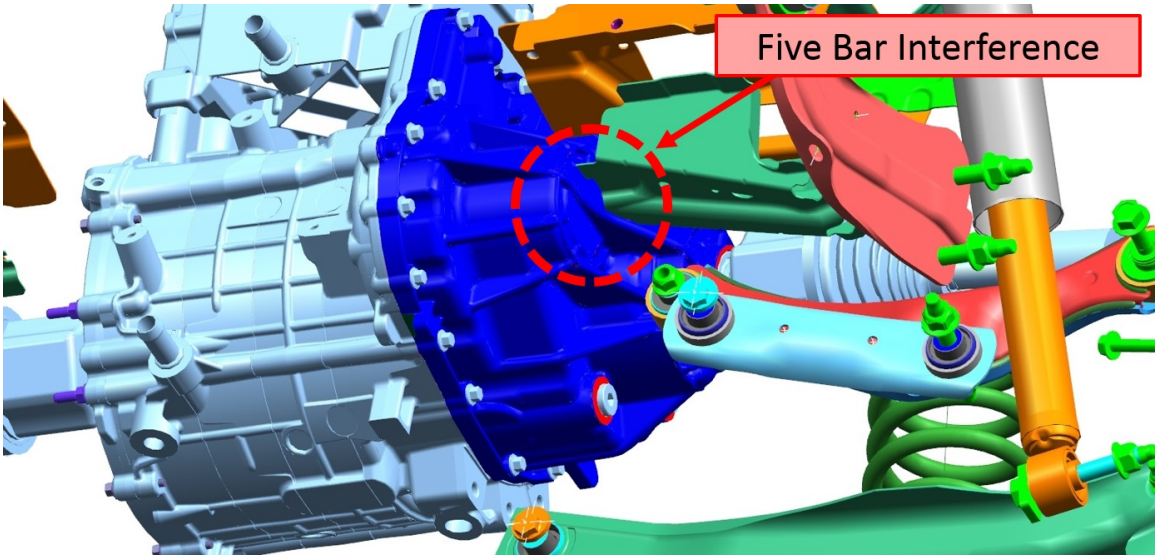

Figure 2.13. Motor interference with the Five Bar - Front isometric view.

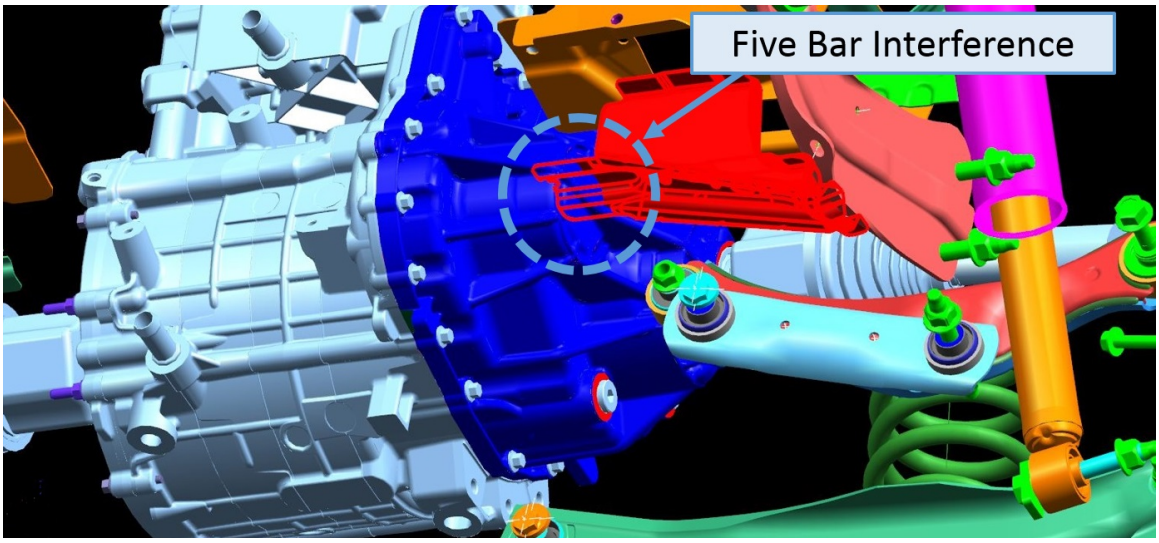

Figure 2.14. Motor interference with the Five Bar - Front isometric view.

2.1.2 Buick AWD Suspension

Since the Mailbu suspension would not fit the motor, the rear suspension from a 2013 Buick Lacrosse was used. Since the 2013 LaCrosse is available as an All-Wheel-Drive (AWD) vehicle, the linkages of the rear suspension are capable of allowing a rear differential to be placed in-between the inboard bearings of the suspension control arms. Additionally, since the Buick Lacrosse and the Chevrolet Malibu are both built using the GM epsilon format, the suspensions were compatible with both vehicles. Shown below is an image of the LaCrosse linkages in relation to the desired placement of the rear traction motor.

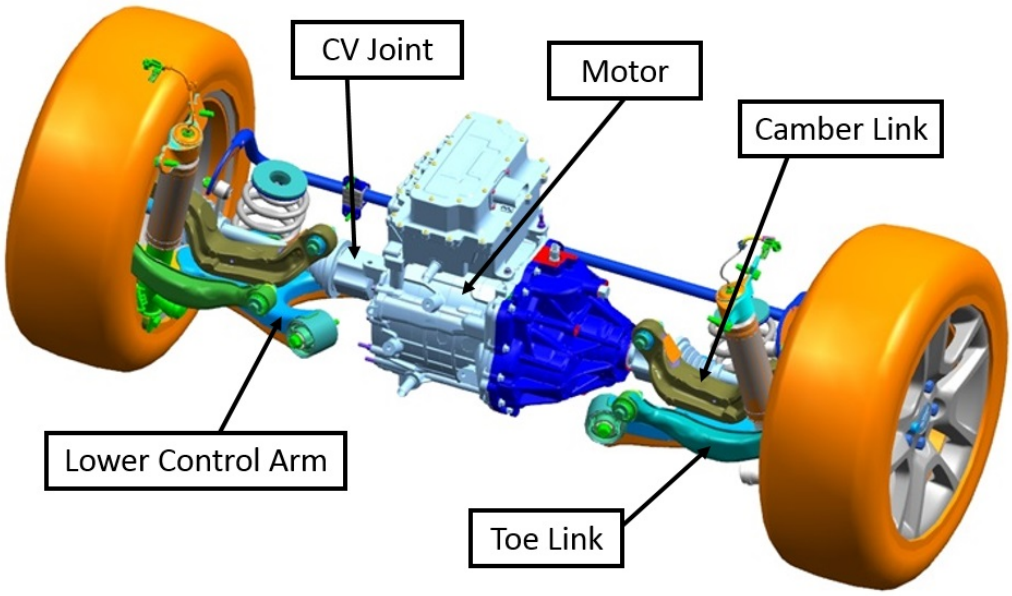

Figure 2.15. Buick LaCrosse AWD rear suspension with motor in place - front isometric view.

During the initial design stages, it was assumed that if the motor were placed with its axle collinear with the axle of the LaCrosse suspension, a set of drive shafts may be made for usage by the motor which would not interfere with the linkages of the LaCrosse, given that the drive shafts would perform similarly to those of the AWD

LaCrosse suspension. Although the suspension links would not interfere with the rear traction motor, the rear suspension cradle would greatly interfere if used.

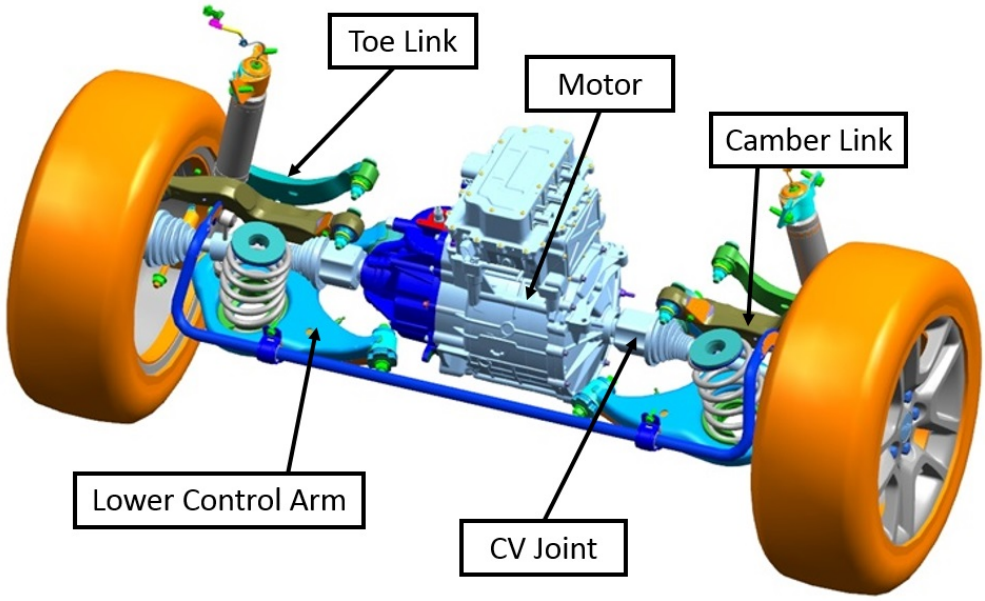

Figure 2.16. Buick LaCrosse AWD rear suspension with motor in place - rear view.

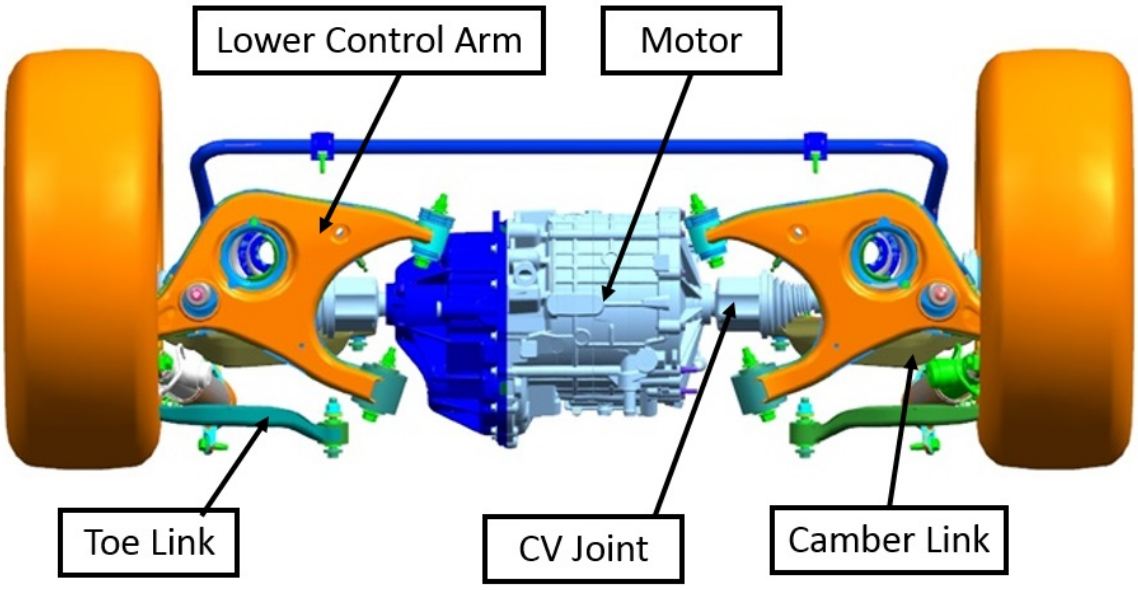

Figure 2.17. BareBones view of Buick LaCrosse AWD rear suspension with motor in place - bottom view.

2.1.3 Stock Cradle Interference

Shown in Figure 2.18 is the rear suspension linkages, cradle and rear traction motor when placed together in one assembly.

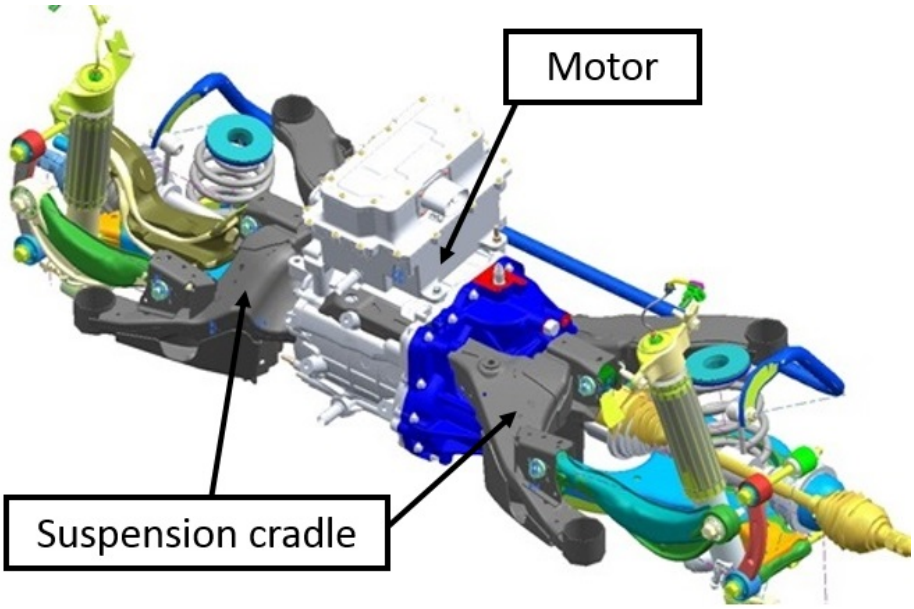

Figure 2.18. Complete Buick LaCrosse AWD rear suspension with motor in place.

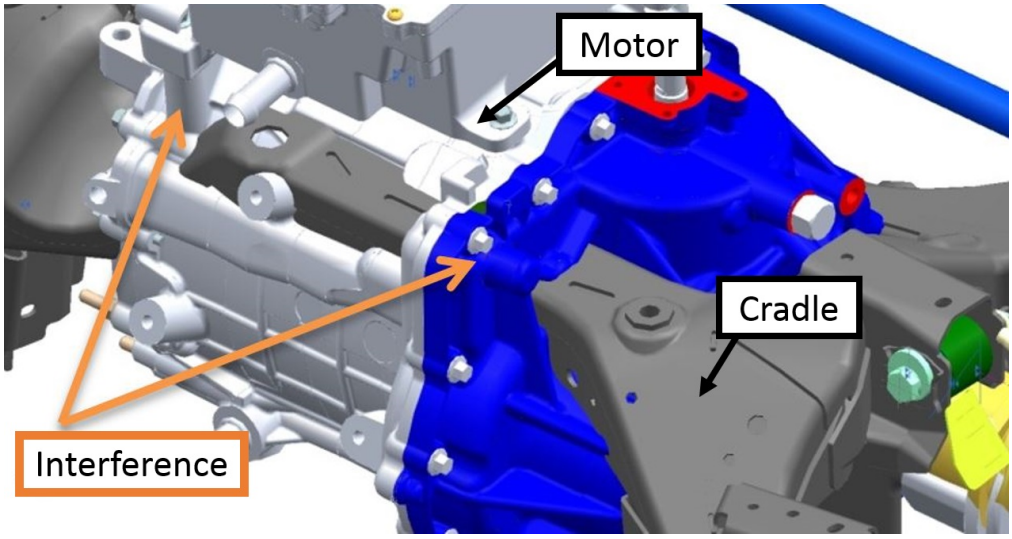

Figure 2.19. Stock cradle interference - Front view.

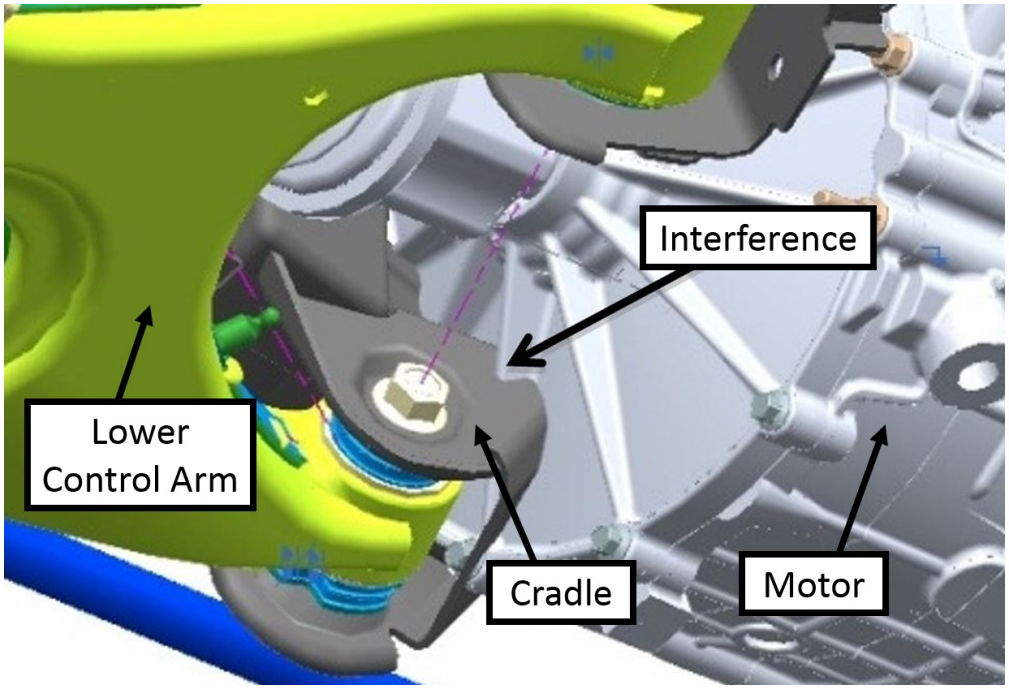

Figure 2.20. Stock cradle interference - Bottom right side of vehicle.

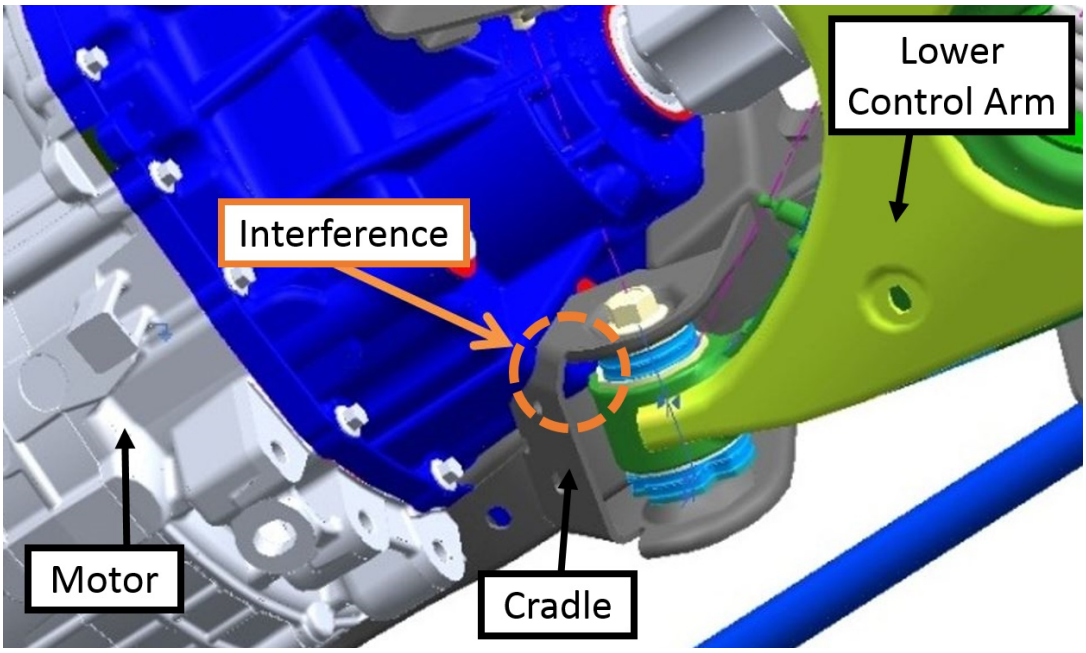

Figure 2.21. Stock cradle interference - Bottom left side of vehicle.

As can be seen in Figures 2.18 - 2.21, there were severe interferences between the motor and the AWD suspension cradle. However, since this was the desired position of the rear traction motor, it was required that the Purdue EcoMakers create a custom suspension cradle that would safely hold the motor in place and maintain the inboard bearing locations of the rear suspension links. As described by the NYSR, it was necessary that any custom component installed on the vehicle have a Factor of Safety (FOS = Yield Stress / Max Stress) greater than or equal to 2 when compared to the stock component (ie: Custom Component FOS/ Stock Component FOS). Additionally, it was required by GM that the custom suspension cradle use the same four chassis mounting locations as the stock suspension cradle.

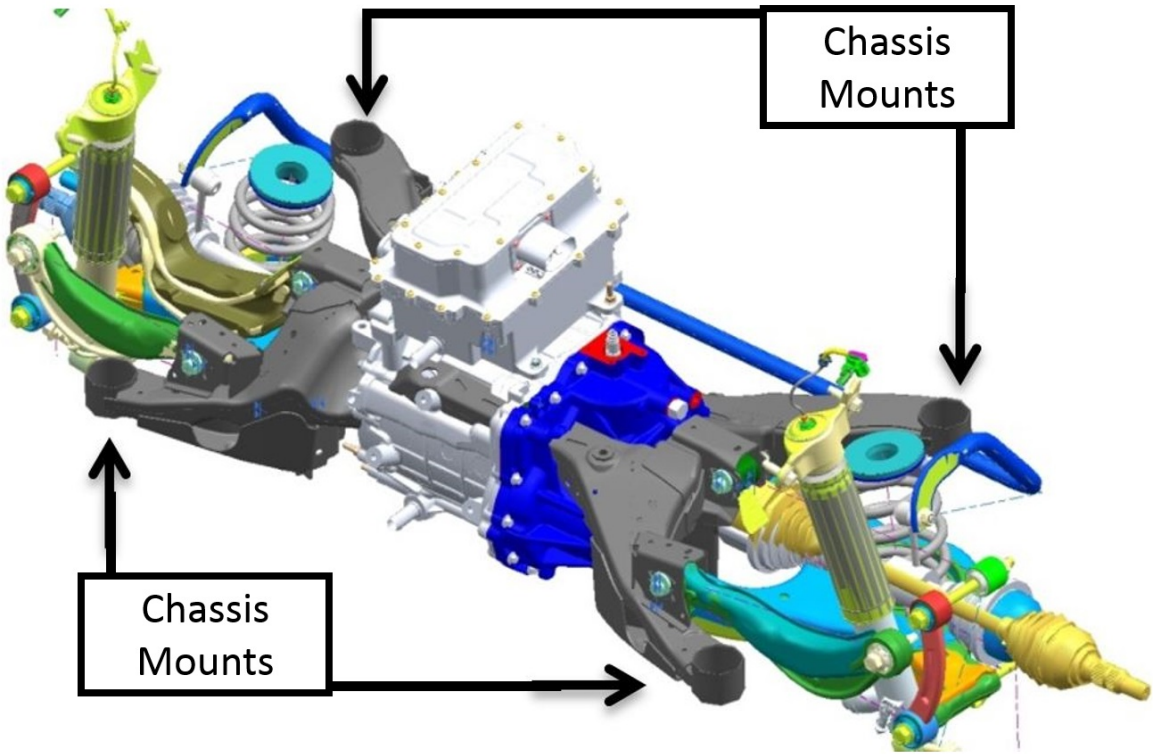

Figure 2.22. Chassis mount locations of Rear Cradle.

Overall, it can be seen that the packaging constraints determined by the NYSR of the competition caused the Purdue EcoMakers to decide to design, analyze, fabricate

and install a custom rear suspension cradle which would also hold the mounting locations of the rear traction motor. Figures 2.23 - 2.25 depict the mounting locations of the Magna E-Drive.

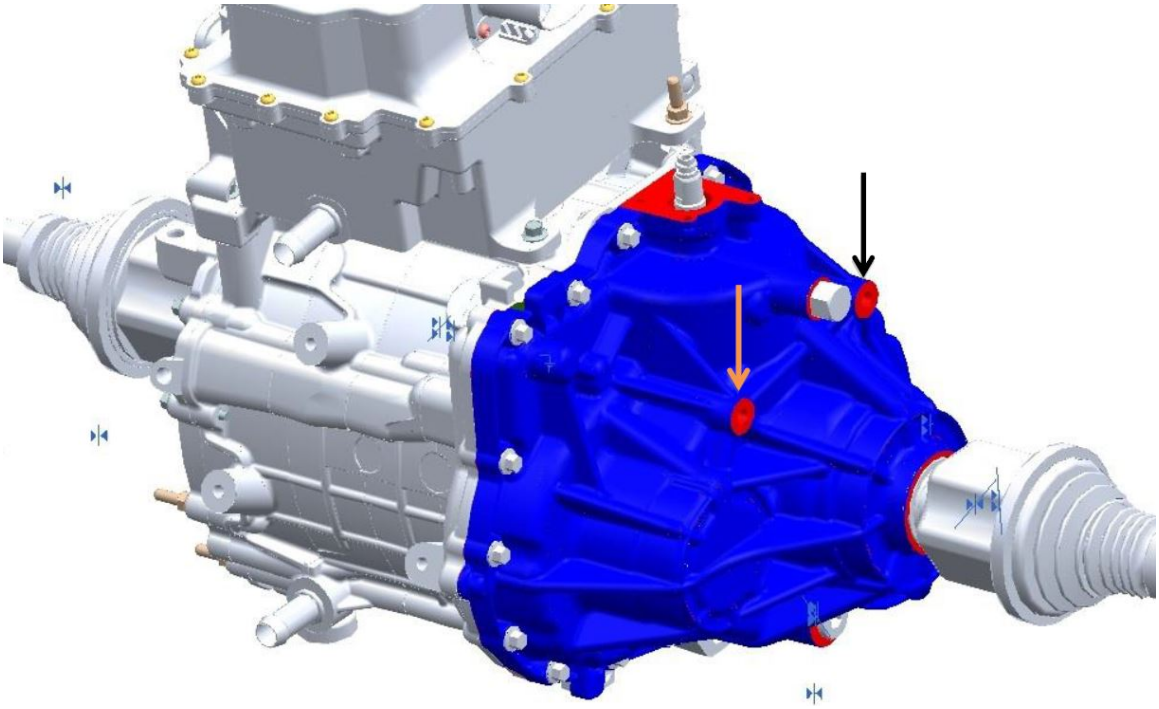

Figure 2.23. Driver's Side Mounting Points on Magna E-Drive.

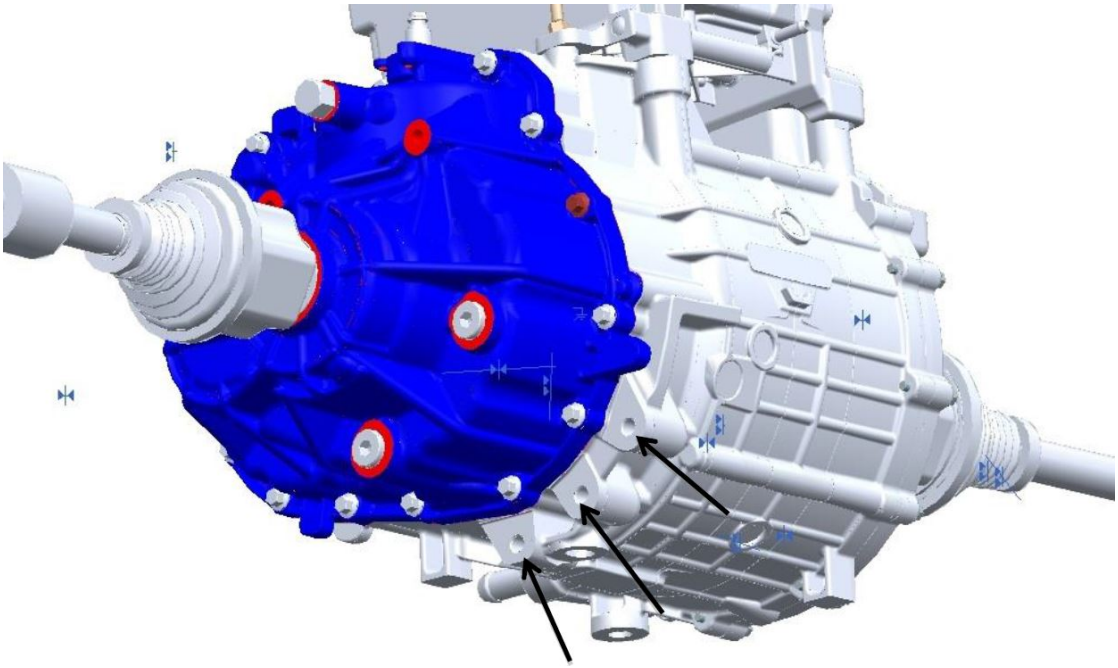

Figure 2.24. Torsion-Resistanct Driver's Side Mounting Points.

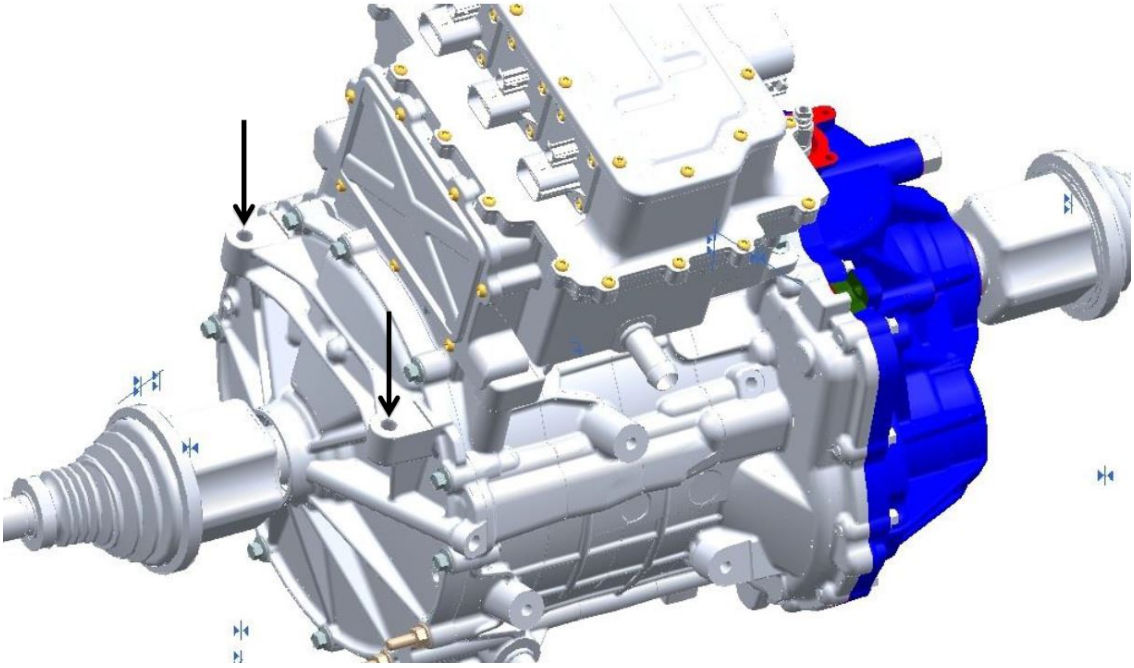

Figure 2.25. Passenger's Side Mounting Points on Magna E-Drive.

2.2 Custom Rear Suspension Cradle.

2.2.1 Design

The proposed modification was an entirely custom-made steel structure which located all inboard bearings of the rear suspension linkages while also supporting the rear traction motor without interference. Additionally, during the design procedure, the routing path of the exhaust pipe was mentioned frequently. Due to the movement of the rear suspension control arms, and the substantial volume occupied by the rear motor there was very little available cross sectional area to allow an exhaust pipe to pass through.

However, there was a gap on the passenger side between the motor and the inner bearing of the upper camber link that was capable of allowing an exhaust tube to pass through, as long as it passed over the inboard CV joint of the half shaft used by the motor. Therefore, this gap was needed as an exhaust pass-through as shown in Figure 2.26. One design criterion was to have adequate room to allow an exhaust pipe with ample air cushion to pass through. After consultation, it was determined by the Purdue team that a 2in OD exhaust tubing would be used which required a 0.5in air cushion around it for proper heat dissipation. Therefore, a 3in OD tubing representation was using during CAD design to represent the size requirement of the exhaust. Shown below is the stock 2013 LaCrosse cradle compared to the proposed custom cradle of the Purdue EcoMakers.

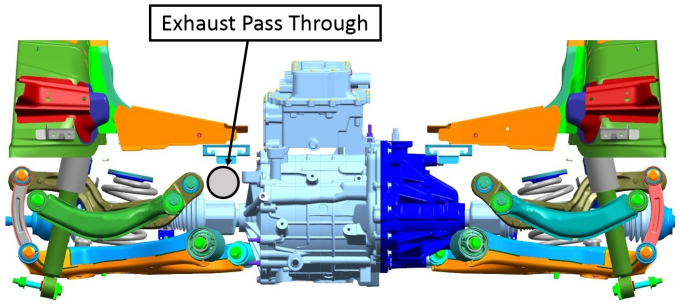

Figure 2.26. Exhaust Pass-Through Clearance.

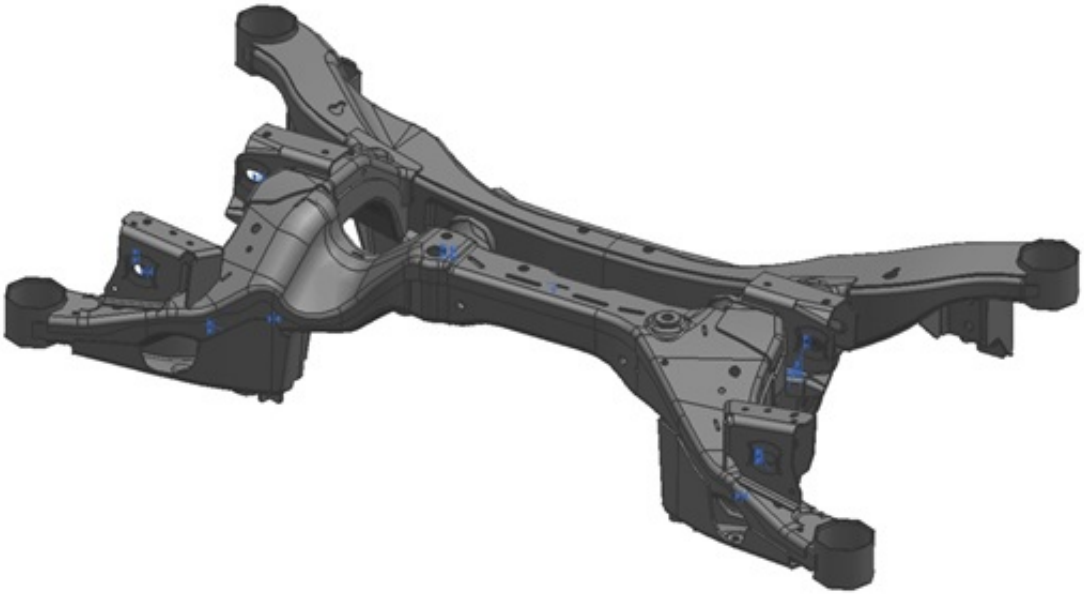

Figure 2.27. Stock 2013 Buick LaCrosse AWD rear suspension cradle.

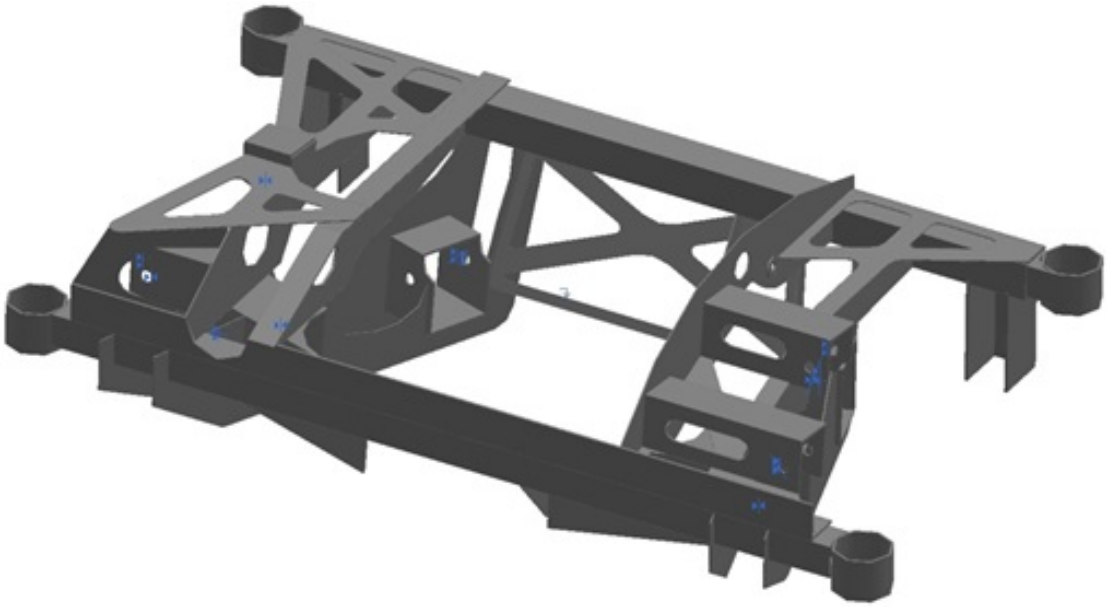

Figure 2.28. Custom Purdue rear suspension cradle.

The basis for the structure relies on two square-profile steel tubes which bridge the gap between the chassis mounts of the vehicle.

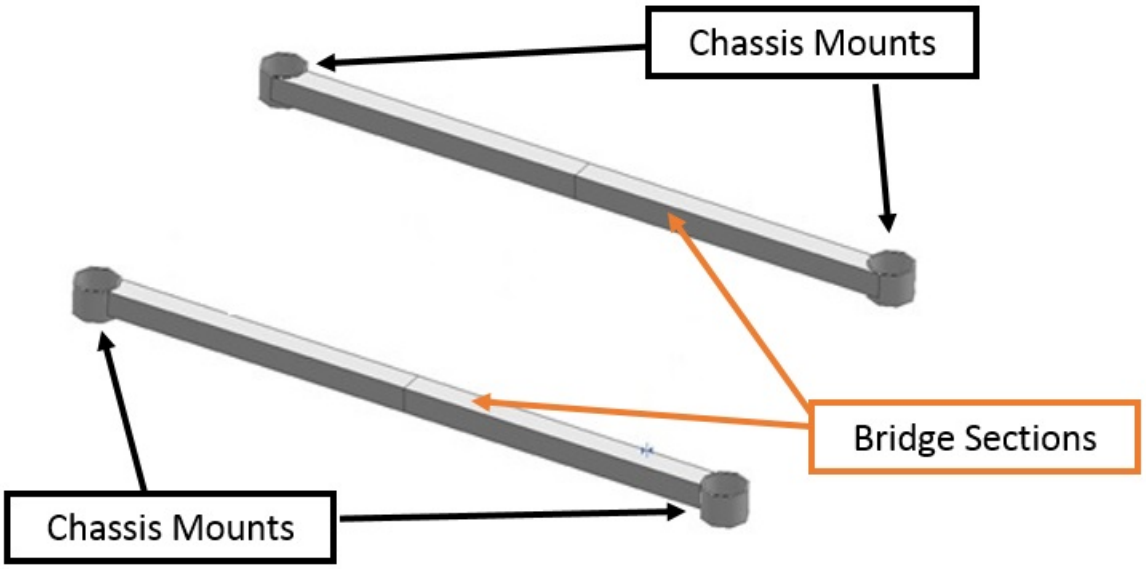

Figure 2.29. Bridge Components of custom cradle.

In the proposed design, there are rigid metal components which entirely encompass the motor. Therefore, if the proposed cradle consisted entirely of welded metal components, it would be impossible to remove the motor without undoing irreversible welds of the assembly during fabrication. With this in mind, it was desirable that the assembly consist of two or more rigid sections to be connected by reversible connection techniques. Therefore, it was decided that the proposed structure consist of an upper shell and a lower shell, both of which were rigid, welded assemblies. As the two sections connect to each other, they were bolted together to ensure that the connections may be undone in the case that the motor needed to be removed from the sub-frame. Shown below is the lower section of the structure which hold the bearings for the lower control arms as well as the torque-resist mount of the motor.

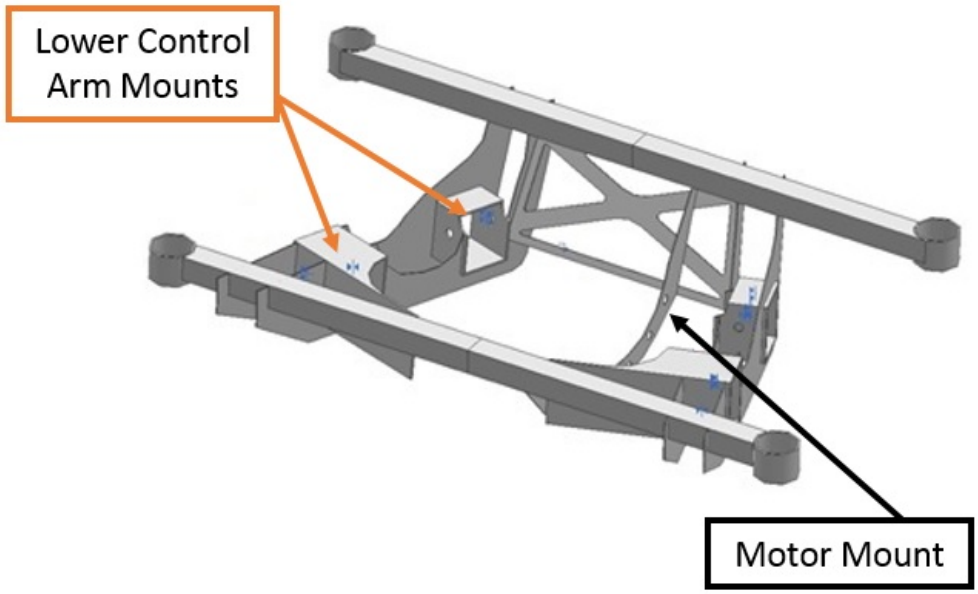

Figure 2.30. Front-Driver's view of lower portion.

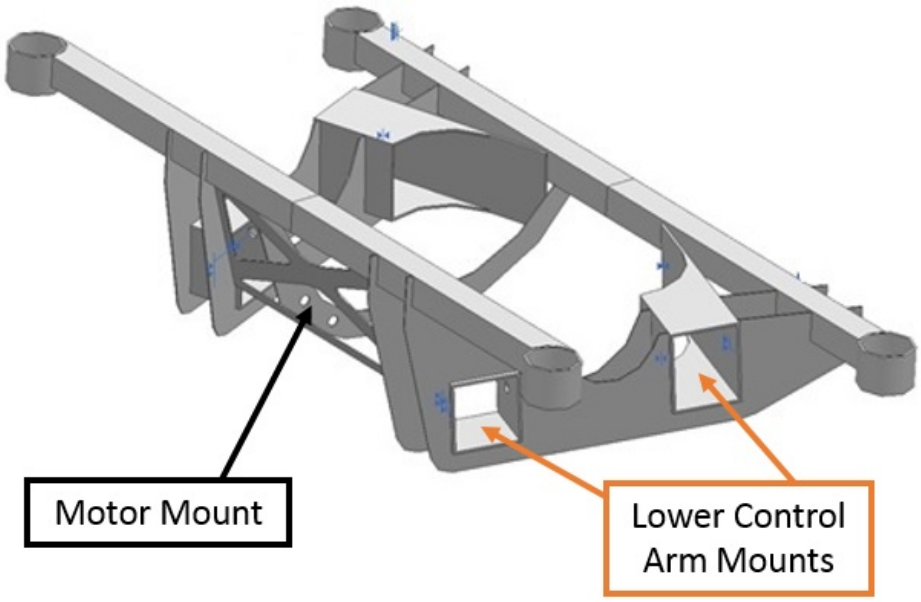

Figure 2.31. Rear-Passenger view of lower portion.

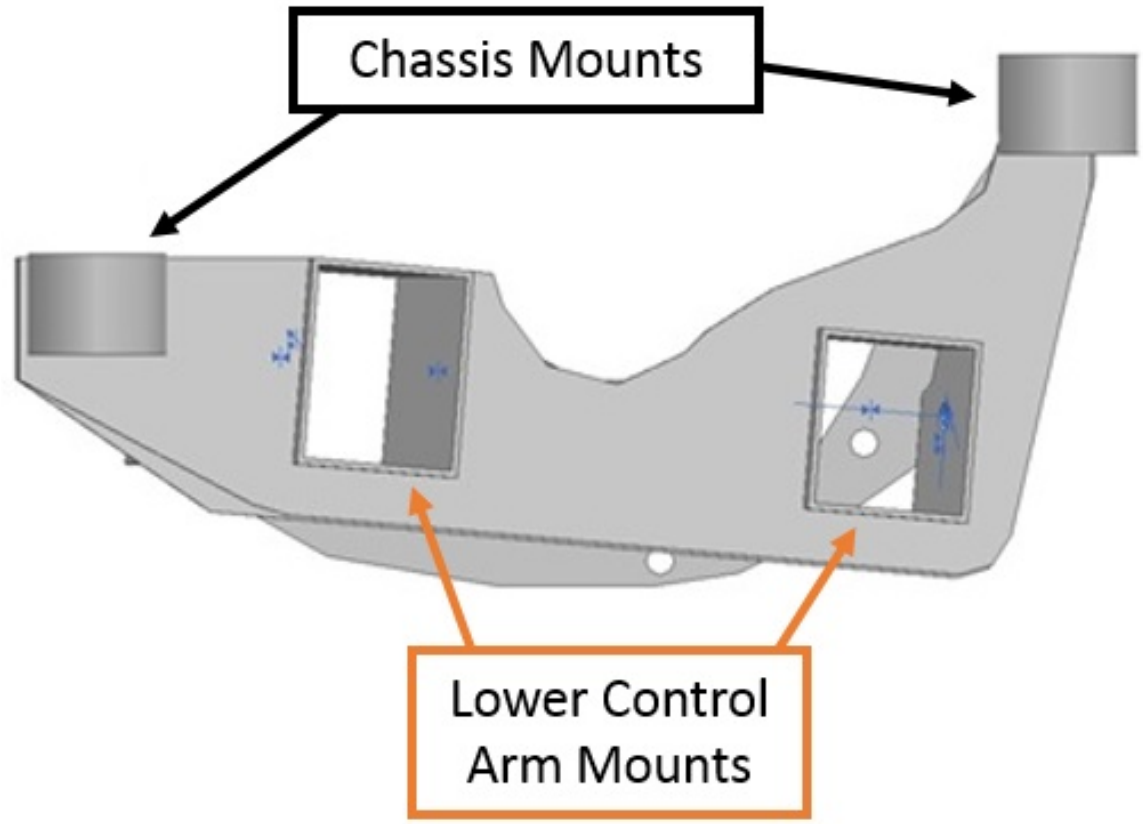

Figure 2.32. Driver's side profile of lower portion.

In order to ensure proper alignment of the suspension bearings, it was decided that the planes of metal be cut using a water-jet to ensure accuracy and precision. In order to ensure proper placement of each plane upon the square tube bridge sections, it was decided that a precision end-mill be used to mark the locations upon the square tubing where the planes are desired to sit. Therefore, the square tube sections which held the bearings of the lower control arms fit neatly into the recesses of the planes which connected between the square tube bridge sections.

Since the upper faces of the square tubing being used as bridge sections were left untouched, it was decided that the upper section of the custom sub frame should be able to sit flush upon these faces. Therefore, angle steel sat upon the square tubing of the lower section and served as fixture locations for all components of the upper

structure. Shown in Figure 2.33 is a depiction of how the angles sat upon the square tubes.

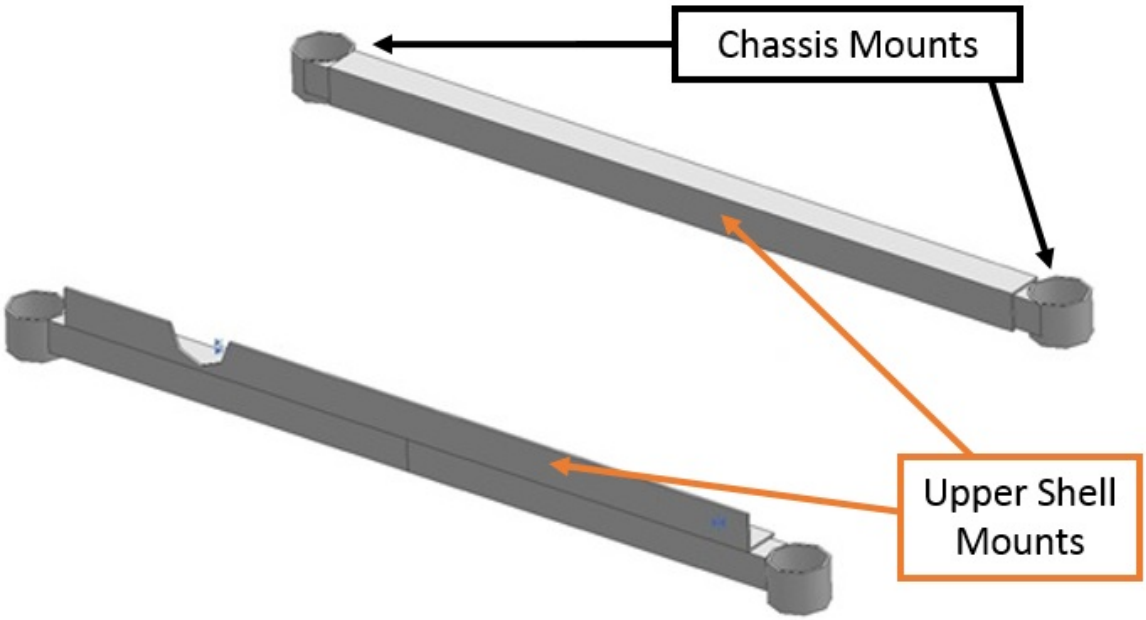

Figure 2.33. Angle rods placed flush upon square tubing.

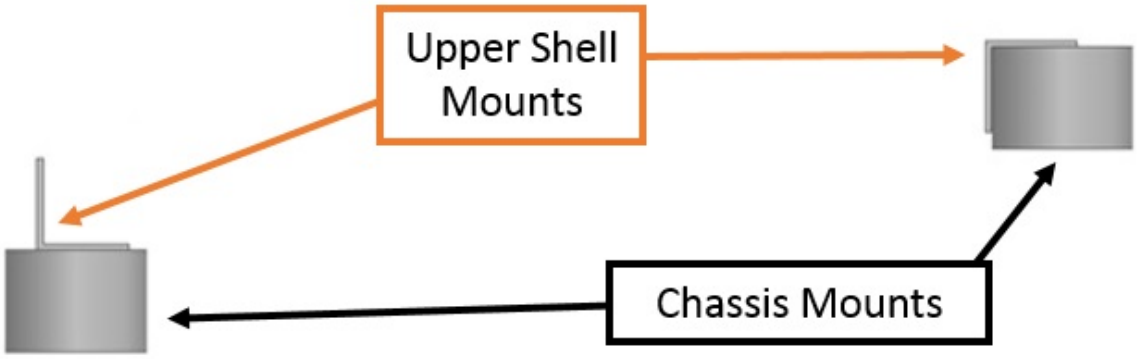

Figure 2.34. Side view of angle rods placed flush upon square tubing.

Once new permanent-fixture points were designated for the upper structure, it was possible to weld new elements to the cradle. Shown in Figures 2.35 - 2.37 is the upper section of the cradle which held the bearing locations for both upper camber links, both toe links, and four upper mounting locations of the rear traction motor.

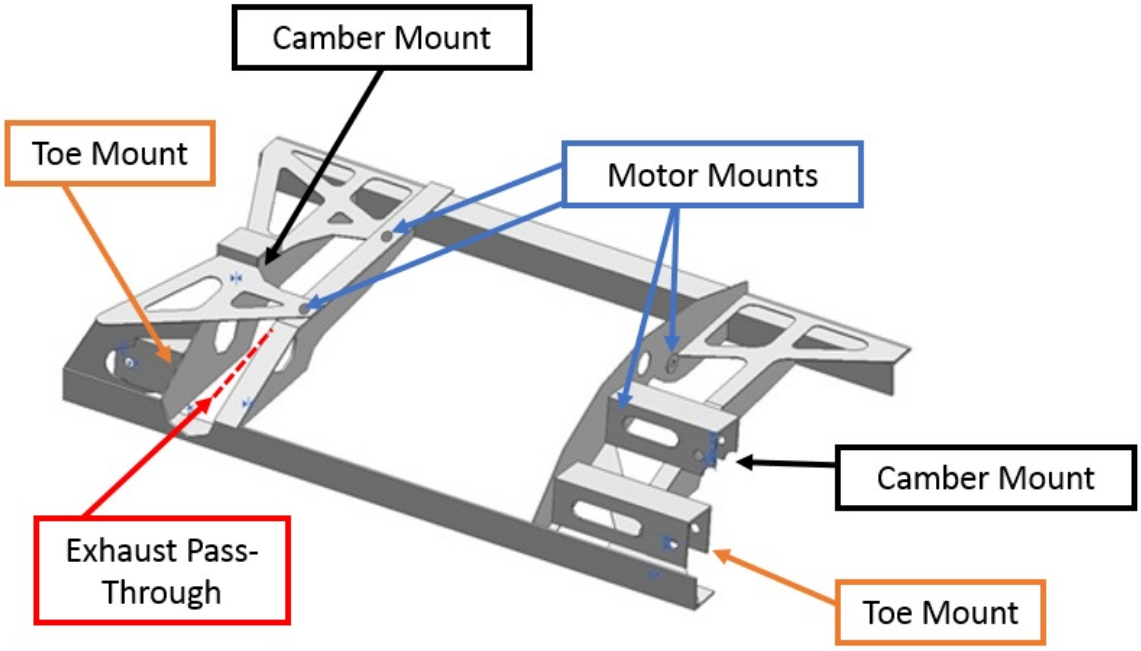

Figure 2.35. Front-Driver's side view of upper portion.

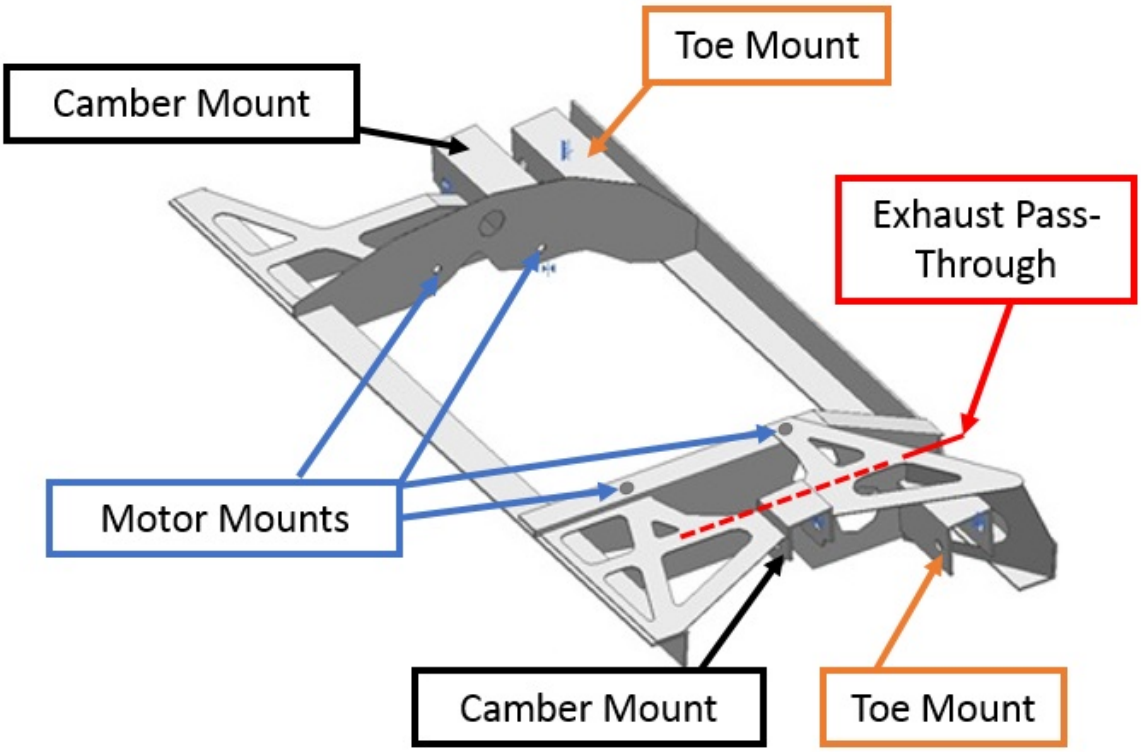

Figure 2.36. Rear-Passenger perspective of upper portion.

Shown in Figures 2.38 - 2.42 are images of the comprehensive cradle design after the upper and lower halves are bolted together.

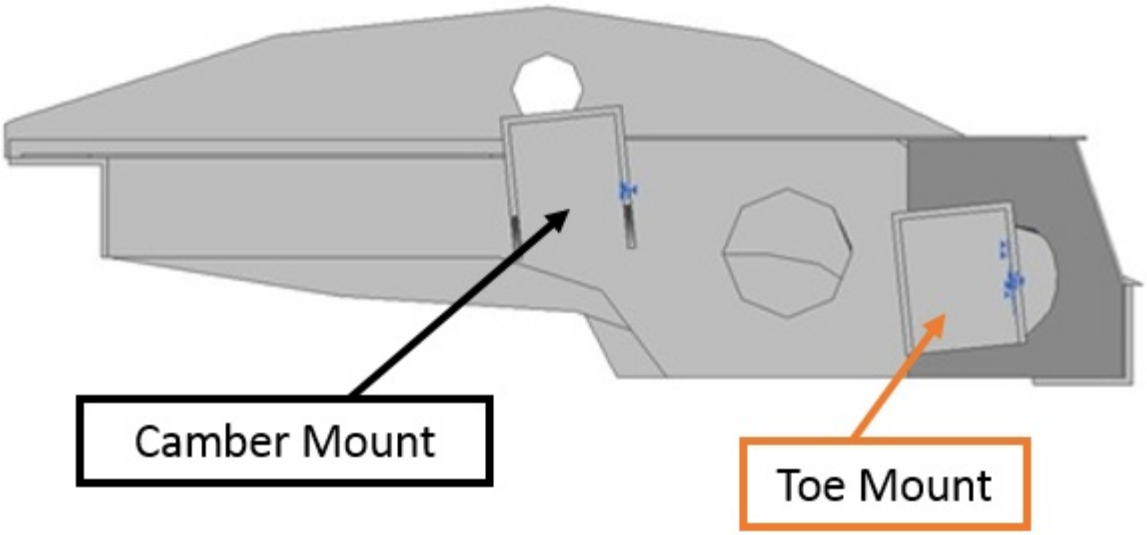

Figure 2.37. Passenger profile view of upper section.

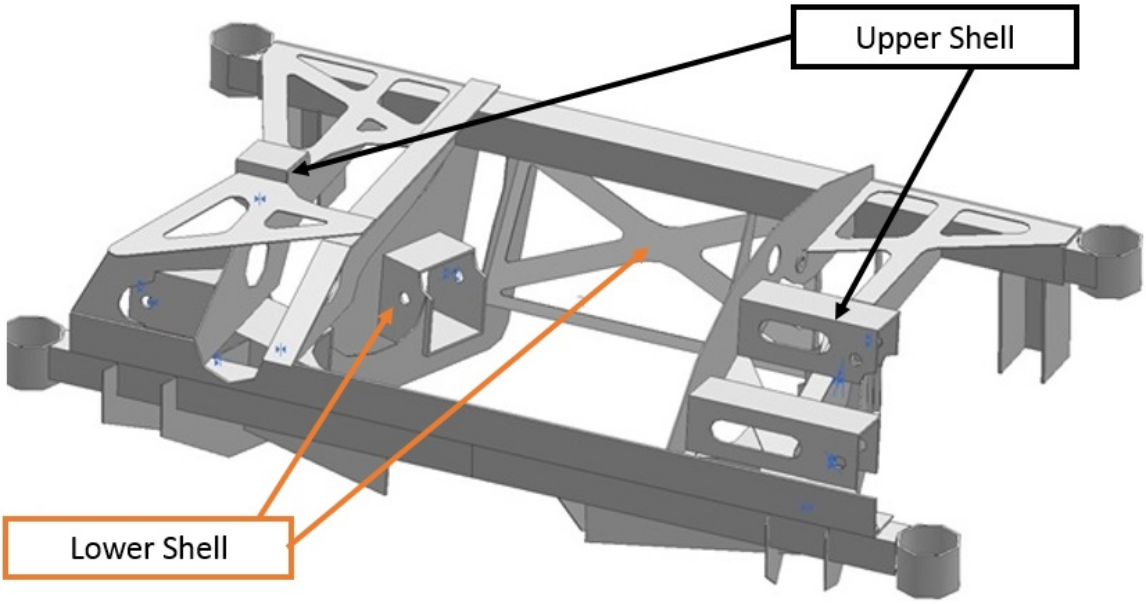

Figure 2.38. Proposed custom cradle design.

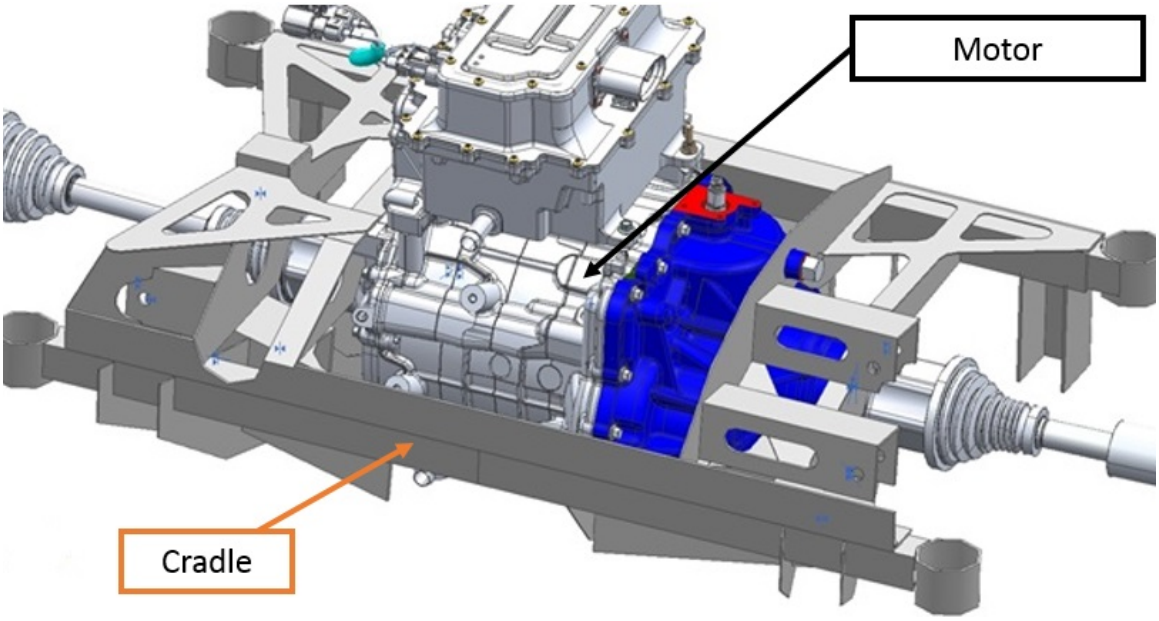

Figure 2.39. Custom cradle with motor and drive shafts.

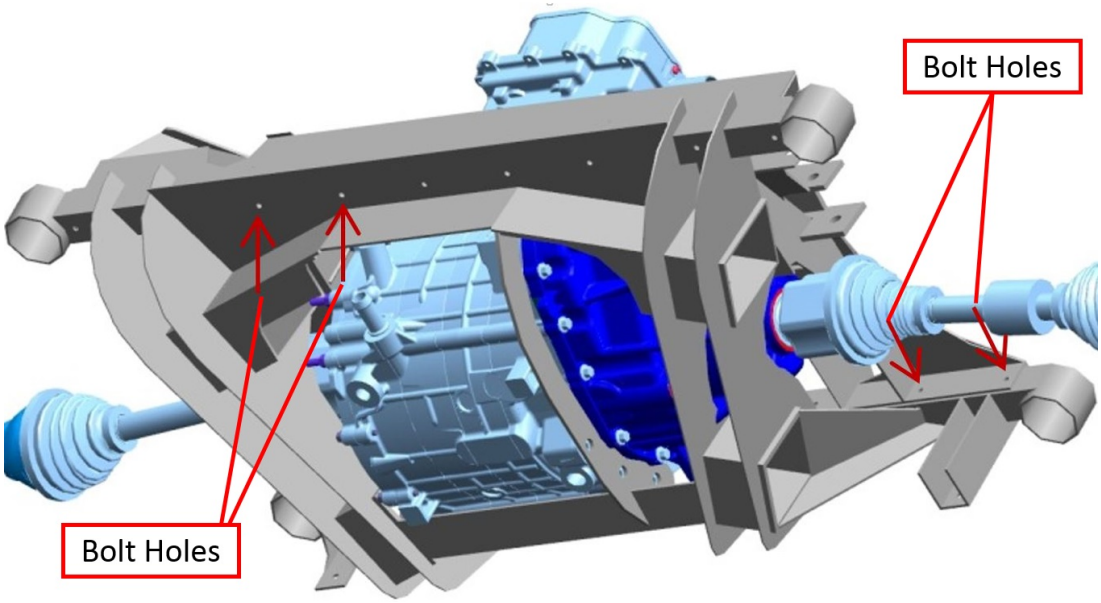

Figure 2.40. Underside view of assembly emphasizing bolt holes to attach two halves together.

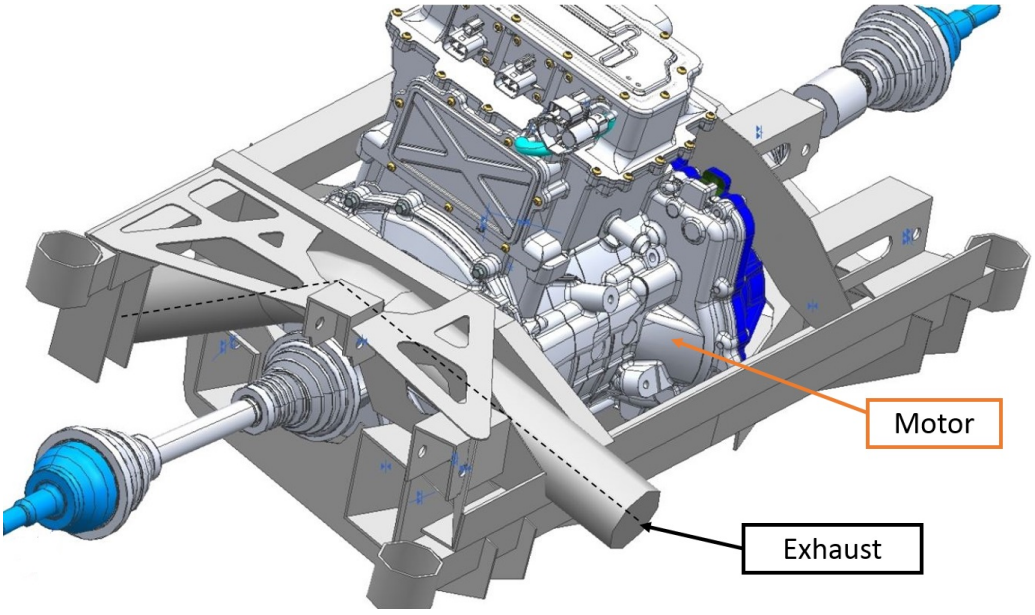

Figure 2.41. Custom sub-frame with motor and representation of exhaust with surrounding air cushion.

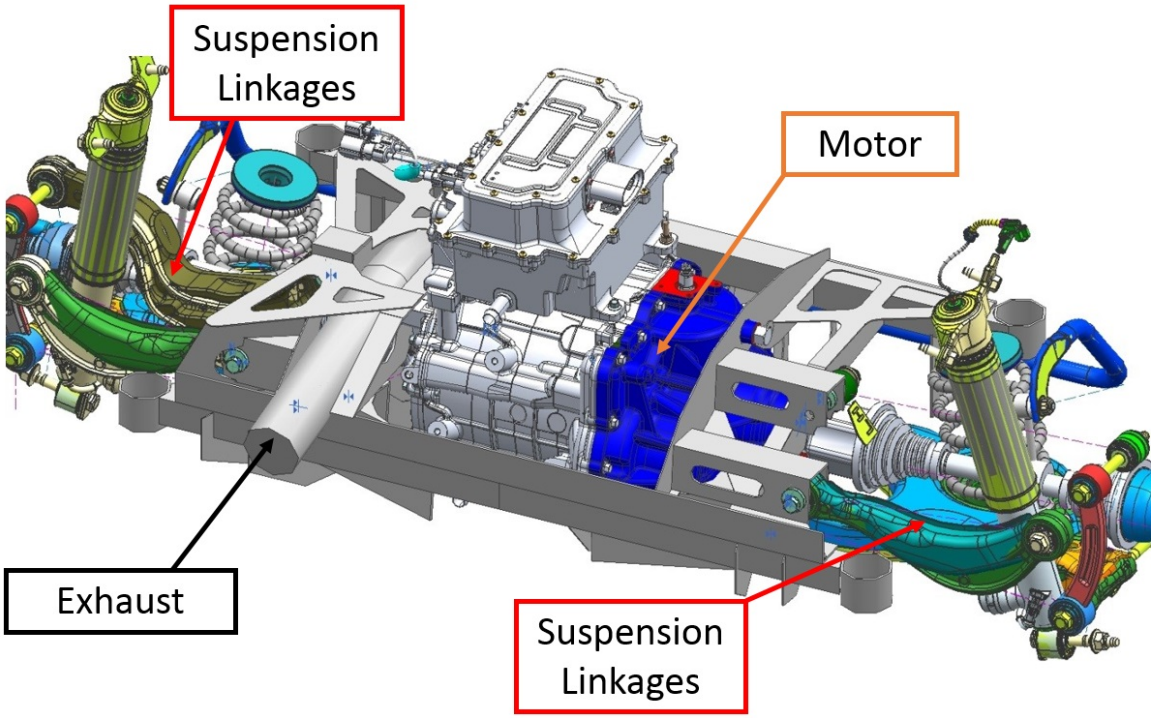

Figure 2.42. Front-passenger side view of assembly.

Figures 2.43 and 2.44 depict the custom cradle design after fabrication and assembly. As can be seen, it successfully held the rear traction motor and suspension bearings in place.

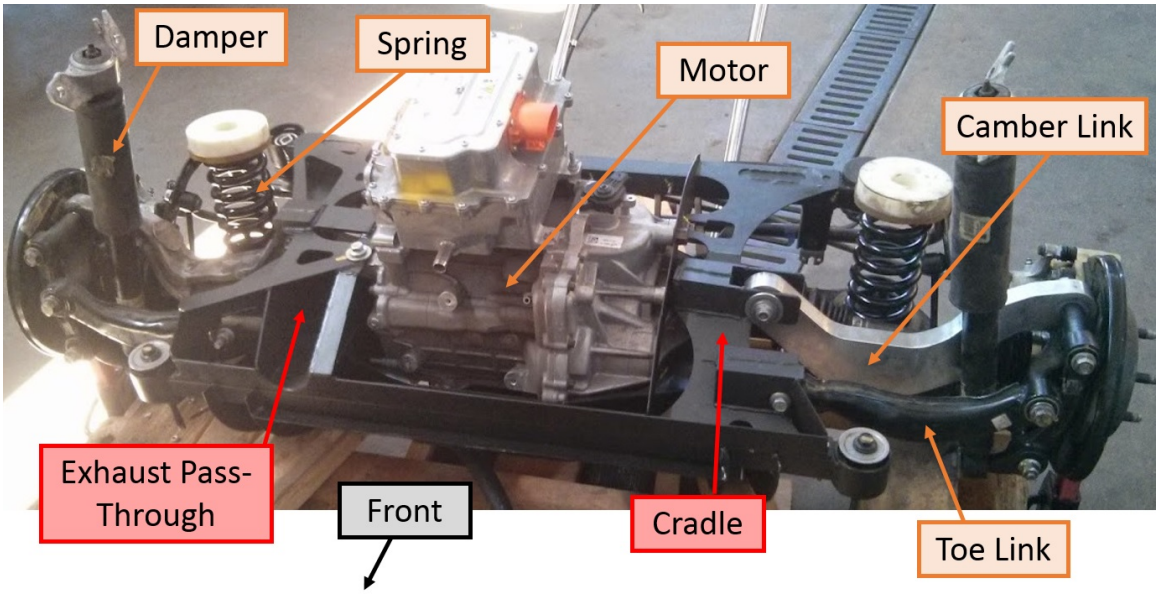

Figure 2.43. Front view of rear suspension assembly after fabrication.

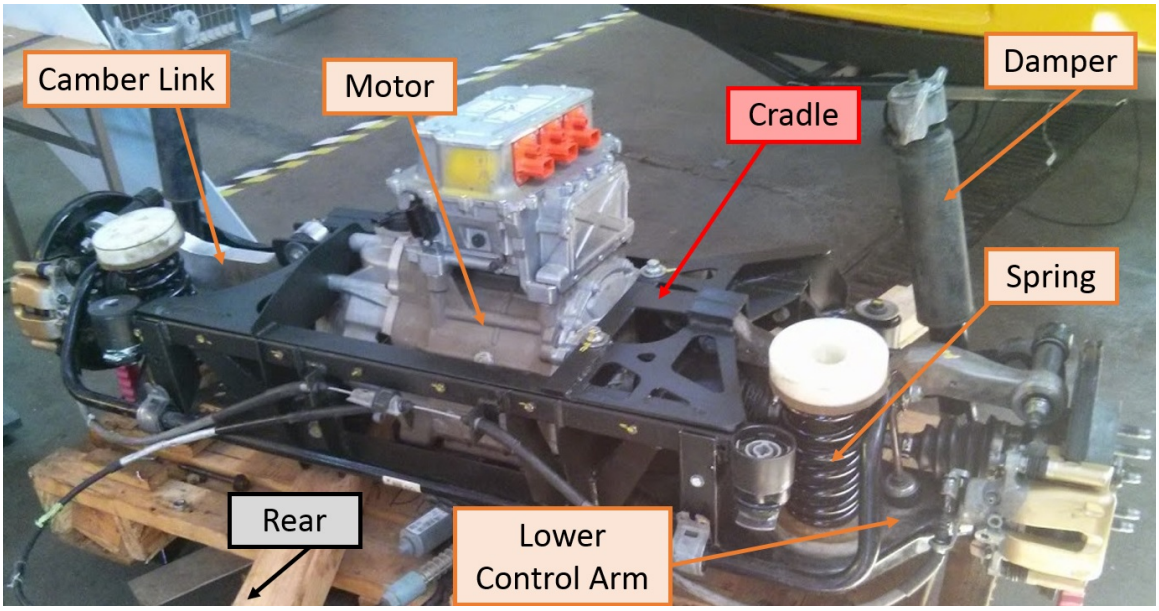

Figure 2.44. Rear view of rear suspension assembly after fabrication.

Direct Load Paths

When designing rigid support structures, it is very efficient to add material along direct pathways between load locations and ground locations. The goal of such a technique is to transform each pathway into a member of the structure that will experience direct compression or tension in order to maximize structural efficiency. Additionally, it was determined that the outer metal casing of the electric motor may be used as a lumped, rigid mass capable of transferring load between members of the custom cradle. Shown in Figure 2.45 are the theoretically desired pathways between the chassis mounting locations and the upper mounting locations of the motor. It was the intention of the cradle design to add material as close to these pathways as possible.

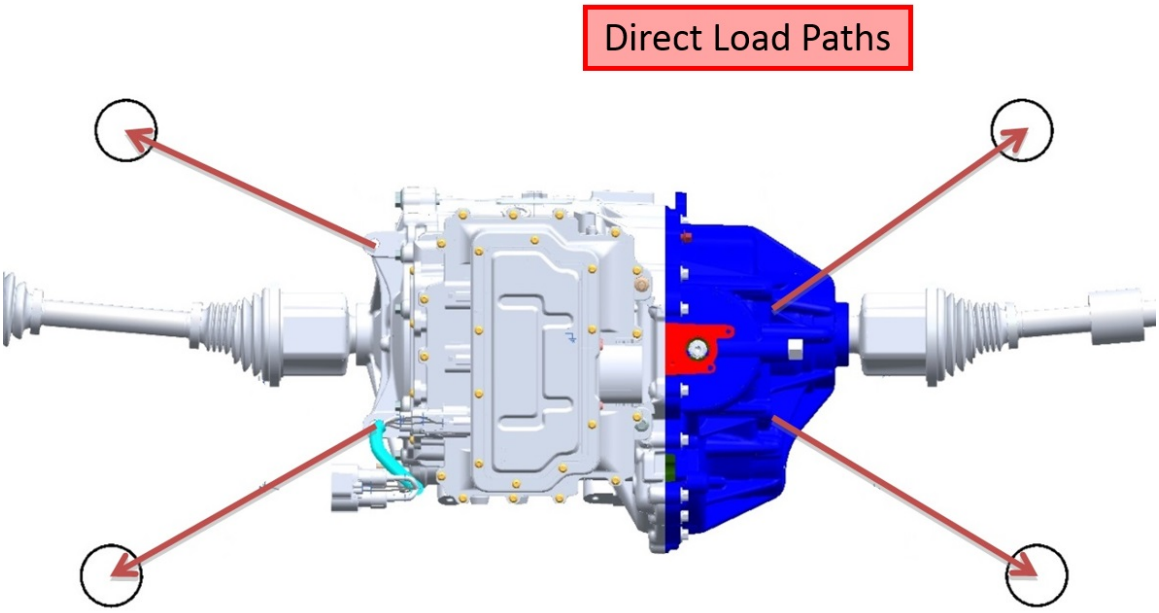

Figure 2.45. Theoretical direct force paths from motor mounts to chassis mounts.

Figure 2.46 shows how material was added along the desired pathways. The pathways near the dotted lines were not possible to be made absolutely direct due to the inner bearings of the toe links.

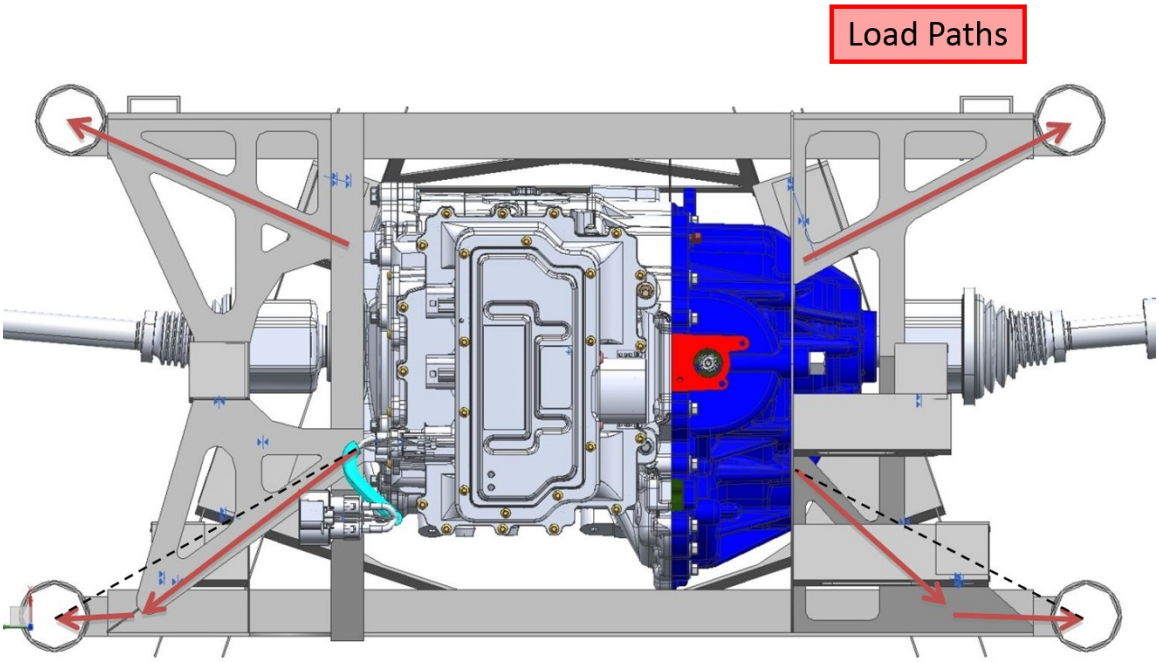

Figure 2.46. Realistic near-direct force paths used by custom cradle.

Figures 2.47 and 2.48 show the force paths between the mounting bosses of the motor encasement and the nearest chassis mount of the cradle.

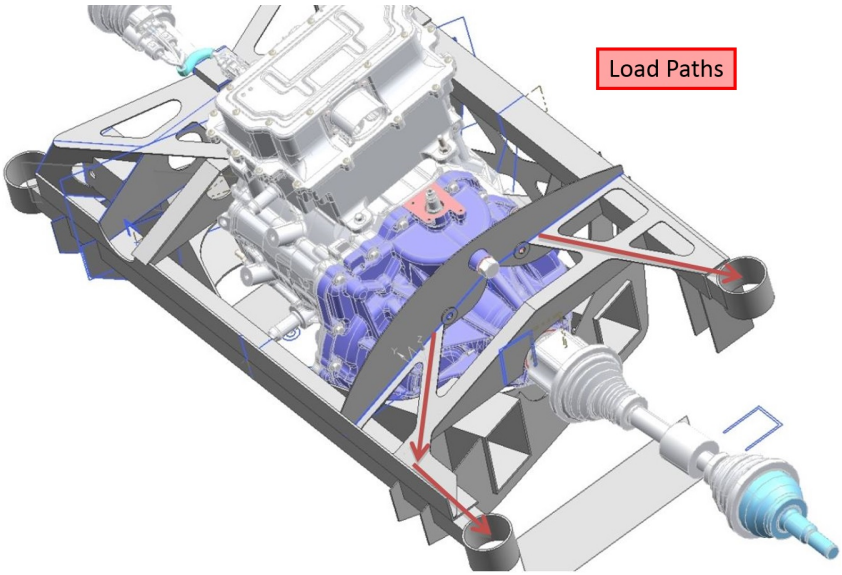

Figure 2.47. Front-driver's side view of assembly.

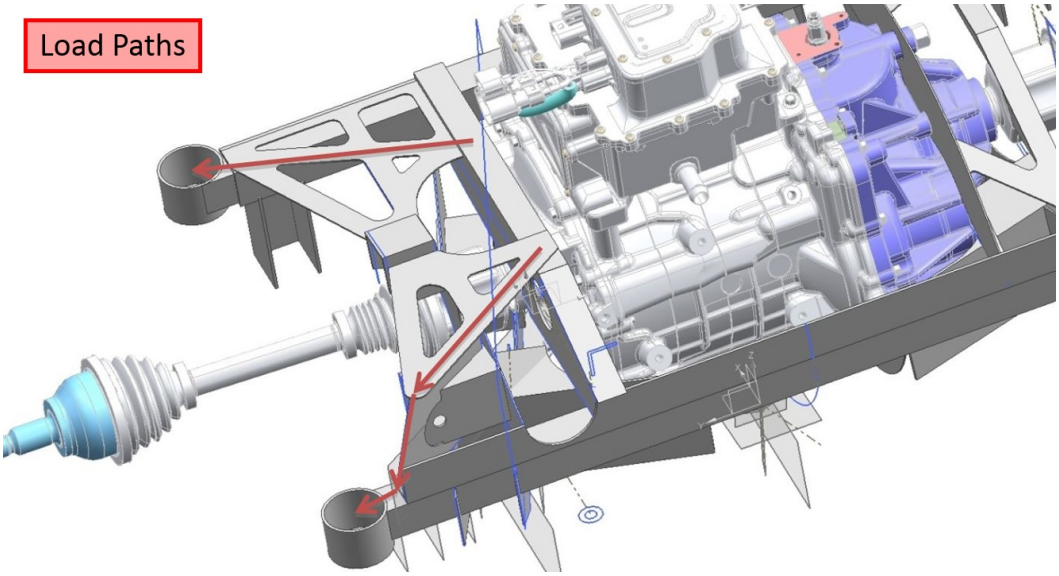

Figure 2.48. Front-passenger side view of assembly.

Figures 2.49 and 2.50 show how forces are transferred by the lower A-arm links of the Buick Suspension into direct compression and tension of two force paths within the cradle.

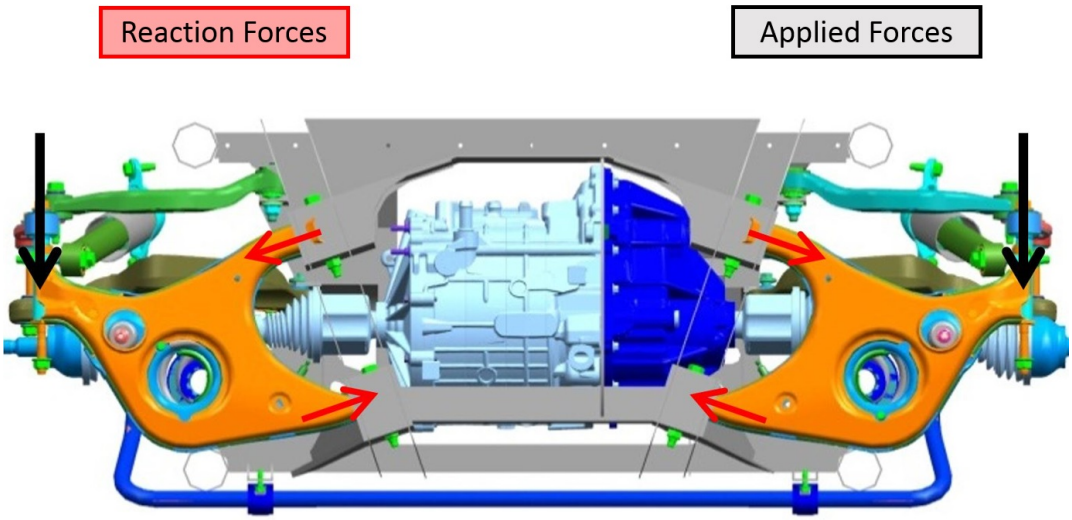

Figure 2.49. Force-reactions applied to cradle by the suspension's lower A-arms - underneath view of suspesion.

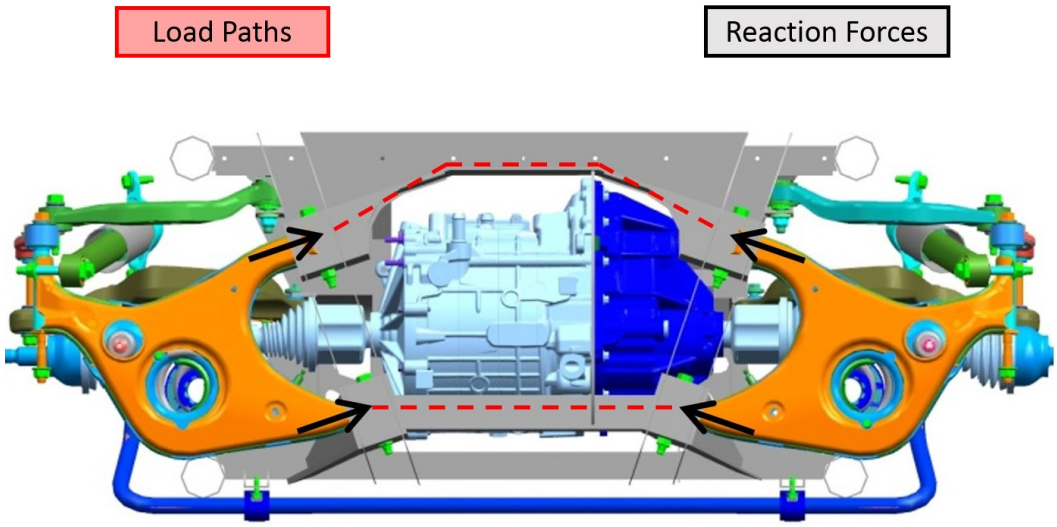

Figure 2.50. Direct and near-direct force paths used by cradle - underneath view of suspesion.

After briefly observing the magnitudes of the forces experienced at each bearing location for all load sub-cases to be tested, it was found that the most significant forces were inward compression of the upper camber mounts and compression/tension of the two force paths shown in Figure 2.50. Therefore, both of the significant forces mentioned previously were prepared for by a respective direct force path. Additionally, since the upper camber links contain the motor encasement between them, structural efficiency was obtained by compressing the rigid mass.

2.2.2 Analysis

Due to the complex shape and geometry of the custom cradle, a Finite Element Analysis (FEA) model was required in order to create a reliable static stress analysis across several load cases specified by General Motors. Since the FOS calculation required a comparison between stock and custom components, it was required to create FEA models for both the stock and custom suspension cradles. While each model was being constructed, several assumptions were made concerning the boundary conditions of the force analysis.

Since the bushings used to isolate the four corners of the sub-frame were made of rubber, they allowed a small amount of rotation in all directions without allowing a significant amount of linear displacement to occur. In order to represent these connections, spider-webs of rigid 1-D connections were used to connect the inner faces of the chassis mounts to 0-D points located at the middle of each cylinder. Once the spider-webs were made, the 0-D points were constrained in linear movement, but allowed to rotate freely in all directions. Figure 2.51 depicts the spider-web assembly and Figure 2.52 demonstrates the rotational capability of each spider-web. After seeing a result such as the one in Figure 2.52, it was assured that this particular boundary condition was satisfied.

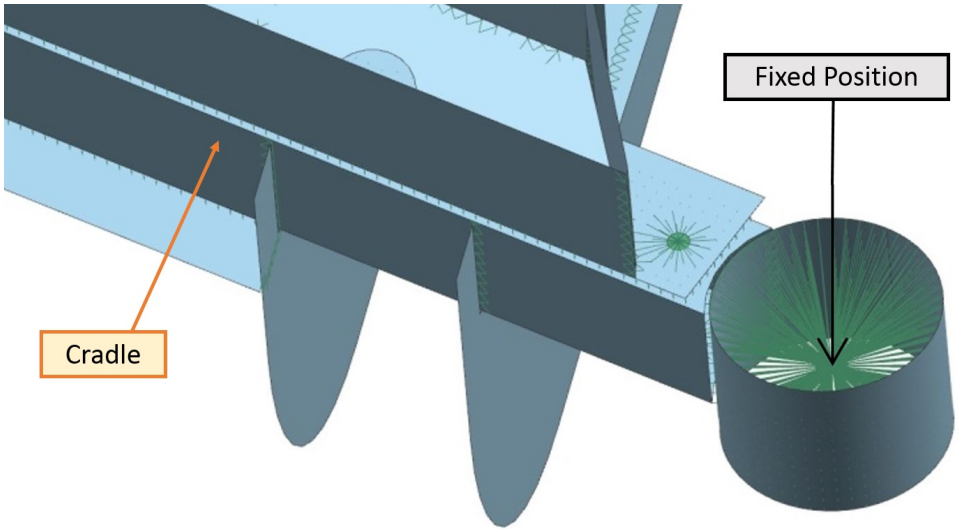

Figure 2.51. Front-Left view of the FEA assembly with Chassis-Mount 1-D Spider-webs implemented.

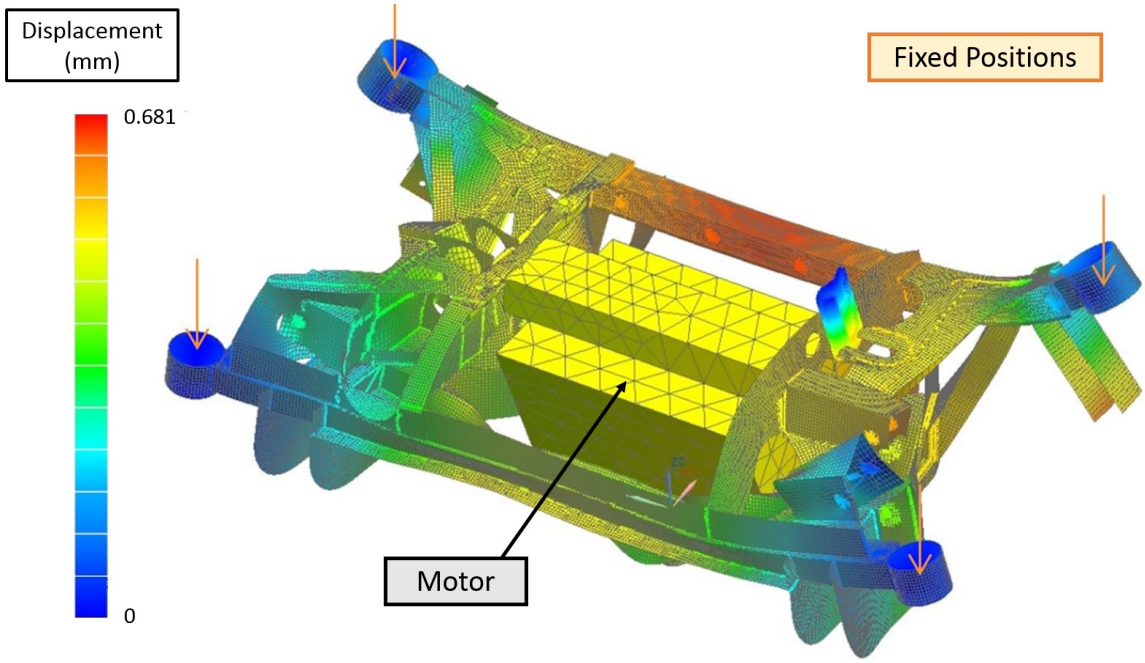

Figure 2.52. Displacement on custom cradle.

In practice, if all the bolts which contain the inner bearings of all the camber links are torqued properly, the friction caused by the contact of the bolt faces will transfer force along with the shank of the bolt. Therefore, at all bearing locations of the cradle, a bolted connection was made in order to represent the physical bolts of the structure which will transmit load from the camber links. Therefore, the force and torque vectors being caused by the camber links were applied to the bolted connections seen in Figure 2.53

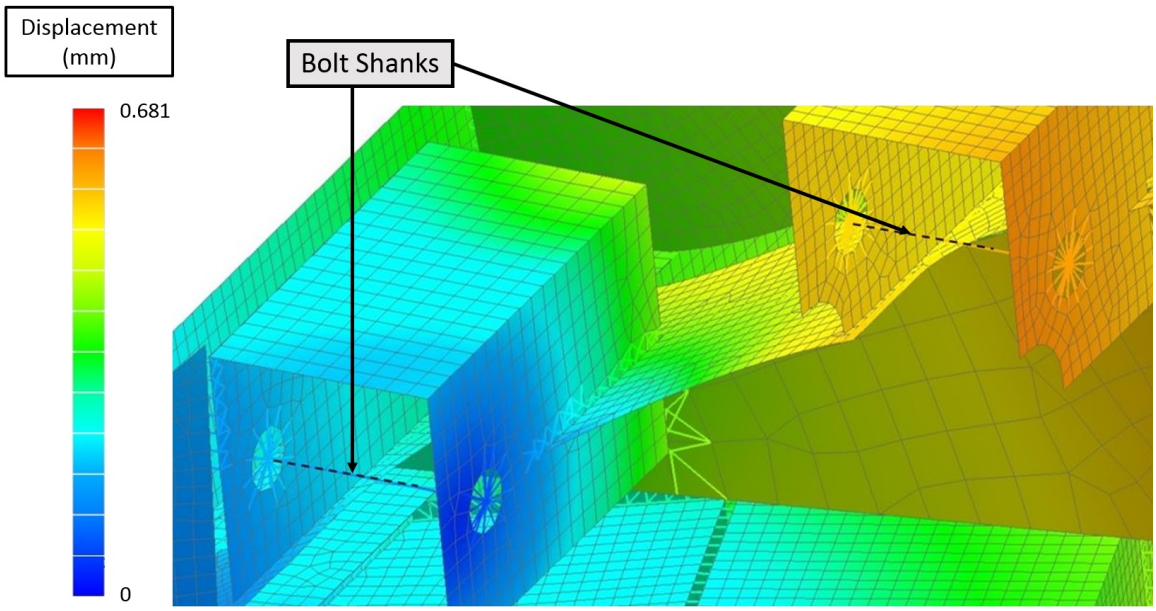

Figure 2.53. Bolted Connection of the bearing mounts.

Additionally, these 1-D bolted connections were used to represent the bolts that will hold the two halves of the steel cradle together as seen in Figure 2.54.

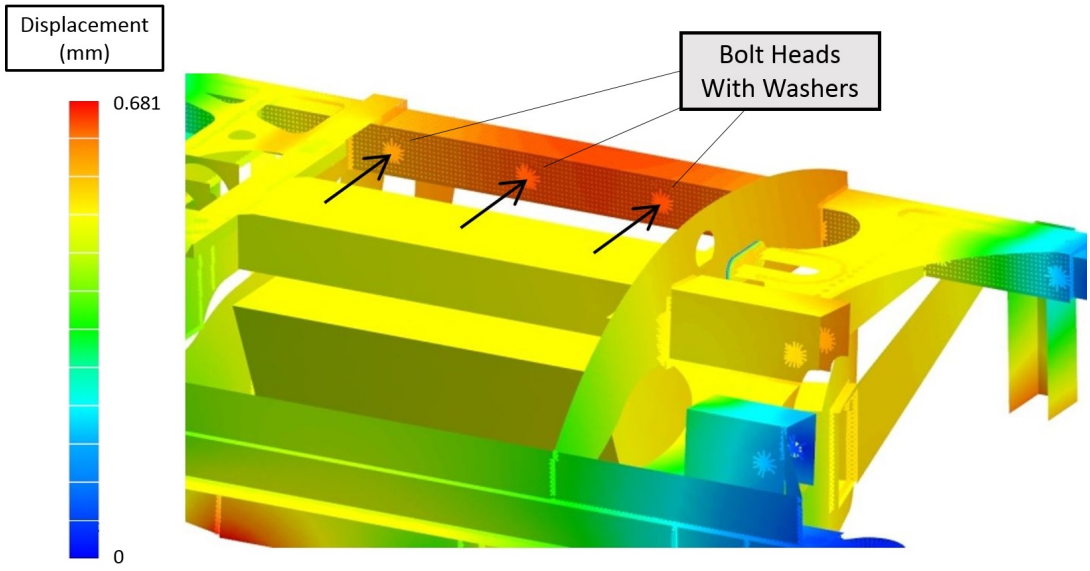

Figure 2.54. Bolted Connections of the two halves of the cradle.

For all welded connections, rigid 1-D connections were made between an element edge and its adjoining face shown in Figure 2.55.

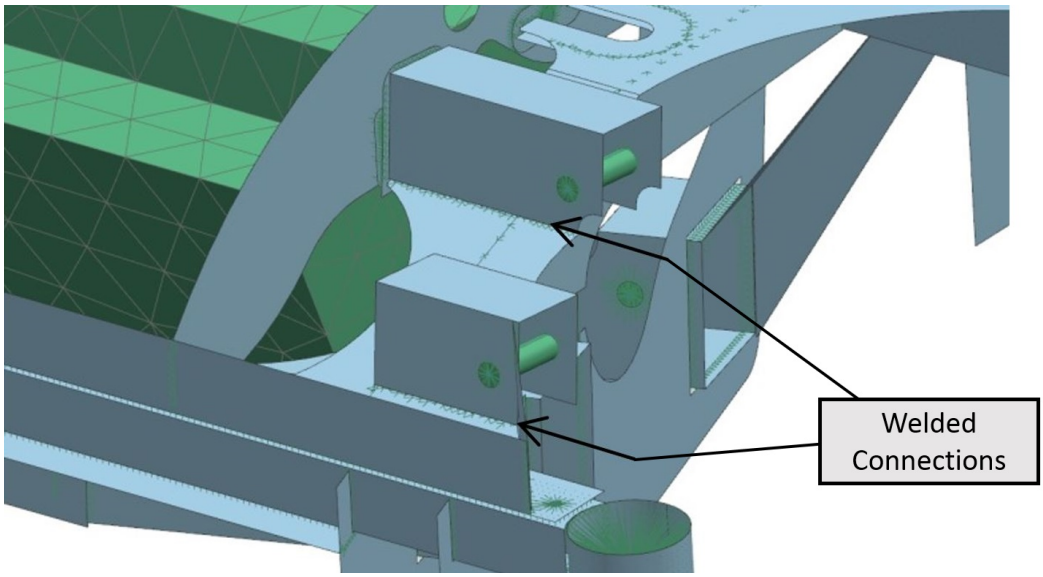

Figure 2.55. Front-Left view of the FEA assembly with 1-D welded connections implemented.

Shown in Table 2.1 is a table of material properties used in the analysis.

Table 2.1. Material Properties used in Analysis.

	Yield Strength (MPa)	**Ultimate Tensile Str. (MPa)**
Stock	275	475
AISI 1020 CR Steel	350	420

Shown in Table 2.2 is a sample force matrix used for one of the bearing locations of the suspension cradles. Similar matrices were used for all sections of the cradle which would be experiencing a load during operation. In total, there were 10 locations across the cradle which experience load during analysis [9].

Table 2.2. Sample force subcases for inner bearing locations.

	LForce on CROSSMEMBER from TOELINK BUSH_INNER right side							
Loadcase	Fx [N]	Fy [N]	Fz [N]	Tx [Nm]	Ty [Nm]	Tz [Nm]	Fm [N]	Tm [Nm]
Two-Wheel Bump	456	3254	1198	15	-10	-6	3498	19
One-Wheel Bump- LHS	157	1019	364	13	-6	-3	1093	14
One-Wheel Bump- RHS	739	5523	1952	15	-13	-8	5904	21
Twist - LHS jounce, RHS rebound	-11	-38	-29	-5	4	1	49	7
Twist - LHS rebound, RHS jounce	999	7802	2565	14	-16	-8	8273	22
Forward Braking	743	4088	1296	13	-14	-19	4353	27
Reverse Braking	-171	-1119	-221	13	-2	12	1154	18
Cornering - Left Turn	-765	-6545	-2040	16	-3	-7	6898	17
Cornering - Right Turn	197	1559	60	1	0	-2	1573	2
Forward Acceleration	-174	-765	-143	13	-13	16	798	24
Reverse Acceleration	515	2565	713	12	-1	-16	2712	20
Max Torque - Forward	-321	-2381	-481	10	-13	24	2450	29
Max Torque - Reverse	871	4006	1068	12	2	-24	4236	27
Reverse Bump	-315	-2309	-488	10	-14	24	2381	30
Forward Impact	1558	6705	1872	14	6	-33	7133	36

2.2.3 Results

Once realistic results were achieved, the first aspect that was analyzed was the effectiveness of the direct force paths used within the design. This was done initially by viewing the discoloration of the 2-D planes within the stress results of the load scenarios.

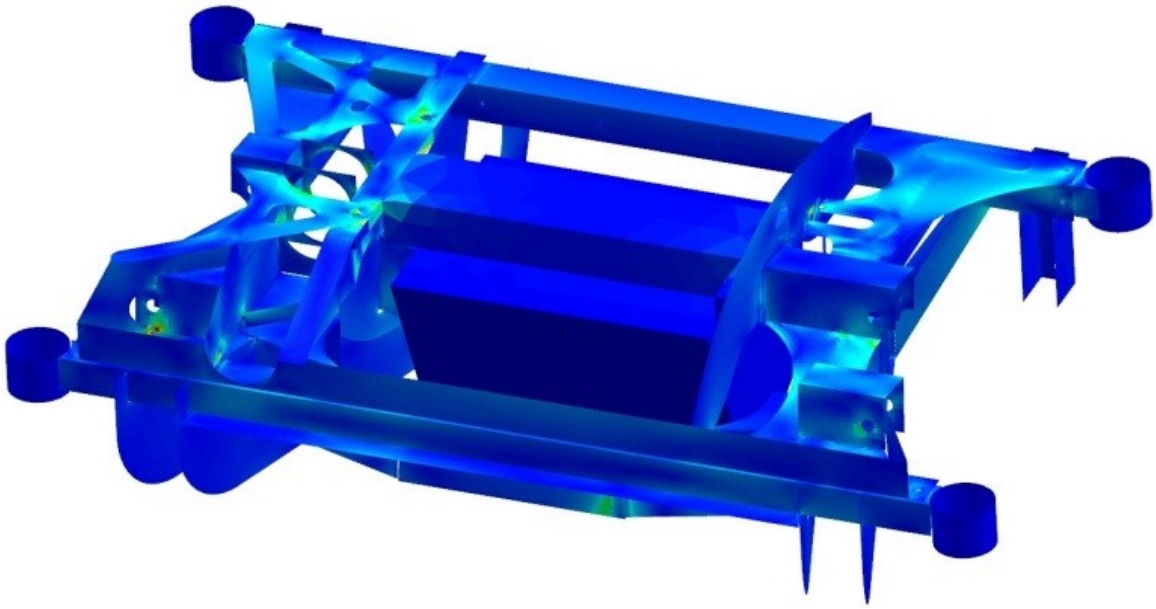

Figure 2.56. Stress result of one of the simulation load sub-cases.

Figure 2.57 shows three different results gained from viewing the discoloration of FEA planes under loading. The direct force path of leg A shows an even light-blue coloration, showing that there are no weak points along the leg. Also, since the color is not dark blue, it is concluded that the member is contributing a notable force during this load scenario. Conversely, leg B shows a less-direct force path between camber mount and motor mount which shows a green coloration at the apex of its inner curve, implying that it is at higher risk of failure than leg A and may require more material than leg A. Furthermore, area C shows a highly indirect force path with sharp angles between the front-right chassis mount and front-right motor mounting

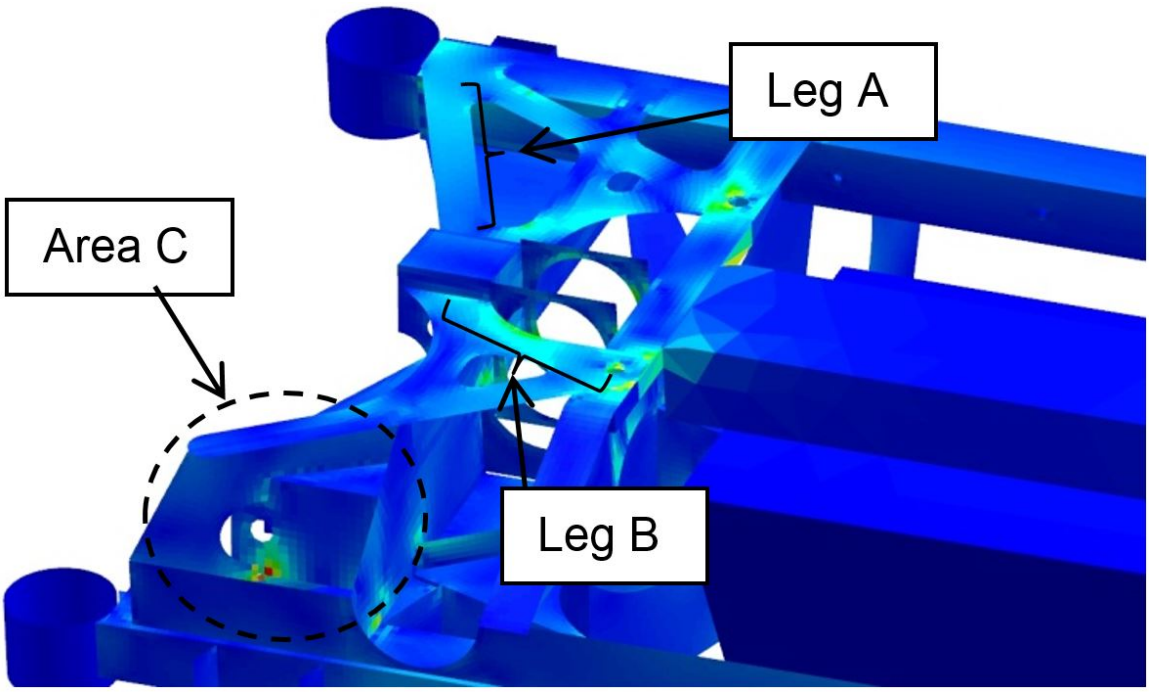

Figure 2.57. Close-up view of right side of cradle under loading with annotations concerning direct/indirect force paths.

location. Due to the shape of area C, the majority of the area is dark-blue, while at the sharp corners the stress spikes upward, causing red coloration.

Much like the links of a chain, the thickness of the material is determined by the failure of its weakest area. Therefore, areas that distribute stress evenly, such as leg A, will ultimately require a much smaller material thickness than areas such as area C. Since less material will yield lower energy consumption of the vehicle, careful analysis of these force paths allowed for much more efficient structures with less weight. During analysis of this simulation, there was much focus towards discovering if there were similarities across all subcases that warranted improvements in the design for all load scenarios.

After identifying the weakest areas of the structure of each sub-case for both the stock and custom cradles, the maximum stresses experienced were tabulated and compared. Shown below are the stress and Factor of Safety results across all 15 load cases for both the stock and custom cradles.

Table 2.3. Final Stress results between custom and stock designs.

Load Case	Stock Max Stress (MPa)	New Max Stress (MPa)	FOS (Stock)	FOS (New)	FOS Ratio (New/Stock)
Two Wheel Bump	406	89	0.76	4.72	6.18
One Wheel Bump (LHS)	507	134	0.61	3.13	5.11
One Wheel Bump (RHS)	689	132	0.45	3.18	7.06
Twist – LHS Jounce, RHS Rebound	795	193	0.39	2.18	5.58
Twist – RHS Jounce, LHS Rebound	725	182	0.43	2.31	5.41
Forward Braking	408	220	0.76	1.91	2.51
Reverse Braking	312	164	0.99	2.56	2.58
Cornering (LH Turn)	629	195	0.49	2.16	4.38
Cornering (RH Turn)	579	166	0.53	2.53	4.74
Forward Acceleration	268	124	1.16	3.39	2.93
Reverse Acceleration	411	95	0.75	4.40	5.84
Max Torque - Forward	470	172	0.66	2.44	3.71
Max Torque - Reverse	532	154	0.58	2.73	4.69
Reverse Bump	469	171	0.66	2.46	3.72
Forward Impact	907	306	0.34	1.37	4.02

As can be seen in Figure 2.3, the new cradle achieves a FOS ratio greater than 3.13 for all load cases given. Although there were cases where the new FOS dropped

below 2, the FOS ratio compared to the stock part was well above 2 for all sub cases. With this justification, the structure was determined safe to fabricate, install and use.

Deformation of a structure under loading has implications towards its dynamic safety and performance. Therefore, the displacement of each inboard bearing location was also analyzed. This was done by tabulating the total distance traveled by each inboard bearing location during each load sub-case, then comparing the new design to the stock design to ensure that the new design was at least as stiff as the stock design.

	Custom SubFrame Displacement (mm)					
Loadcase	**Pass_Toe**	**Pass_Camber**	**Pass_LowerFront**	**Pass_LowerRear**	**Pass_Sway**	**Drive_Toe**
Two-Wheel Bump	0.064	0.298	0.175	0.262	0.214	0.15
One-Wheel Bump- LHS	0.104	0.194	0.146	0.25	0.21	0.097
One-Wheel Bump- RHS	0.218	0.337	0.237	0.244	0.194	0.077
Twist - LHS jounce, RHS rebound	0.147	0.151	0.185	0.172	0.127	0.121
Twist - LHS rebound, RHS jounce	0.283	0.376	0.317	0.231	0.124	0.148
Forward Braking	0.321	0.248	0.686	0.511	0.136	0.249
Reverse Braking	0.115	0.182	0.397	0.541	0.432	0.146
Cornering - Left Turn	0.205	0.124	0.163	0.406	0.311	0.025
Cornering - Right Turn	0.036	0.118	0.12	0.3	0.163	0.11
Forward Acceleration	0.076	0.175	0.3	0.397	0.269	0.132
Reverse Acceleration	0.137	0.202	0.228	0.32	0.246	0.082
Max Torque - Forward	0.174	0.194	0.535	0.559	0.305	0.223
Max Torque - Reverse	0.25	0.268	0.489	0.475	0.237	0.201
Reverse Bump	0.171	0.195	0.527	0.554	0.303	0.223
Forward Impact	0.449	0.409	0.996	0.84	0.259	0.406

Figure 2.58. Inboard bearing displacement of the custom cradle.

Figures 2.58 and 2.59 show that the stiffness values for the custom design were on average much higher than the stock design; specifically, the bearing displacement was on average 2.4 times greater in the stock design than the custom design. This is in large part due to using the E-Drive as a rigid-lumped mass. Concerning the weight of the cradle, the total weight of the custom cradle is approximately 24.45 Kg, while the stock cradle is 26.2 Kg, indicating that the custom cradle is approximately 6.7% (1.75 Kg) lighter in weight while also having higher factors of safety concerning stress and being stiffer as well. However, the weight of the custom design could have been optimized further since the right side of the custom cradle uses indirect load paths to

	FOS (Stock/Custom)					
Loadcase	Pass_Toe	Pass_Camber	Pass_LowerFront	Pass_LowerRear	Pass_Sway	Drive_Toe
Two-Wheel Bump	6.20	2.24	3.19	3.05	1.28	2.62
One-Wheel Bump- LHS	3.25	3.09	3.59	3.13	1.57	5.21
One-Wheel Bump- RHS	2.42	2.28	2.84	3.55	1.57	4.01
Twist - LHS jounce, RHS rebound	3.14	4.34	3.58	4.51	3.20	4.71
Twist - LHS rebound, RHS jounce	2.11	1.98	2.40	3.58	4.60	2.29
Forward Braking	3.14	4.31	2.25	3.62	3.84	3.53
Reverse Braking	3.73	0.69	1.58	1.62	0.92	2.37
Cornering - Left Turn	1.69	3.89	2.70	2.17	0.89	8.88
Cornering - Right Turn	3.33	1.21	0.58	0.63	1.36	1.91
Forward Acceleration	2.21	1.38	1.05	1.37	0.49	1.17
Reverse Acceleration	3.26	3.02	2.19	2.90	1.53	5.67
Max Torque - Forward	2.07	1.65	1.17	1.62	0.57	1.63
Max Torque - Reverse	2.80	3.07	1.77	2.91	2.09	3.79
Reverse Bump	2.08	1.62	1.17	1.62	0.57	1.62
Forward Impact	2.55	2.83	1.60	2.46	2.68	2.91

Figure 2.59. Displacement comparison betwen the stock and custom cradle.

accommodate for the exhaust tunnel. Since the placement of the battery pack forced an indirect routing of the exhaust tubing, the tunnel was required to be made in the custom cradle. If this were not the case, the tunnel would not be necessary.

Shown below in Figures 2.60 and 2.61 are images of the custom cradle with the two sides of the upper half highlighted separately. In Figure 2.60, the side which contains the exhaust tunnel is highlighted. The total weight of all highlighted components is approximately 6.40 Kg.

In Figure 2.61, the left side is highlighted. The total weight of all highlighted components is approximately 2.95 Kg. As can be seen, the exclusion of the exhaust tunnel allows for a more efficient structure to be made. From this efficiency, the left side is 3.45 Kg (54.9%) lighter than the right side. From this, two conclusions can be drawn; the usage of direct load paths allowed for a weight reduction of approximately 50% between comparable components of the custom cradle and that the exclusion of the exhaust tunnel would take approximately 3.45 Kg of weight off of the custom cradle.

Shown below in Figure 2.62 is a concentrated view of the mounts used to hold the inner bearings of the upper camber links. The wall thickness of these components

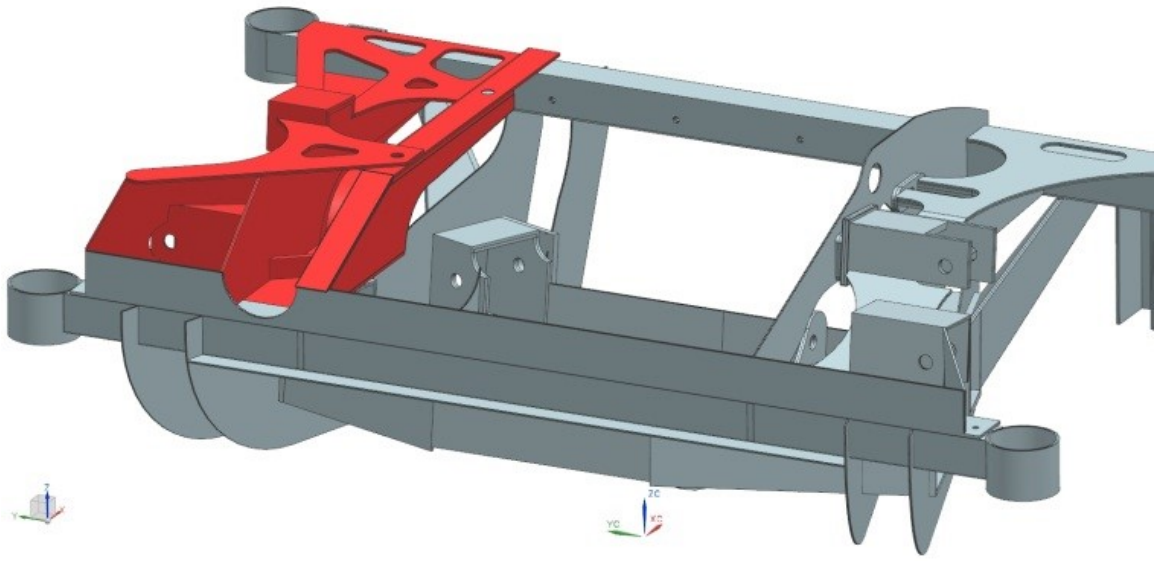

Figure 2.60. Custom cradle with right side of upper shell highlighted.

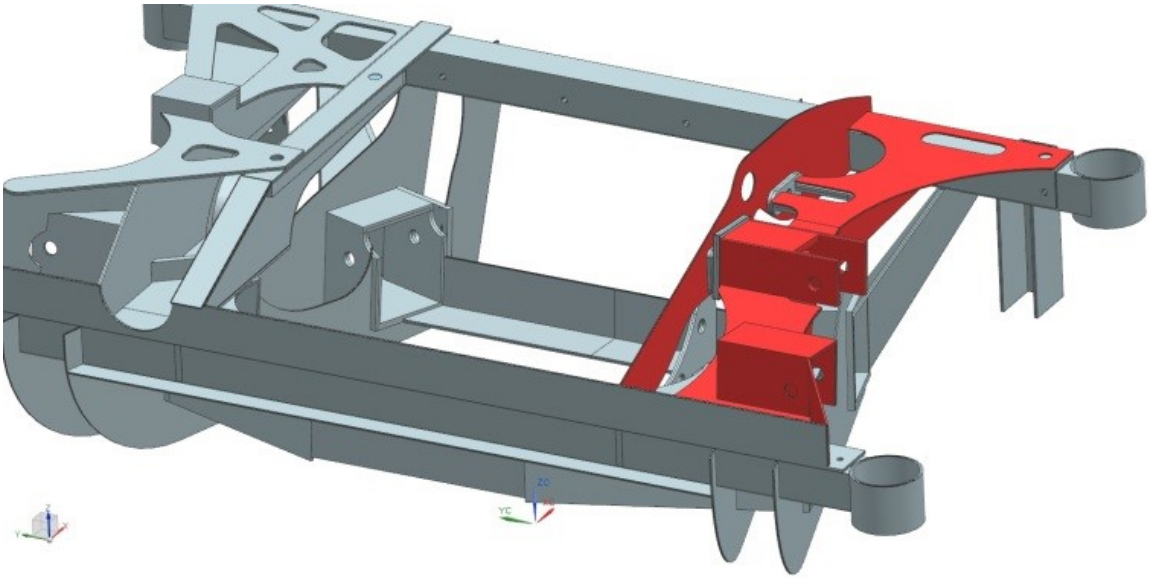

Figure 2.61. Custom cradle with left side of upper shell highlighted.

is 6.35mm. The reason for this was due to the high stress concentrations seen around the bearing locations during modeling. However, this seems to be an over-estimation since the wall thickness for these components of the stock cradle is 3mm which appears more realistic.

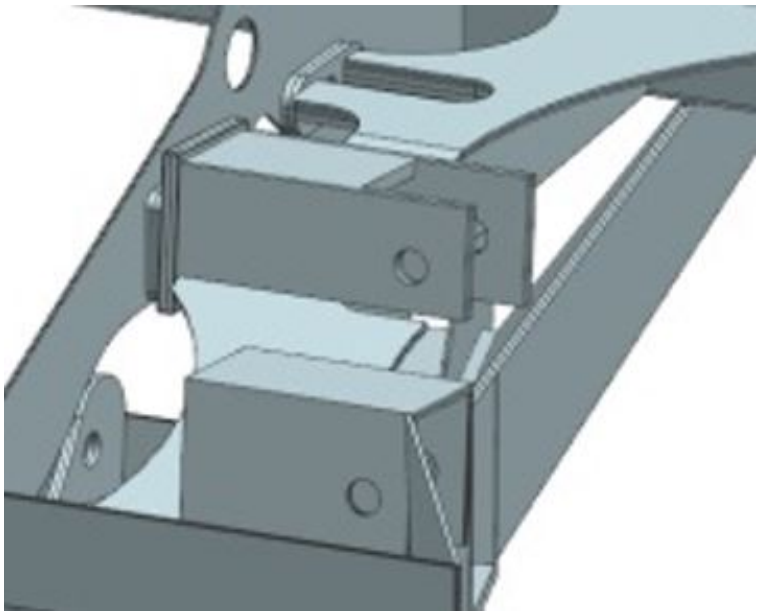

Figure 2.62. Camber link mounting locations on the custom cradle.

If it is assumed that the custom camber mount wall thickness is over-estimated, it can be said that these camber mounts could have been reduced to a wall thickness of 3mm, as the stock cradle uses. If this was implemented, the total weight of the camber mounts used in the custom cradle would have changed from 5.88 Kg to 2.78 Kg, yielding an additional theoretical weight reduction of 2.78 Kg. If added to the previous weight reduction, the total theoretical weight difference between the custom cradle and the stock cradle would have been 7.98 Kg. Overall, the custom cradle made was restricted due to the exhaust tunnel, the allotted time for design iteration and the availability of materials. However, if these restrictions were removed or reduced, it is reasonable to conclude that the custom cradle could have been 30% lighter than the stock cradle.

2.2.4 Main Take-aways

From the analysis of the suspension cradle, much was learned concerning direct load paths and correct FEA procedures. This knowledge was used by the team in order to create a custom camber link for the rear suspension, a custom five-bar brace for the vehicle body as well as a custom trailer hitch for the vehicle all of which are shown below in Figures 2.63, 2.64 and 2.65, respectively.

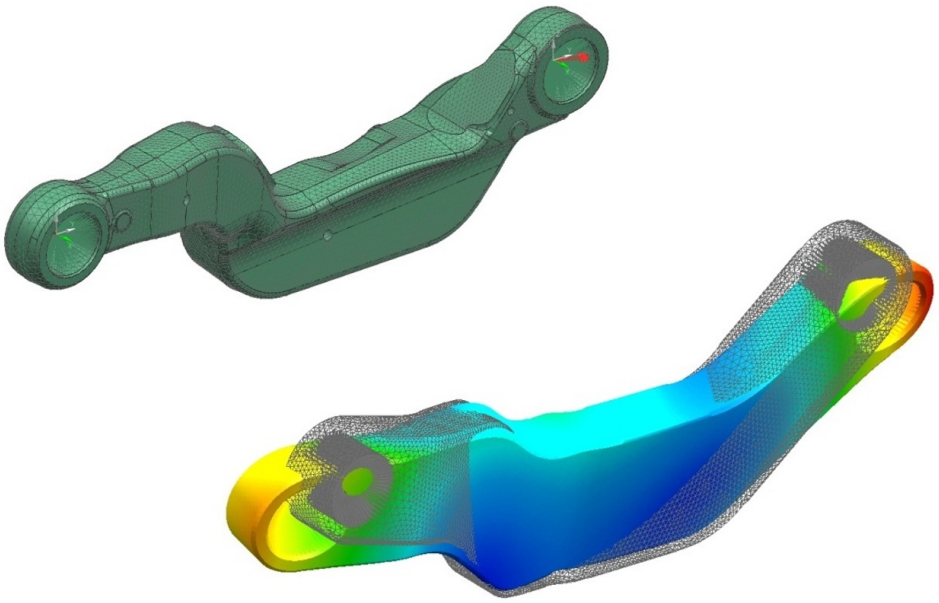

Figure 2.63. Custom Camber link.

As can be seen in Figures 2.63, 2.64 and 2.65, similar FEA modeling and analysis was used for other custom components for the vehicle, all of which were designed on CAD and tested using FEA before fabrication began. All three of the components shown in Figures 2.63, 2.64 and 2.65 worked successfully at the competition.

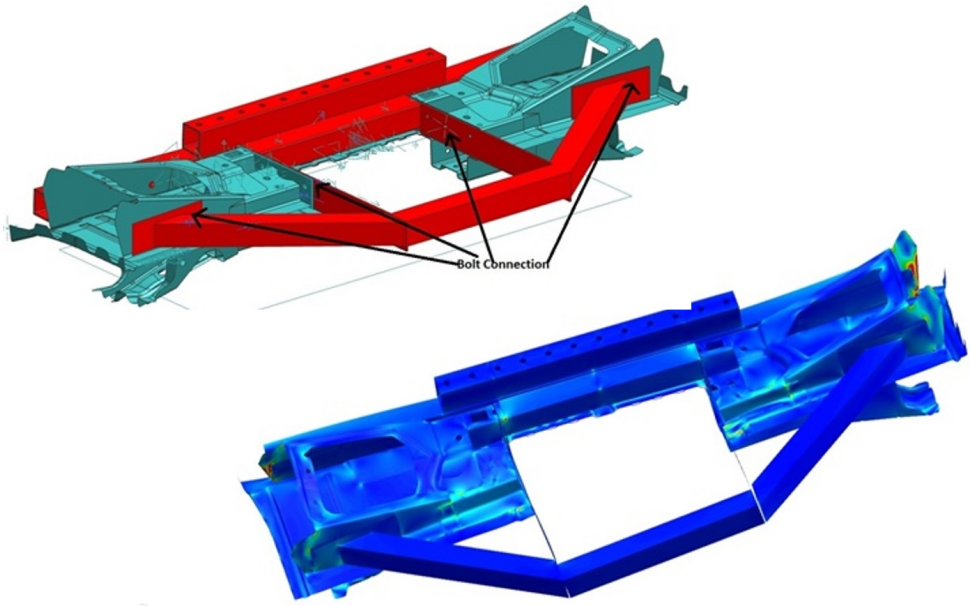

Figure 2.64. Custom Five-Bar brace.

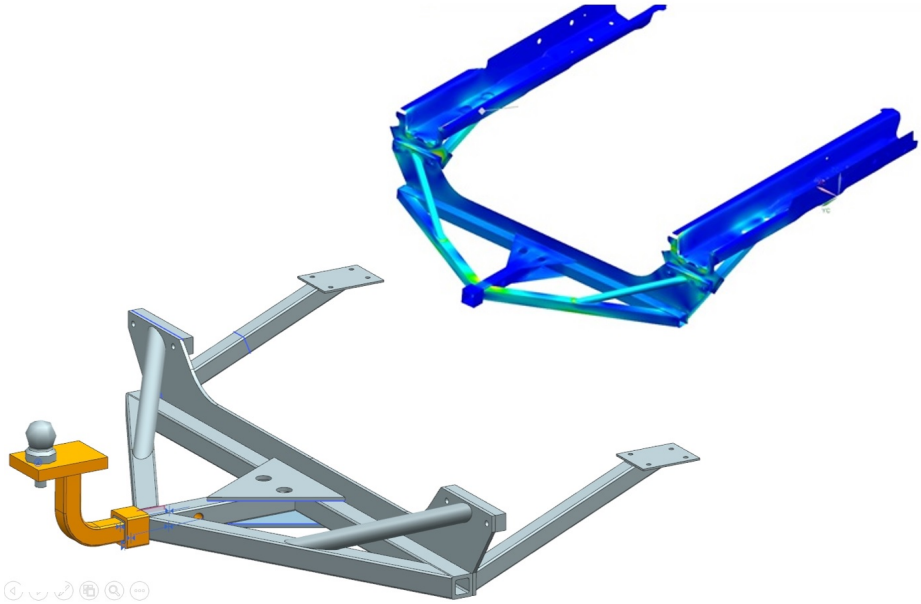

Figure 2.65. Custom trailer hitch.

3. ENERGY STORAGE SYSTEM

As previously mentioned, the vehicle used by the Purdue Team in EcoCar2: Plugging Into the Future was a Plug-in Hybrid-Electric Vehicle which used a B20 combustion engine in parallel with an electric drivetrain. The energy sources for these two drivetrains were a B20 diesel fuel tank for the combustion engine and a 16.2 kWh Lithium-ion High Voltage (292 V nominal) Battery Pack for the electric drivetrain.

3.1 Electrical Architecture

Throughout the development of the vehicle, it was important to determine the power demands (nominal and peak) of each electrical component as well as whether they were a high voltage or low voltage component. Since each team was given a Stock 2013 Chevy Malibu, there was an existing 12v (low voltage) circuit to work from. However, since the team was going to add a high voltage drivetrain to the vehicle along with a high voltage Energy Storage System, there were some components which became redundant once both systems were integrated into the vehicle.

A prime example is the alternator of the Malibu versus the Accessory Power Module (APM) of the electric drivetrain. An alternator converts mechanical work of the combustion engine into 12 V electrical energy, while an APM converts high voltage electrical energy into 12 V electrical energy. Both components were capable of charging the 12 V system of the vehicle. With this in mind, whether or not to include the stock alternator was discussed within the team during early design phases in the effort of saving weight and reducing complexity. However, it was decided to keep both components so that there was an on-board backup option in case either component experienced malfunction. Overall, the vehicle developed an electrical architecture consisting of both high and low voltage components which ensured that all compo-

nents were capable of receiving their required electrical demand at all necessary times during vehicle operation.

3.1.1 Vehicle Electrical Schematic

Figure 3.1 depicts a diagram which details the high and low voltage connections between major components of the vehicle.

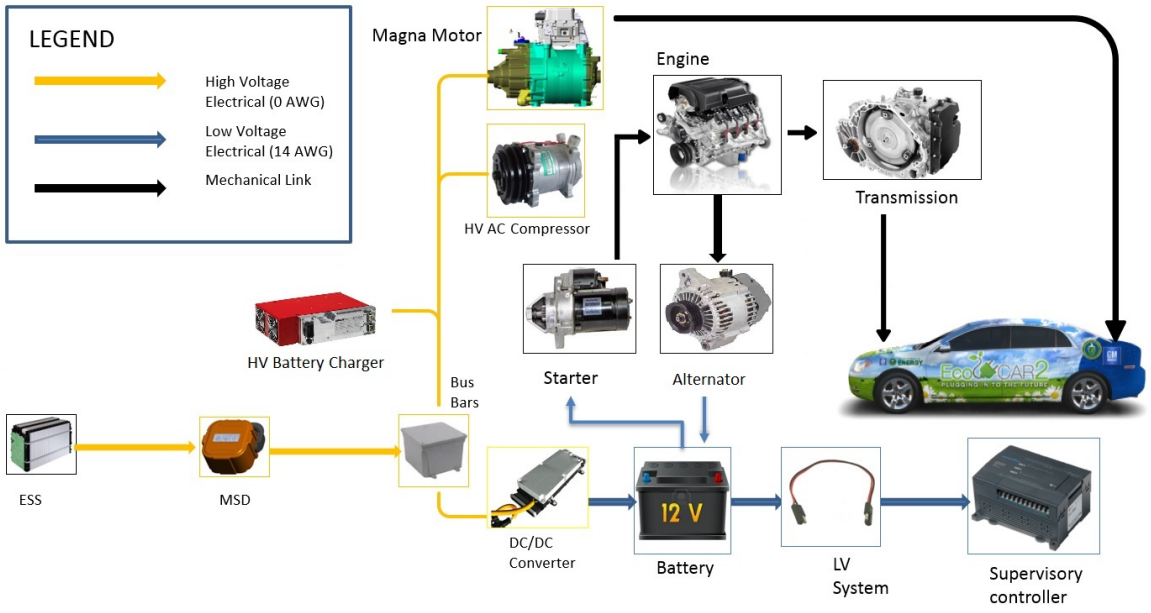

Figure 3.1. Diagram detailing the High and Low voltage architecture of the vehicle.

3.1.2 ESS Components

Since the ESS is the primary energy source for electrical energy onboard the vehicle, it was imperative that it be capable of sending and receiving high voltage electrical energy without failure at all times. In order to accomplish this, battery modules, a current sense module, electrical distribution module, battery monitoring

module and a manual service disconnect switch were all components required to be included within the ESS.

Battery Modules

Since it was determined that the vehicle have approximately 30-40 miles of charge depleting range at full charge, it was necessary to consider what battery pack options available for the competition were capable of achieving such a range. Since Eco-Car2 was sponsored by A123 systems, several A123 battery pack arrangements were available for donation. The two highest capacity options available were a 16.2 kWh (6 battery modules) and an 18.9 kWh (7 modules) battery pack. Due to packaging considerations, the 6 module (16.2 kWh) pack was used.

Each module consisted of a stack of thermally conductive metal cells with plastic LV balance boards at each end. Additionally, each balance board contained heat fins on one side to allow the modules to be air cooled as long as proper temperature air is convected across them. However, it was the decision of the Purdue team to liquid cool the battery modules in order to have a more powerful and faster responding cooling system.

Figure 3.2. Example of a single battery module used.

Manual Service Disconnect Switch

According to the high voltage schematic, all six battery modules were to be connected in series such that their individual voltages add together in order to attain a higher pack voltage of 292V. Since this high voltage energy would be lethal if handled improperly, safety of the high voltage electrical system was paramount during all phases of development. Part of this safety consideration was the inclusion of a Manual Service Disconnect Switch (MSDS). The switch was to be placed in-line with 6 battery modules via high voltage connection. Therefore, if the switch were opened, the pack would consist of two sections of 3 modules connected in series rather than 6 modules connected in series. This was paramount because if the switch were closed, the total pack voltage would be 292 V, yet if the switch were opened, the total voltage would be 146 V. It was desired to mount the MSDS within the wall of the ESS such that a portion of it be accessible by hand outside the pack. To disconnect the switch, a user of the vehicle would grab the handle of the MSDS located on the exterior and remove the exterior cap of the MSDS. The removal of said cap would open the switch, ensuring that the pack voltage was decreased by 50%.

Figure 3.3. Image of the MSDS used for the Purdue ESS.

Since removal of the MSDS cap would decrease the battery pack voltage by 50%, it was a safety requirement of the battery box design that the MSDS cap require removal prior to opening the battery pack.

3.1.3 ESS Schematic

With all ESS components and vehicle electrical distribution determined, it was possible to create a vehicle electrical schematic such as the one seen in Figure 3.4.

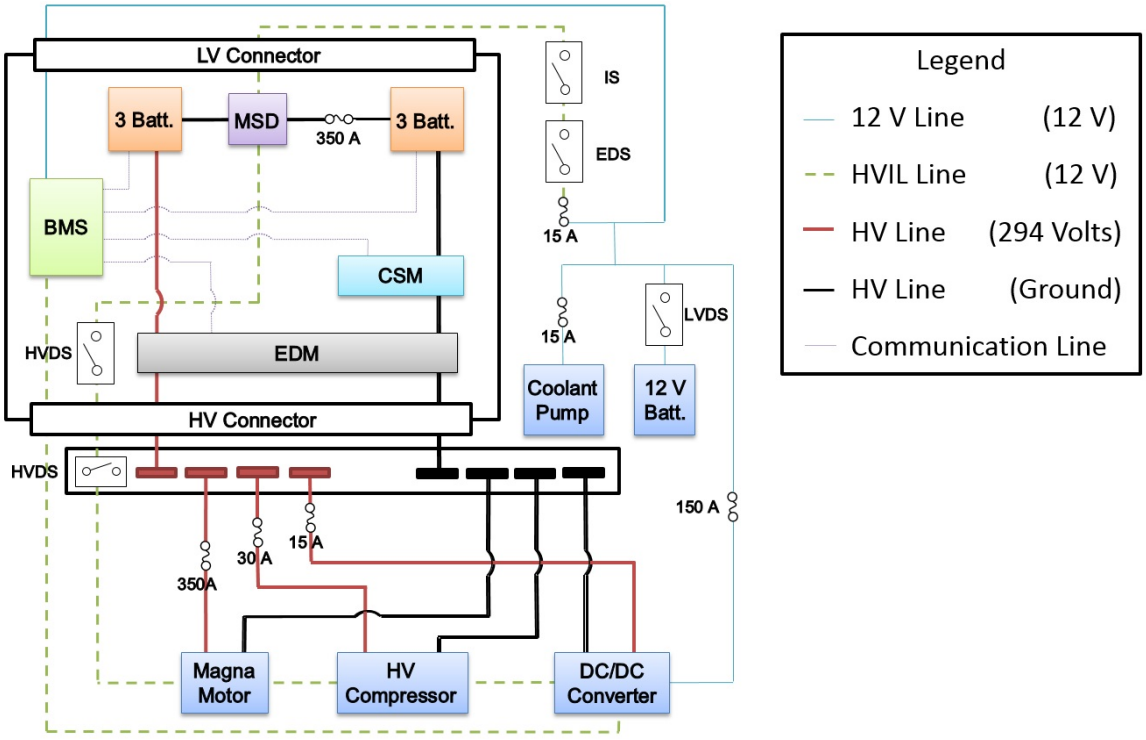

Figure 3.4. Diagram of the ESS electircal wiring.

3.1.4 Module Placement

During the initial design stages of the battery box, many orientations of battery modules were proposed. However, each battery module consisted of a stack of cells,

similar to a loaf of bread consisting of several slices stacked next to each other. Because of this, it was discovered that the battery modules should not be oriented such that the cells were sitting atop one another. Figure 3.5 depicts one such unacceptable orientation.

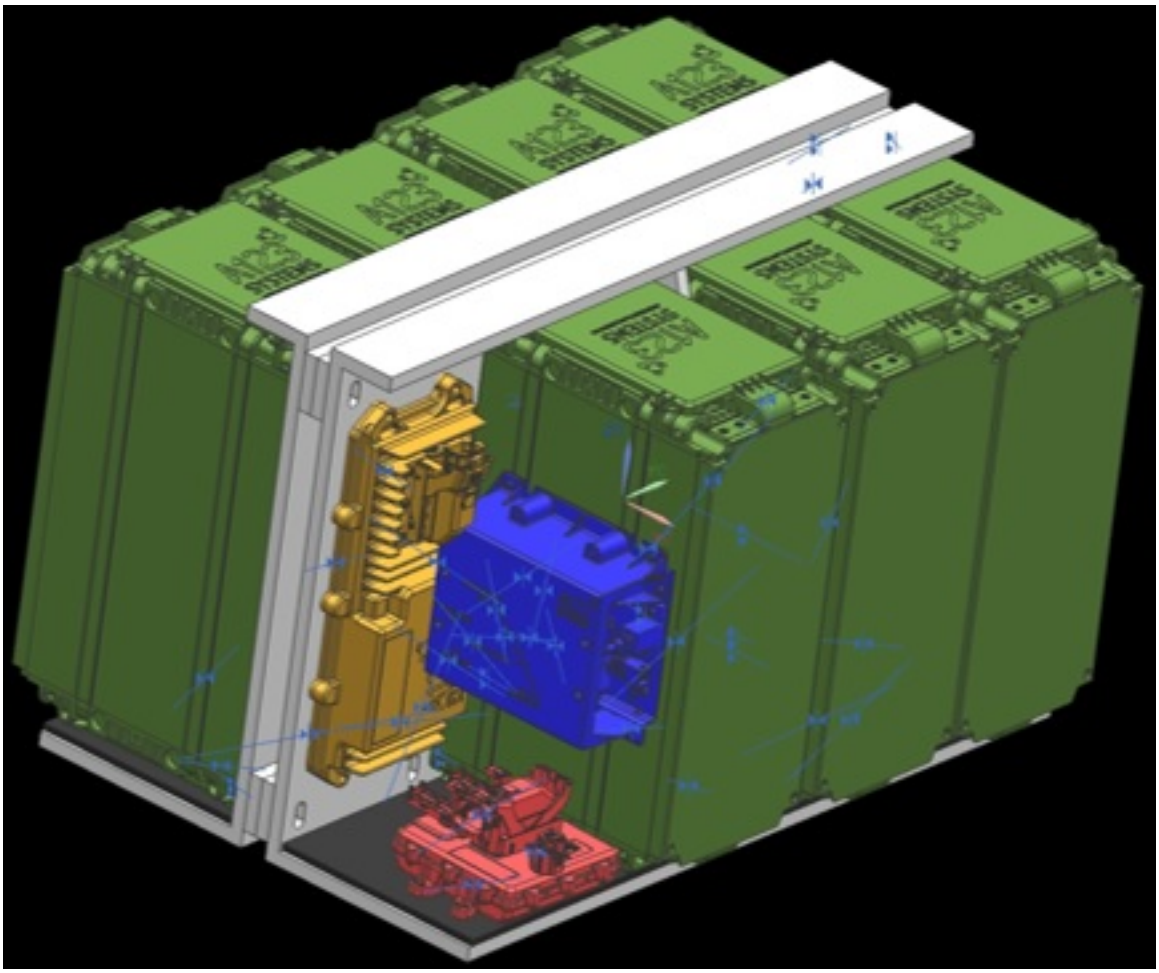

Figure 3.5. Example of an early ESS design.

Once this was discovered, it was determined that each battery would come either as a "vertical" or "horizontal" module. Depending on the orientation desired, the mounting locations would reflect the desired orientation. For both orientations, the intended mounting strategy for each module is to have four metal rods of approxi-

mately 7mm OD placed near each corner of the module. Figures 3.6 and 3.7 depict the different mounting strategies for each module orientation.

Figure 3.6. Battery module with a vertically oriented mount.

Figure 3.7. Battery module with a horizontally oriented mount.

It is important to note that each module can only be in one orientation. Therefore, if the Purdue team were to design a pack requiring only horizontal modules, all module mounts would be a horizontal mounting arrangement with no access to the vertical mounts. This restricted the team from changing mount orientations after the battery modules were received.

Since it was decided that the battery modules be liquid cooled, thermal conduction of the battery modules was an important consideration. From this perspective, battery box designs which favored high module surface area in contact with a liquid cooling plate were the most desirable. Figure 3.8 depicts a battery box arrangement where the modules are oriented "vertically", whereas Figure 3.9 depicts an arrangement with the modules oriented "horizontally". Arrangements such as the one seen in Figure 3.9 were favored since each module had a large amount surface area in contact with a relatively small cooling plate while also having a smaller conduction distance for the thermal to energy to travel across due to the shorter height of the horizontal modules.

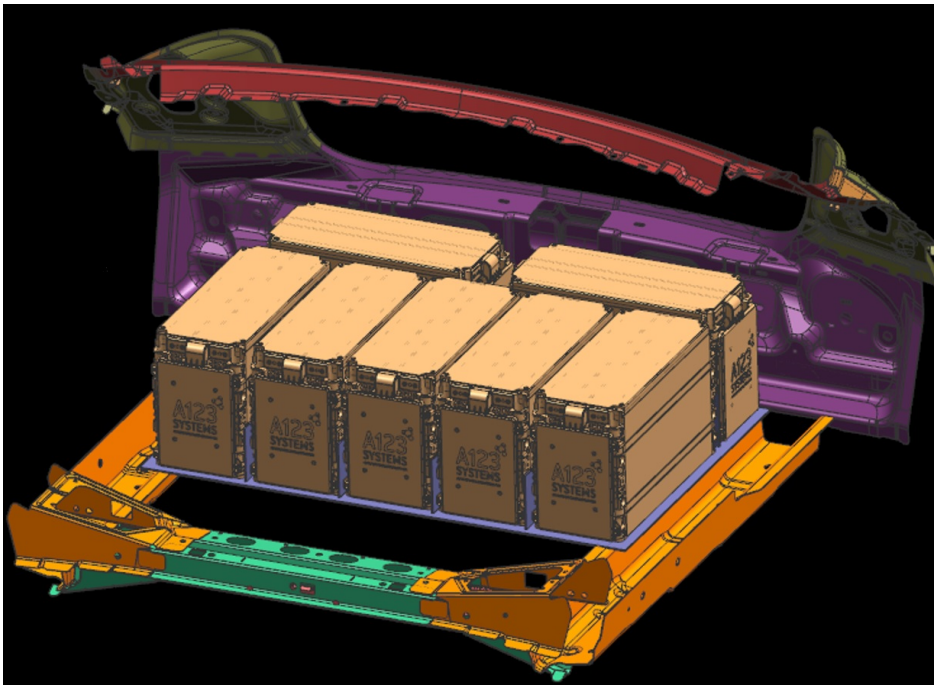

Figure 3.8. Example of an early ESS design with vertical module arrangements.

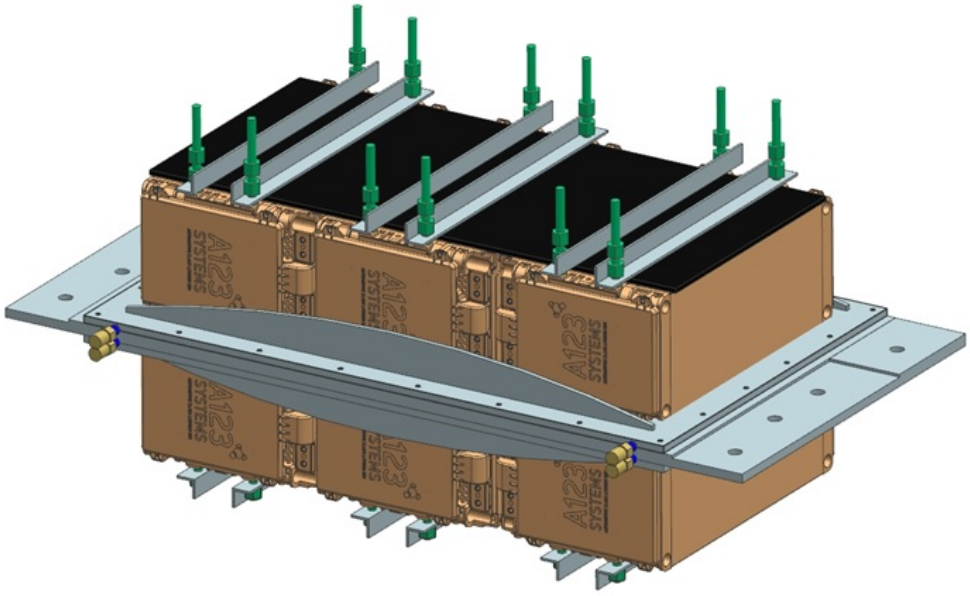

Figure 3.9. Example of an early ESS design with horzontal module arrangements.

3.2 Battery Box

Eventually, it was determined that the battery box to be made by the Purdue team would follow the design seen in Figure 3.9 on page 92.

Aluminum structure

The way in which the battery box was designed centered around a middle aluminum structure that served both as a lightweight structural support as well as a thermal conduit between the coolant and battery modules. Figure 3.10 depicts a partial view of the battery box assembly with the aluminum structure exposed.

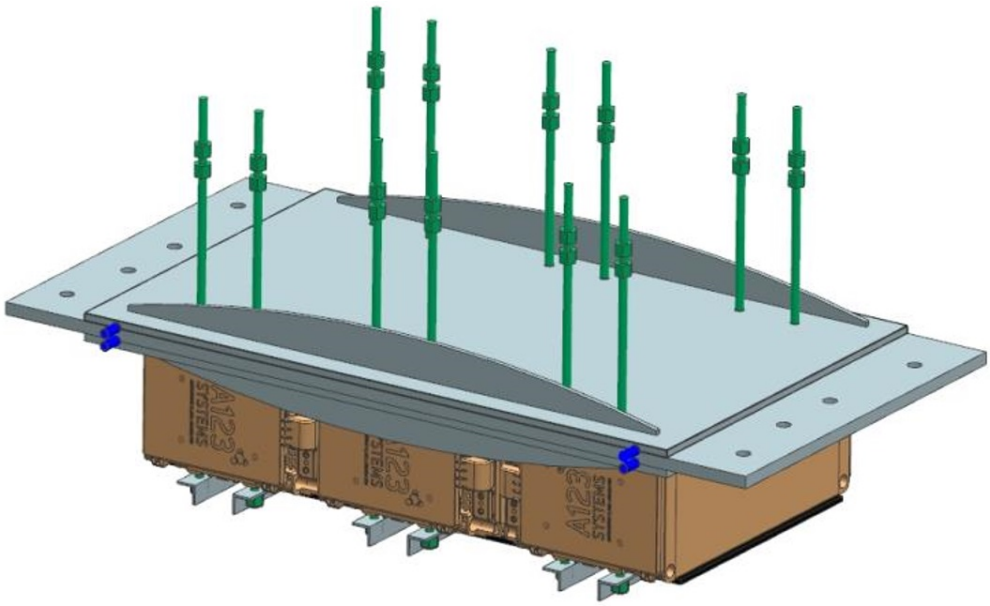

Figure 3.10. Battery Box partial view emphasizing Aluminum Structure.

Since the pack was to be liquid cooled, it was beneficial to insert a cooling element in the middle of the pack such that all modules would have direct contact with a cooling surface while only requiring a singular cooling element. Initially, it was determined that the cooling element would be a section of copper tubing to be inserted into the aluminum structure. This was to be accomplished by milling round

grooves directly into the aluminum structure, then press-fitting copper tubing into the grooves. Figure 3.11 depicts the grooves to be milled into the aluminum while Figure 3.12 depicts the inclusion of copper tubing.

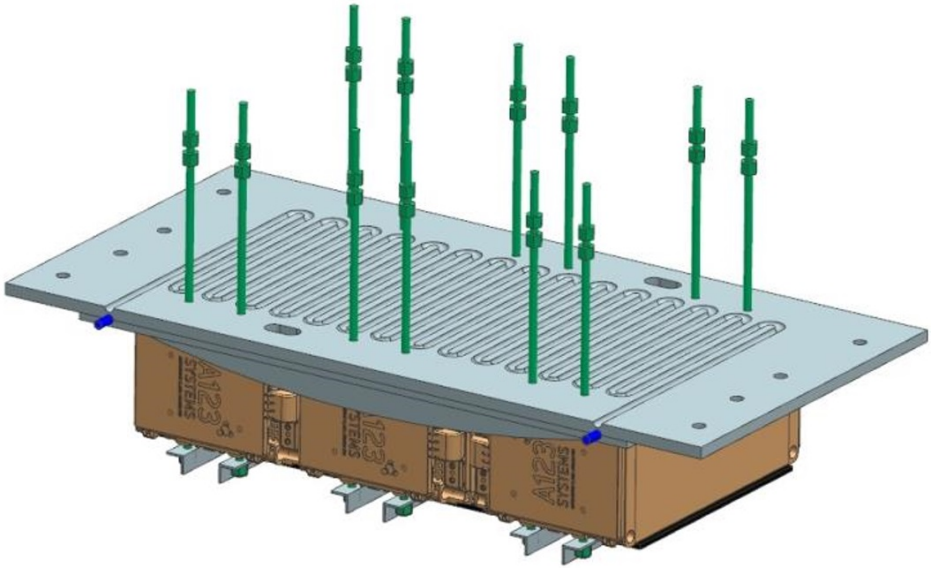

Figure 3.11. Battery Box partial view emphasizing coolant routing.

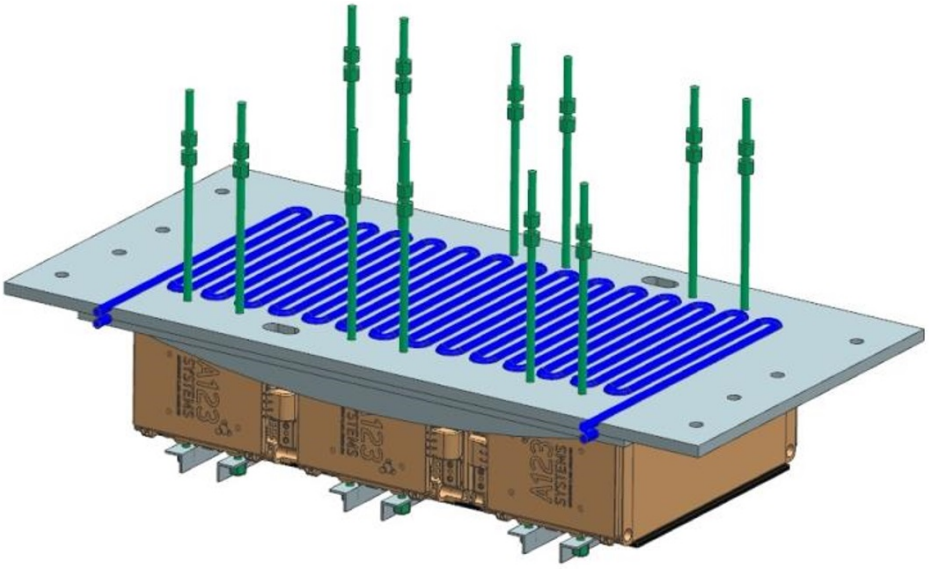

Figure 3.12. Battery Box partial view emphasizing coolant tubing.

Eventually, it was determined that the winding section of copper tubing would be difficult to make. Therefore, the tubing was replaced with several Lytron Cold plates with rectangular aluminum housings as seen in Figure 3.13. These housings would make them easier to precision insert into the aluminum structure of the battery box, as shown in Figure 3.14.

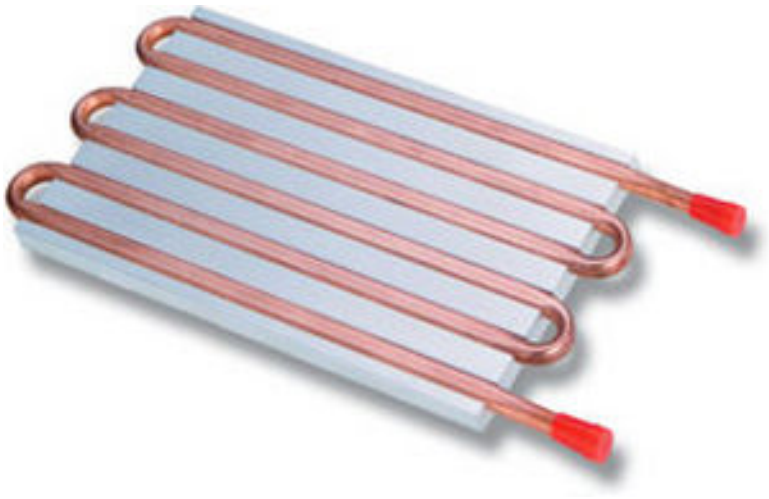

Figure 3.13. Image of the Lytron Cold plates used.

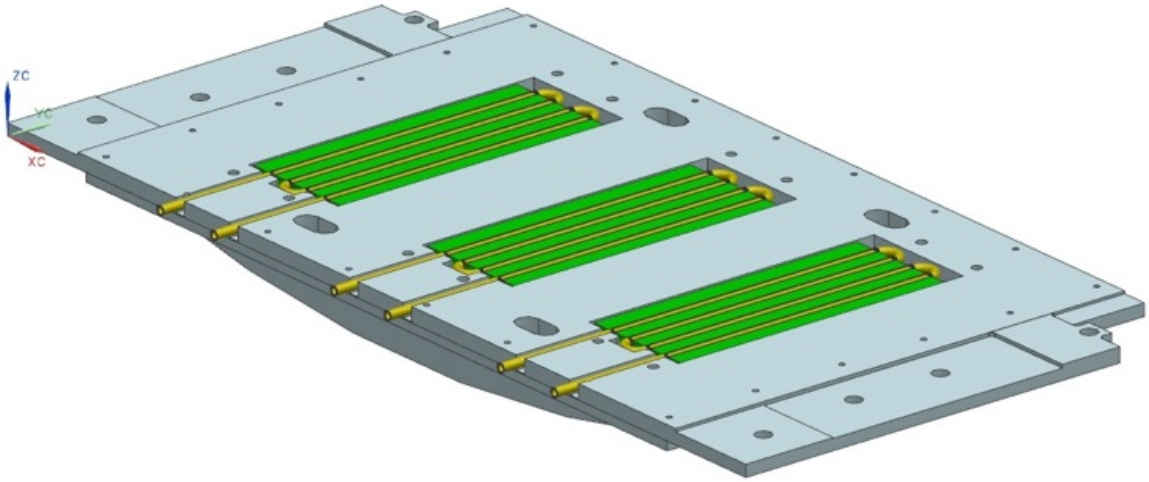

Figure 3.14. Middle aluminum Plate of the battery box.

Battery Box assembly

According to the design of the battery box, the middle aluminum structure consisted of three aluminum sections. The middle section was the widest of the three, allowing it to span across the width of the chassis framerails. The other two sections contained arches for structural rigidity. Therefore, with all three sections assembled together, the aluminum structure was rigid, capable of being directly attached to the bottom face of the framerails and had the capability of conducting heat from the battery modules to moving coolant within the structure.

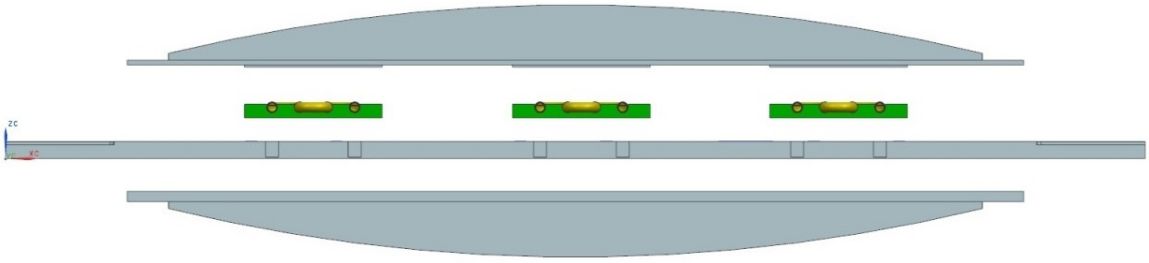

Figure 3.15. Expanded view of aluminum structure with cooling plates included.

Figure 3.16 shows the 5/8 inch thick 6061 Aluminum plate used as the middle structural plate for the battery box. The rectangular seats for the Lytron cold plates were machined to be exactly the same size as the cold plates within a 0.005 inch tolerance. Once the grooves were made, the cold plates were cooled inside a freezer, pressed into their respective seats in the middle plate, then allowed to expand to their natural size within the structure, allowing for lower thermal contact resistance between the surfaces in contact. Once the cold plates were inserted, the middle plate was ready to have the other two aluminum sections placed on each of its two faces. This was accomplished by having the battery modules maintain "squeezing" pressure onto the aluminum assembly.

Between the battery modules and aluminum structure is padding which is both electrically non-conductive and thermally conductive. Aluminum angles were used to

Figure 3.16. Middle aluminum Plate of the battery box - post CNC fabrication.

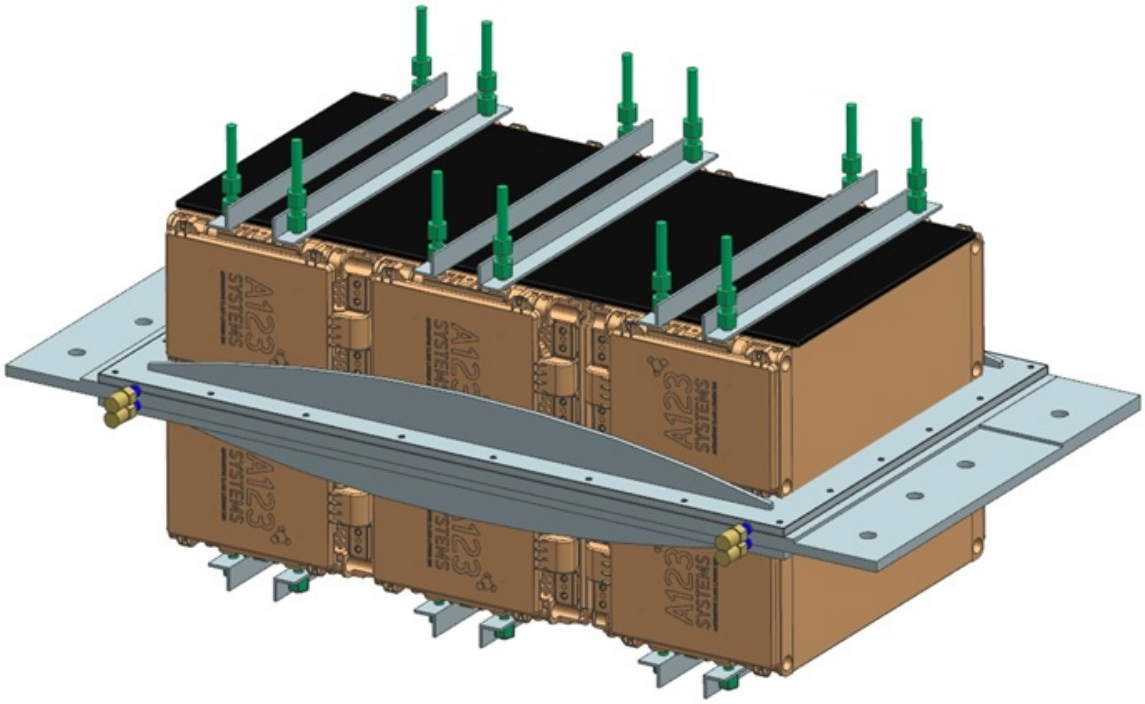

Figure 3.17. Aluminum structure of battery box with all battery modules in place.

spread load evenly across each module, steel threaded rod (shown in green in Figure 3.17) passed through the entire structure to maintain the aluminum angles on each side of the battery box, and vibrational padding was used to isolate (vibrationally and electrically) the modules from the aluminum angle. Once the battery modules were held in place, the structure was oriented upright while a fiberglass plate was placed above the top row of modules. This plate acted as a mounting source for the Current Sense Module, Battery Monitoring Module, Electrical Distribution Module and Manual Service Disconnect Switch.

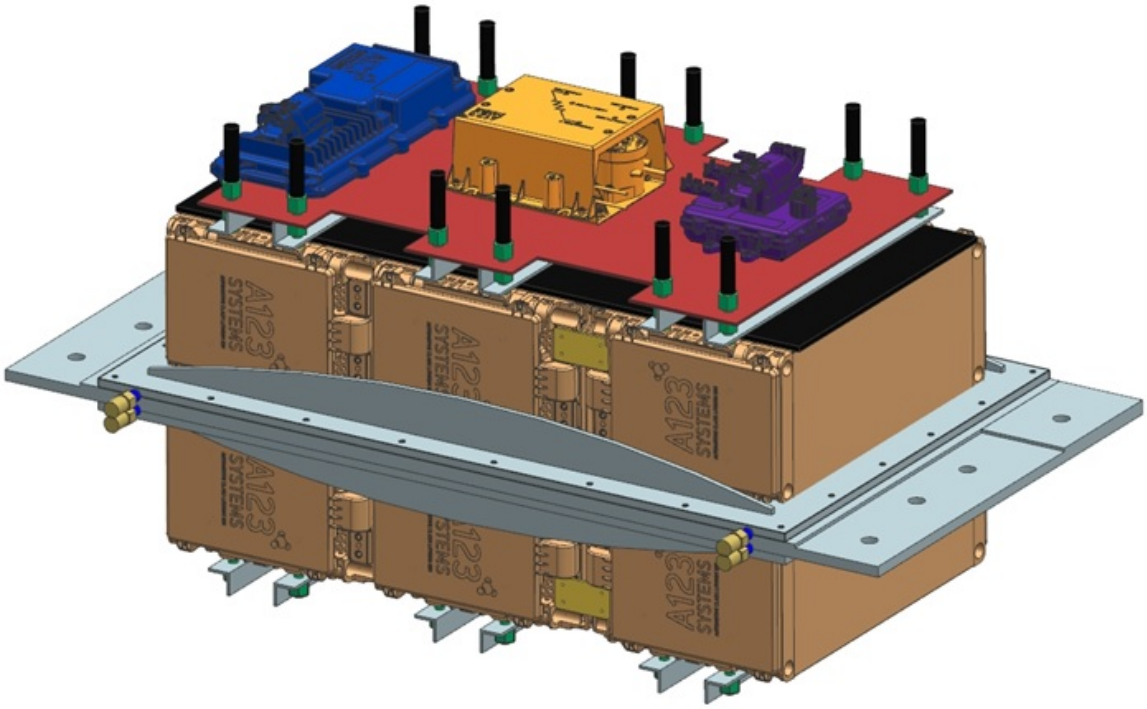

Figure 3.18. Aluminum structure of battery box with all battery modules and power electronics in place.

Electrical Routing

Since high voltage cable is capable of handling high electrical power, it is inherently very thick and heavy. Therefore, by reducing the length that high voltage cable must travel, it was possible to reduce overall weight of a battery pack. With this in mind, two of the battery modules were oriented such that their respective high voltage connection points were within 3 inches of each other. To connect this short distance, a section of copper sheet with the same cross sectional area as the required cable equivalent was used to connect the modules. For other connections, two similar yet longer copper plates were used to connect modules together. These copper plates were referred to by the team as "Bus Bars" and were coated in electrically insulated orange tape for safety considerations. Figure 3.19 emphasizes the longer set of bus bars, while the shorter two can be seen in Figure 3.18.

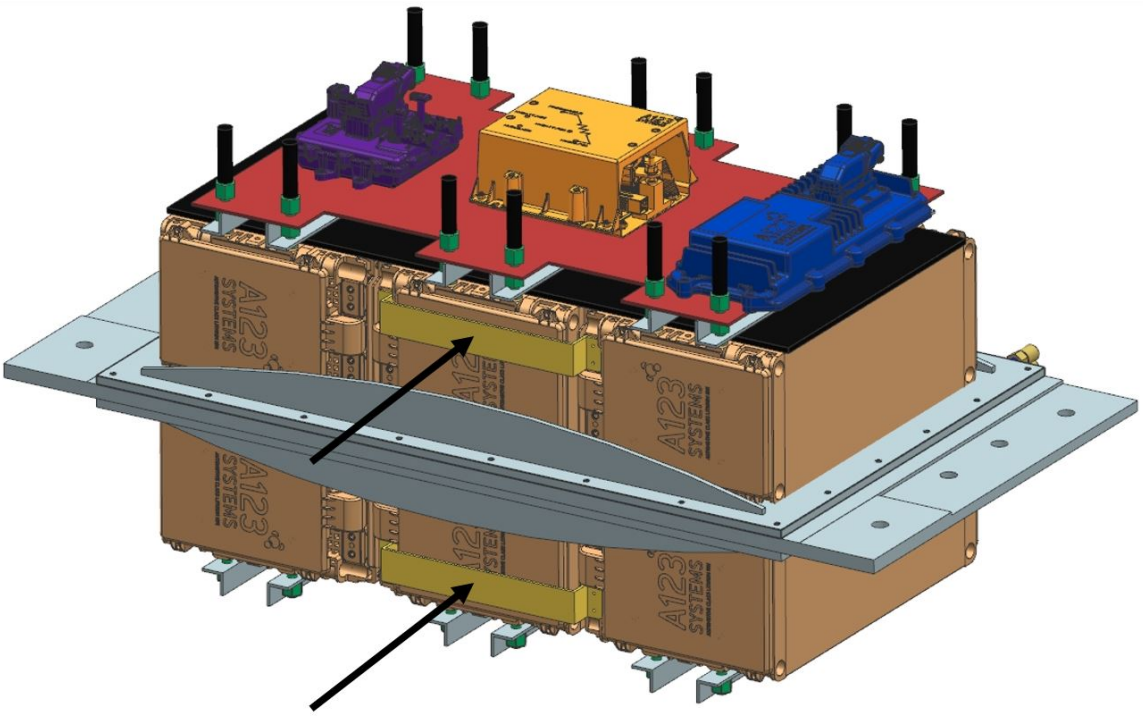

Figure 3.19. Battery Box with bus bars emphasized.

Figure 3.20 depicts the low-voltage wiring harness (shown in blue) used to connect the battery modules, EDM, CSM and BMM together, while Figure 3.21 includes the high voltage harness (shown in translucent orange) used to connect the battery modules, MSDS, CSM and EDM together. Making these harnesses on CAD was useful since it was possible to program the minimum bend radius of each cable into the module, assuring the team that each cable (particularly high voltage cable) was capable of fitting physically as it did on CAD. Additionally, it was necessary to mill large oval sections (seen in Figure 3.22) out of all aluminum plates such that high and low voltage wiring could pass from one side of the battery box to the other.

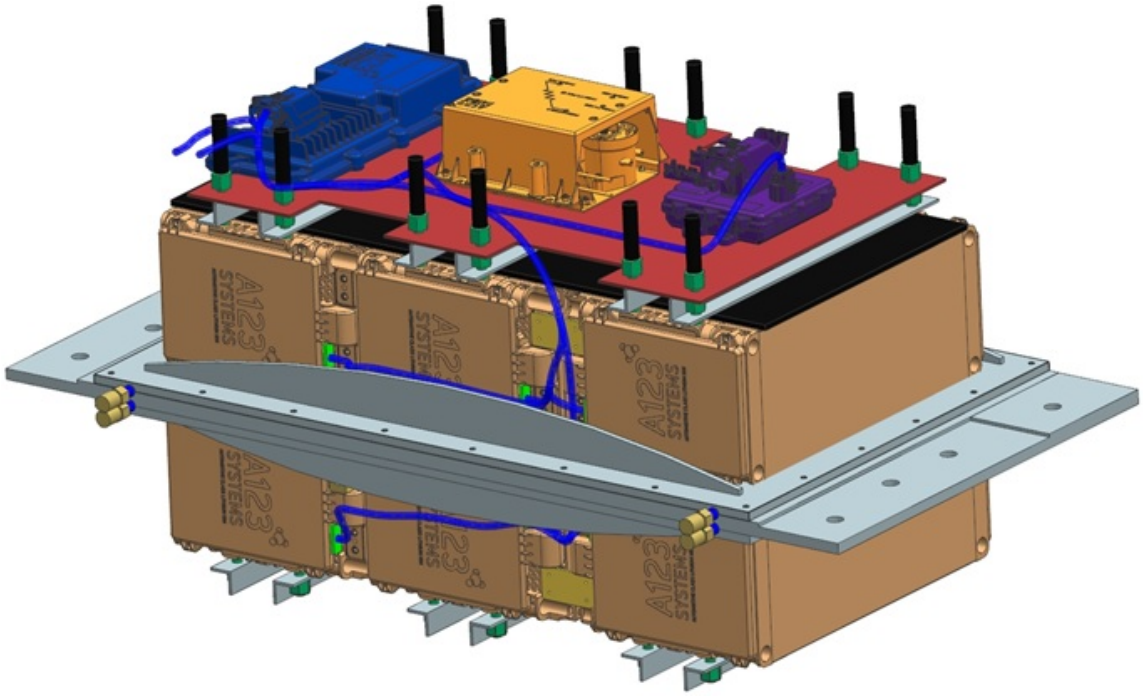

Figure 3.20. Battery Box with low voltage harness emphasized.

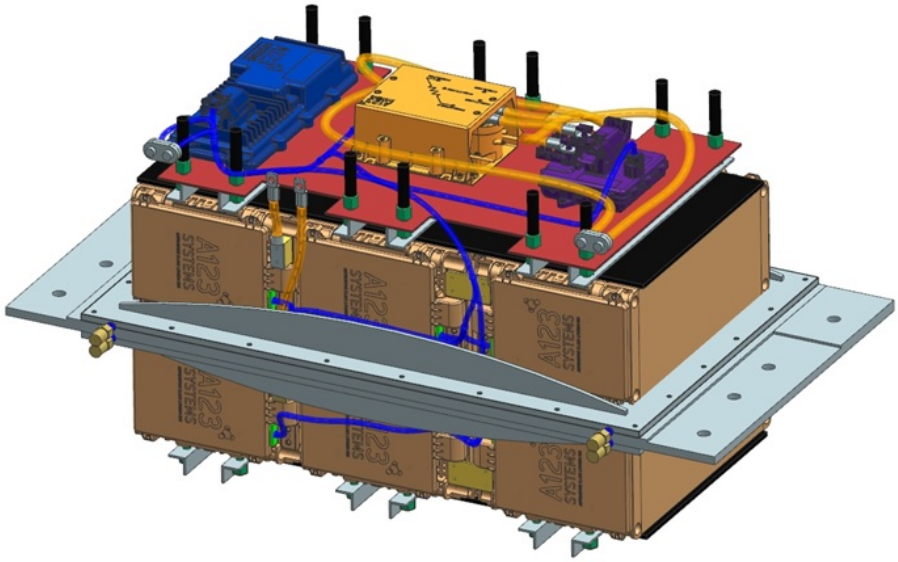

Figure 3.21. Battery Box with high voltage harness emphasized.

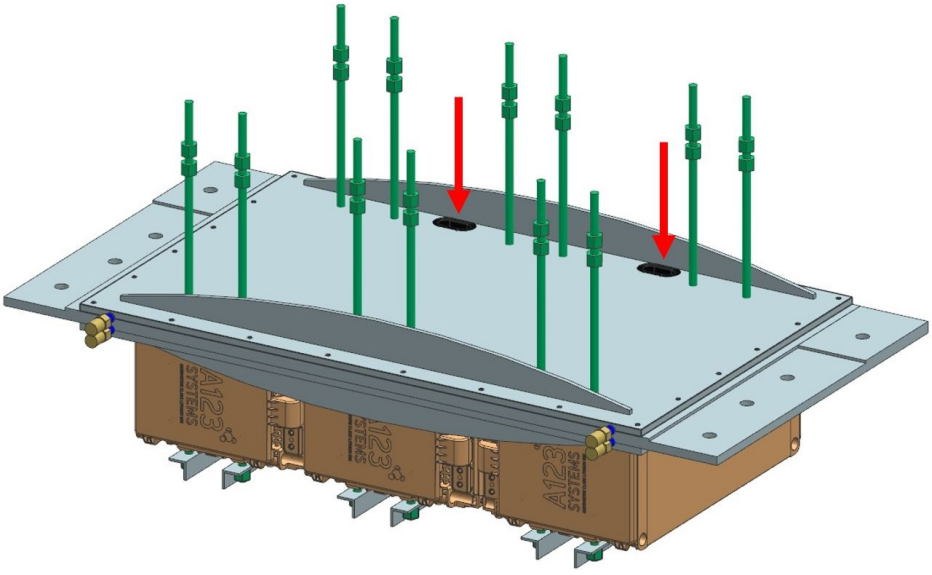

Figure 3.22. Battery Box with high voltage pass-throughs emphasized.

However, in order to ensure that the battery box design was sufficient, there were several additional considerations that must have been satisfied including structural, and thermal integrity of the pack.

3.2.1 Structural Analysis

The rules of the competition stated that the ESS must be capable of withstanding a 20G lateral static load in all lateral (left, right, fore, aft) directions as well as a static 8G load in all vertical directions (up, down). To ensure this, Finite Element Analysis was performed on the aluminum structure of the ESS as well as the threaded rod and aluminum angle used to hold the battery modules in place. Due to the "I-Beam" style shape of the aluminum structure, the Purdue team was confident that it would be capable of withstanding the static loads required. However, the constraint of how thin of material may be used was not based on static load. Since it was intended that Lytron cold plates be press fit into the middle aluminum plate, the thickness of the middle plate was required to be larger than the height of the cold plate. This thickness was higher than what was required by static load analysis, therefore the middle plate was larger than necessary.

Boundary Conditions

To determine what boundary conditions were required for analysis, it was important to know how the box would be attached to the vehicle. As mentioned previously, the middle aluminum plate of the battery box was wide enough to span across both chassis framerails of the vehicle. Since vibrational damage was a concern, it was determined that hard-mounting the battery box to the chassis of the vehicle would be sufficient vibrational isolation since the body of the vehicle contains sensitive electronics similar to the ones used in the battery box. Therefore, the team determined that if the battery box experienced vibrations similar to those experienced by the body of the vehicle, the electronics within the ESS would remain intact. Therefore,

the mounting conditions for the ESS were that it would be hard-bolted to the bottom face of the rear chassis framerails. After observing the chassis framerails, it was discovered that there were several holes available for use on the bottom surface of the framerails. Since the rules of the competition stated that no new holes may be drilled into the safety cage of the vehicle (shown in Figure 1.19 on page 23), it was highly beneficial to discover that there were existing holes in the framerails that were available to use. Figure 3.23 depicts the battery box placement within the vehicle, while Figure 3.24 depicts the bolt holes used by the ESS.

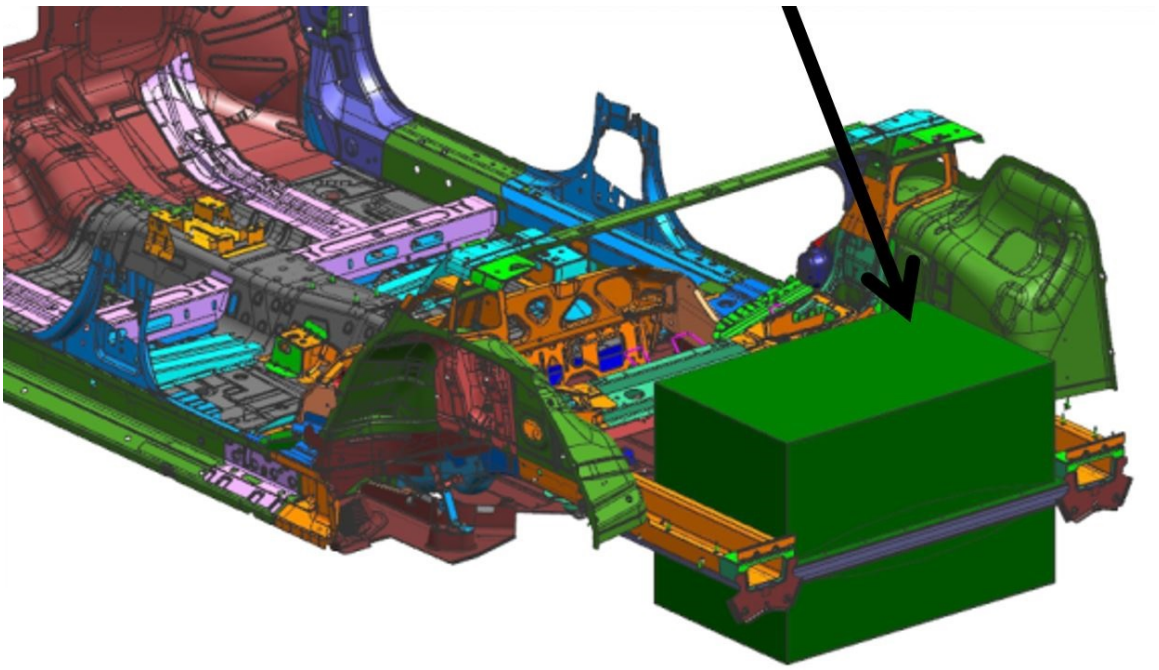

Figure 3.23. Placement of the battery box within the vehicle.

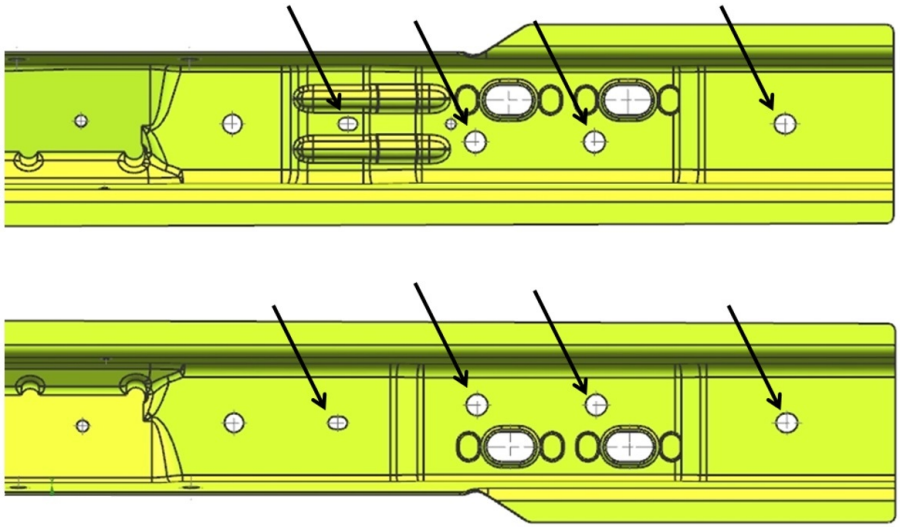

Figure 3.24. Bolt holes to be used by the ESS mounting bolts.

Once this was established, it was possible to create meshed models of the aluminum structure as well as the chassis framerails for the purpose of Finite Element stress Analysis. Shown in Figure 3.25 is a simplified model of the body structure of the rear of the vehicle along with the aluminum structure and battery modules of the ESS. Shown in Figure 3.26 is a similar model with further simplified representations of the chassis framerails.

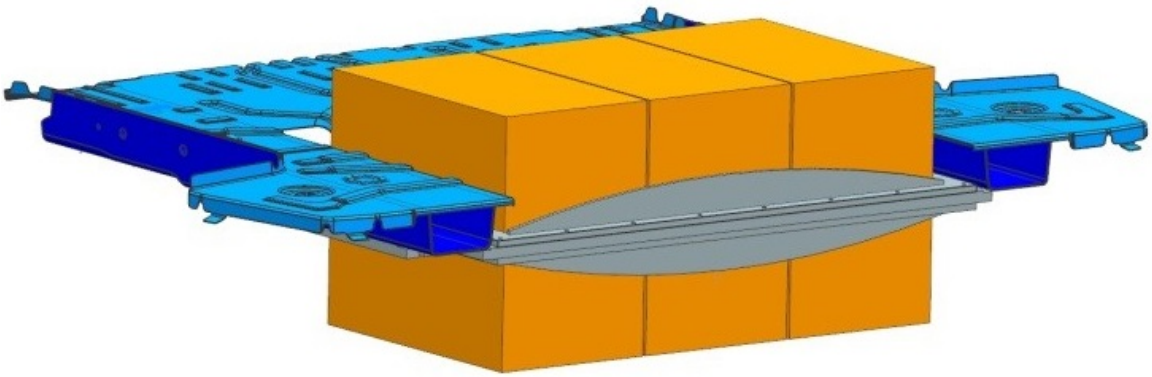

Figure 3.25. Simplified CAD model of the rear of the vehicle including ESS.

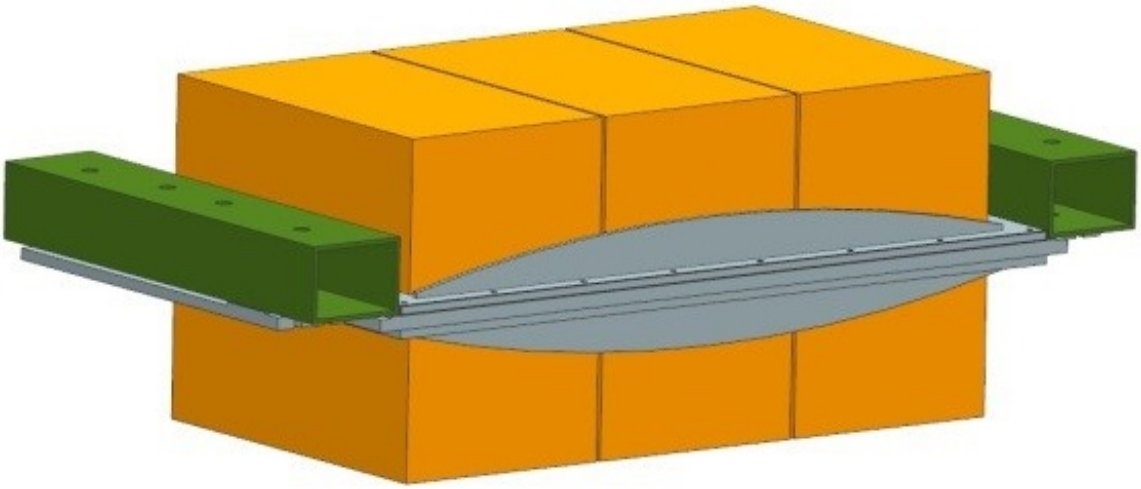

Figure 3.26. Further Simplified model of the rear of the vehicle with ESS.

During this procedure, it was discussed how to fix the framerails during analysis. One suggestions was to fix the front face of the framerails to produce a cantilever style action of the framerails, similar to how the rear end of a vehicle is a cantilever fixed via the middle of the vehicle body. This constraint would determine the extra stress experienced by the chassis framerails due to the added mass of the ESS. After raising this point to the GM mentors of the competition, it was discovered that since the vehicle body is a uni-body structure, proper representation of the cantilever action experienced by the rear of the vehicle would require meshing of the entire rear of the vehicle as seen in Figure 3.27. While this analysis was possible, it was deemed unnecessarily difficult by the GM waiver team as they were confident that the chassis and body of the vehicle were capable of handling the added mass. Therefore, the Purdue team fixed both ends of the chassis framerails during their analysis and focused on the stresses experienced by the ESS structure as well as the bolts that held them in place.

In order to represent the aluminum structure of the ESS, 3-D meshed models of all three sections were created, then surface-to-surface glued to each other. 2-D meshes

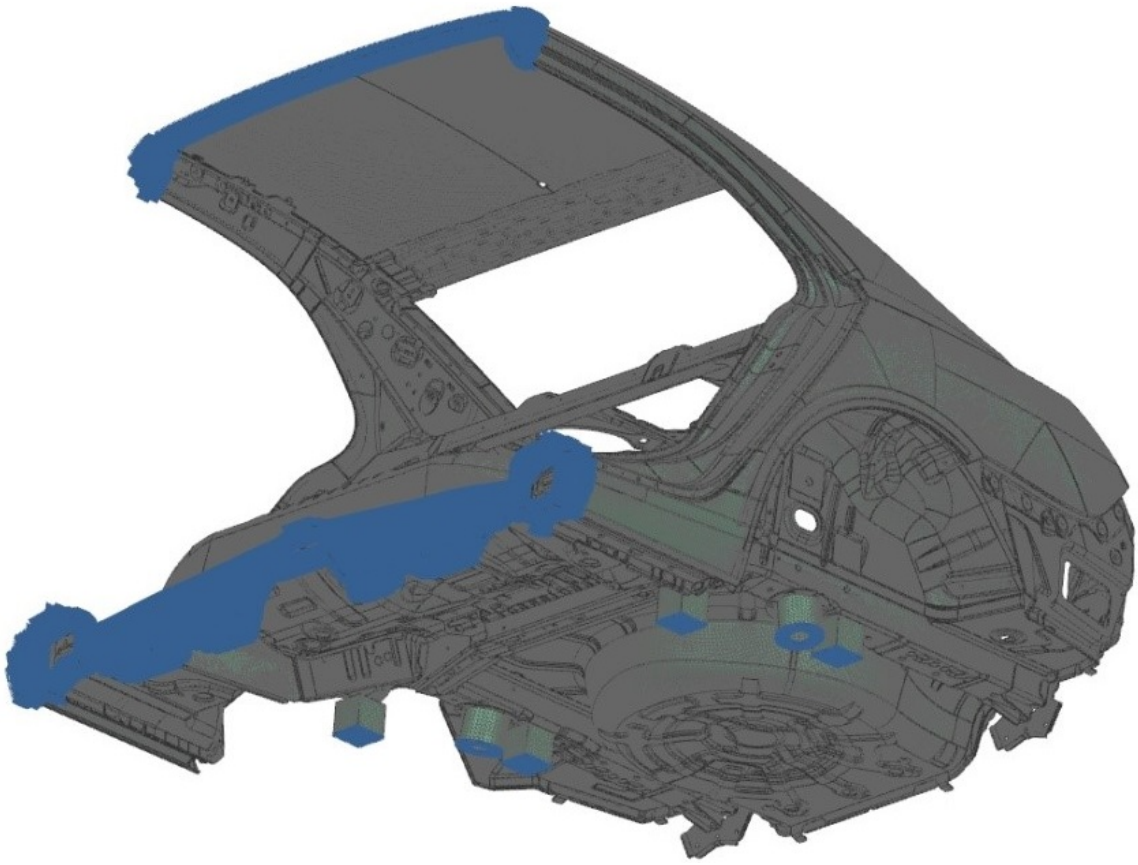

Figure 3.27. Meshed model of the rear of the vehicle.

were used to represent the framerails which were fixed at both the front and rear ends. Next, the two meshes were bolted together at the bolt locations specified in Figure 3.24 on page 104. Next, 3-D meshed models of the battery modules were created, then glued to their respective surfaces of the aluminum structure. Once material properties were assigned to all respective meshes, gravitational loads were applied in all directions required by the load sub-cases specified earlier. Figure 3.28 depicts the stress results from the meshed assembly under an 8G downward load with exaggerated displacement and indications for the mounting locations as well as the load bearing surfaces.

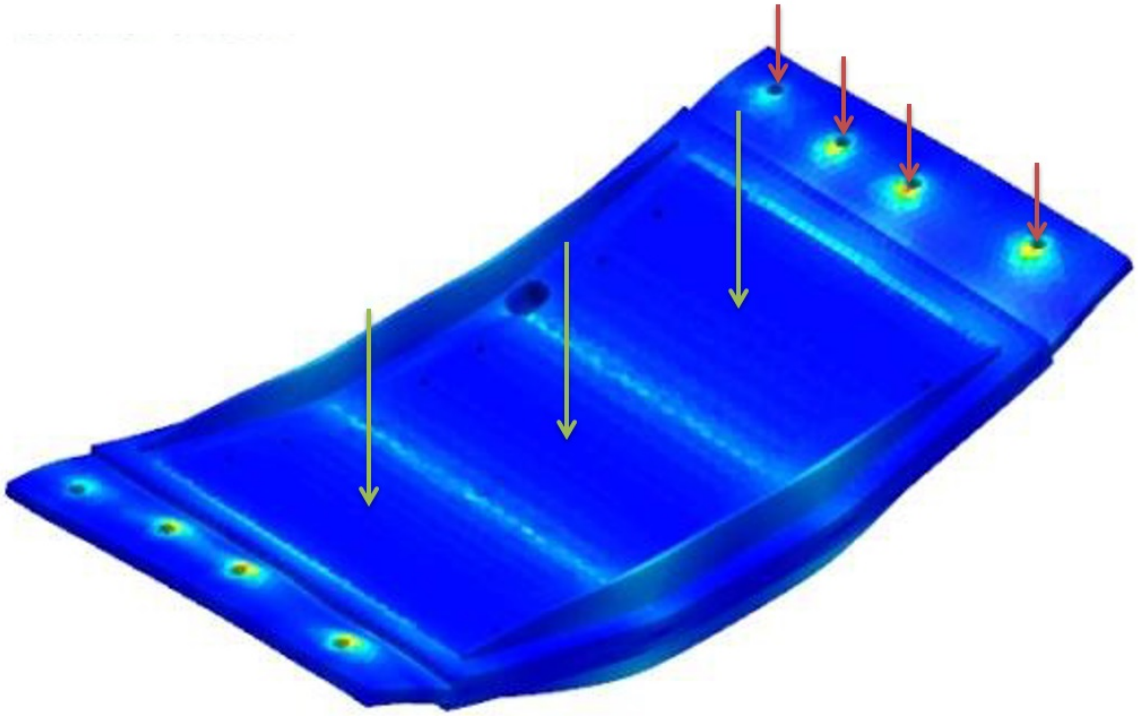

Figure 3.28. FEA model of Aluminum structure experiencing an 8 G vertical load.

Figures 3.29 and 3.30 depict other load cases used during analysis with exaggerated displacement.

Figure 3.29. FEA model of Aluminum structure experiencing a 20 G lateral load (left).

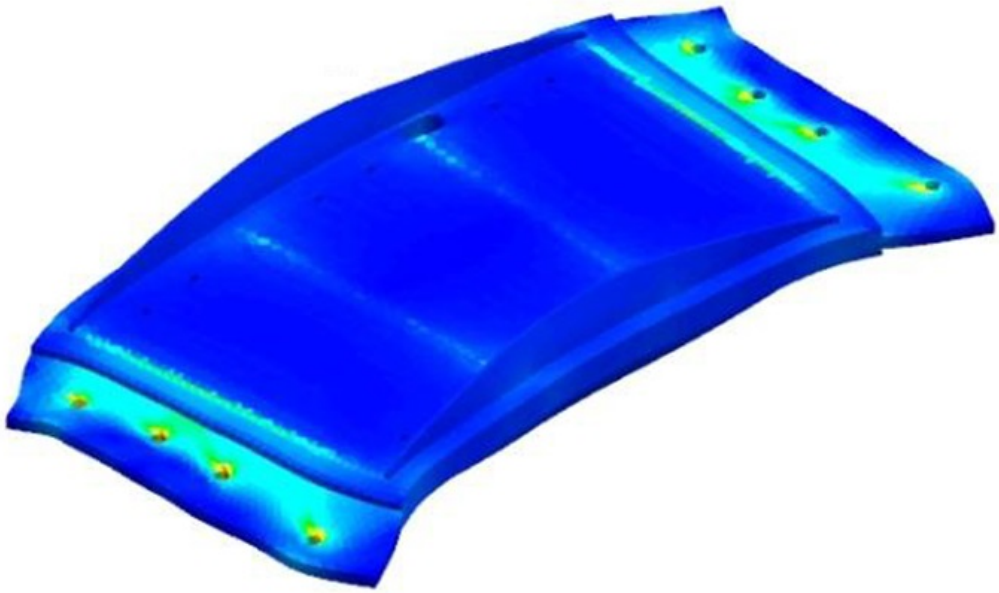

Figure 3.30. FEA model of Aluminum structure experiencing a 20 G lateral load (fore).

Similar to the analysis procedure used to design the rear suspension cradle, by exaggerating displacement and highlighting stress concentration areas, it was possible to determine which parts of each structure were contributing to structural integrity. With this, the Purdue team was able to gain more confidence in their design, allowing them to begin planning for fabrication of the aluminum structure. Figure 3.31 depicts the stress analysis results from the threaded steel rod used in the ESS. Since the OD of the threaded rod was as high as the battery modules would allow, it was crucial that the analysis demonstrate success of the material. Otherwise, the team would have had to either switch material, or use solid rod with retaining rings on each end; an option that was less desirable due to a lack of accessibility.

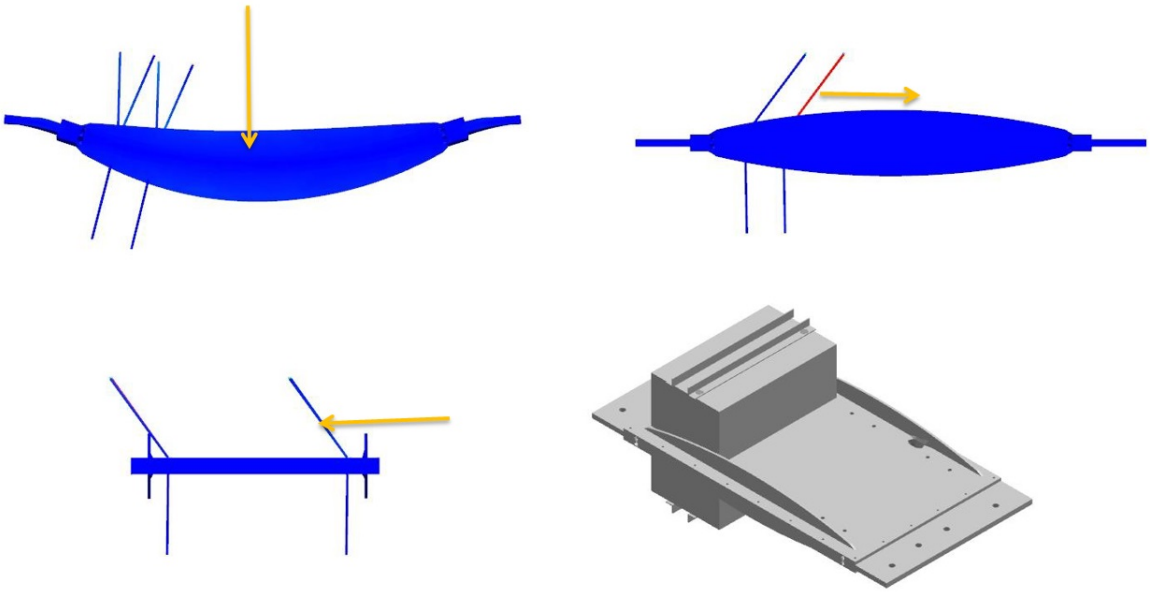

Figure 3.31. FEA model of the threaded steel rod experiencing a all load subcases.

After interpreting the results of the ESS aluminum structure and steel threaded rod analyses, the ANL waiver team gained enough confidence of structural integrity to allow the Purdue team to fabricate and use the ESS design used in the analysis.

3.2.2 Thermal Analysis

When considering the thermal demand of the battery pack, it is important to consider factors such as the peak and nominal thermal output of each battery module, the minimum, maximum and ideal temperature of each module, as well as the minimum and maximum ambient temperatures the ESS will experience during normal vehicle operations. Additionally, since the thermal management system was designed to operate symbiotically with the stock climate control system of the base vehicle, it was necessary to consider how the thermal demand of the climate control system would affect the available power to be used by the ESS thermal management system.

Thermal Demands

The main thermal constraint of the battery pack was that all modules were programmed to reduce power output if their internal temperature reached 50 degrees Celsius (122 degrees Fahrenheit). Additionally, it was known that the Year 2 vehicle competition would take place at Yuma, AZ during May of that particular year. With that, it was researched that the maximum recorded temperature during May in that area was 49 degrees Celsius. Therefore, it was determined that the pack should have sub-ambient capabilities, hence the decision to operate symbiotically with the stock AC system. Additionally, it was discovered that at module temperatures below 10 degrees Celsius, the charging and discharging capabilities of the battery modules would be reduced. Since no vehicle competitions during EcoCar2 occurred during winter months, the Purdue team elected to not include a heating system for the ESS. The ideal temperature range of the battery pack was specified as 10 - 35 degrees Celsius. With this, it was possible to construct a list of requirements for the ESS cooling system as seen in Table 3.1.

Table 3.1. Thermal Properties of ESS used in analysis.

Signal	**Value**
Max Coolant Inlet Temp	40 C
Target Coolant Inlet Temp	30 C
Steady State Heat at 16kW Battery Power Output	160 W
Steady State Heat at 45kW Battery Power Output	1250 W
Target Coolant Flow Rate	15 L/min
Target Coolant Flow Inlet Pressure	0.8 barg
Max Coolant Inlet Pressure	1.5 barg

Figure 3.32 depicts a diagram of the thermal circuit to be used for both the battery pack as well as the climate control system. Figure 3.33 depicts a diagram of how each component will be placed within the vehicle in the effort of maximizing exposure of above-ambient temperature components while minimizing exposure of sub-ambient temperature components. This design philosophy was used to decrease the amount of ambient heat that would contaminate the refrigerant circuit while also increasing the total amount of heat dissipated by the refrigerant system. It should be noted that both the Evaporator/Expansion Valve and the heat exchanger/Expansion Valve connections occur as one singular unit in order to minimize the length of exposed cold refrigerant to ambient air.

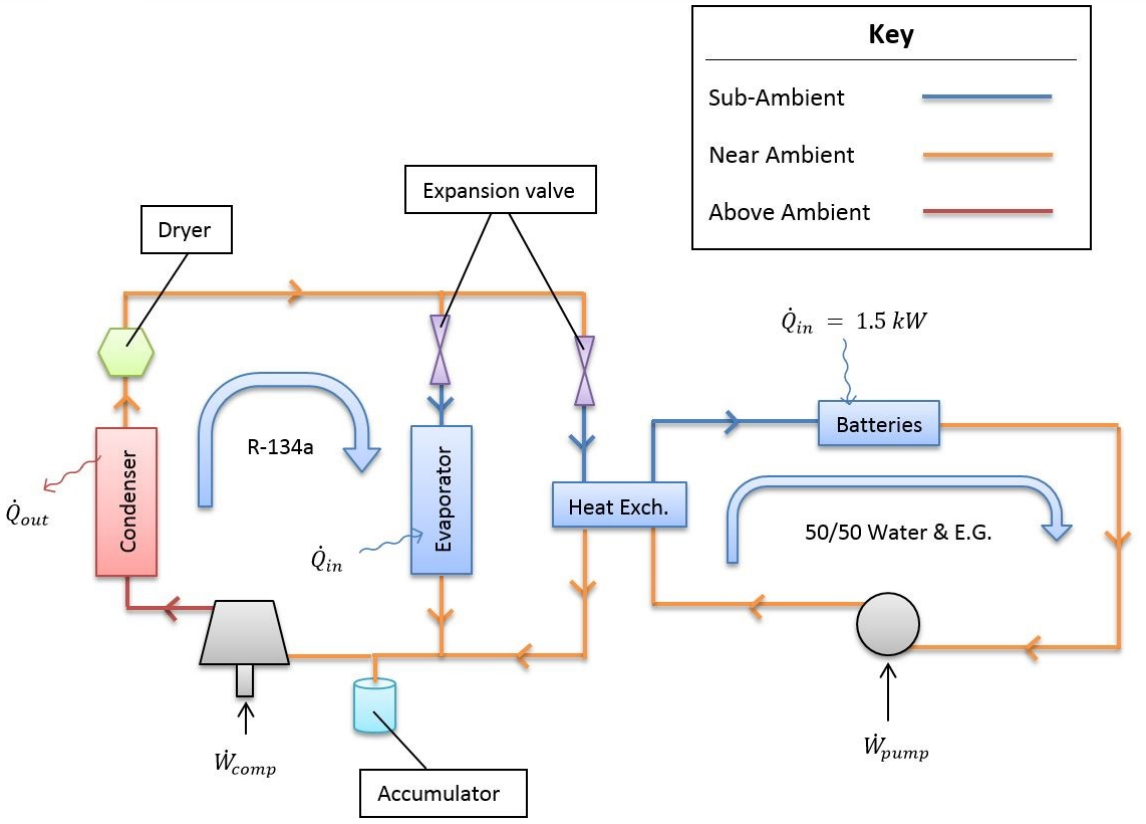

Figure 3.32. Diagram depicting the thermal circuit used within the vehicle.

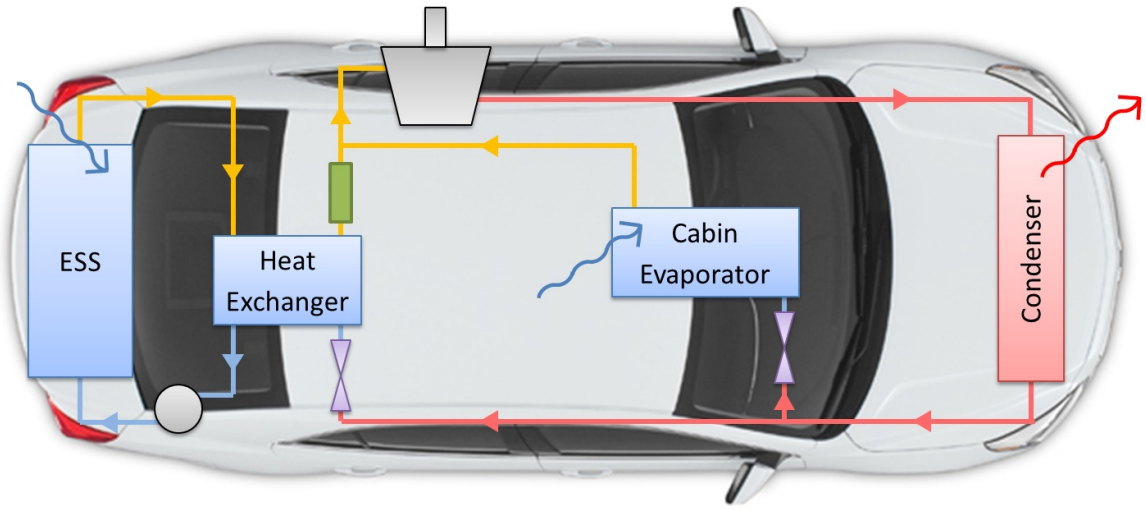

Figure 3.33. Diagram depicting the thermal circuit used within the vehicle.

4. THERMAL MANAGEMENT SYSTEM

Both the ESS and the cabin of the vehicle required sub-ambient cooling systems, which required the use of a refrigerant circuit. The main power draw of the cooling circuit was the compressor, which was driven by high voltage electricity. Since the combustion engine of the vehicle was not always running, it was not feasible to incorporate a belt-driven AC compressor. Since the HV AC compressor was driven via high voltage electricity, reducing its energy consumption increased the total amount of electricity the ESS could use for driving purposes. Most importantly, increasing electrical efficiency increased the Electric-Only range of the vehicle, a very high priority of the design. This chapter will explore how the Purdue team attempted to increase efficiency of the thermal circuit without affecting performance, accessibility or safety.

4.1 Thermal Circuit

4.1.1 Thermal Demands

Figure 4.1 depicts the vehicle with the ESS, Cabin and Condenser represented by colored blocks. The red blocks depict components that remain above ambient temperature, while the blue blocks represent those below ambient temperature. It was desired by the system that the thermal system be capable of absorbing thermal energy from the ESS and Cabin and exhaust thermal energy to the environment.

Figure 4.2 depicts the vehicle with its stock AC system for cabin cooling. Since all of the parts were new and formed to fit easily with the vehicle, it was desired to use as many stock components as possible. However, as mentioned previously, the stock AC compressor was belt driven by the combustion engine and was therefore

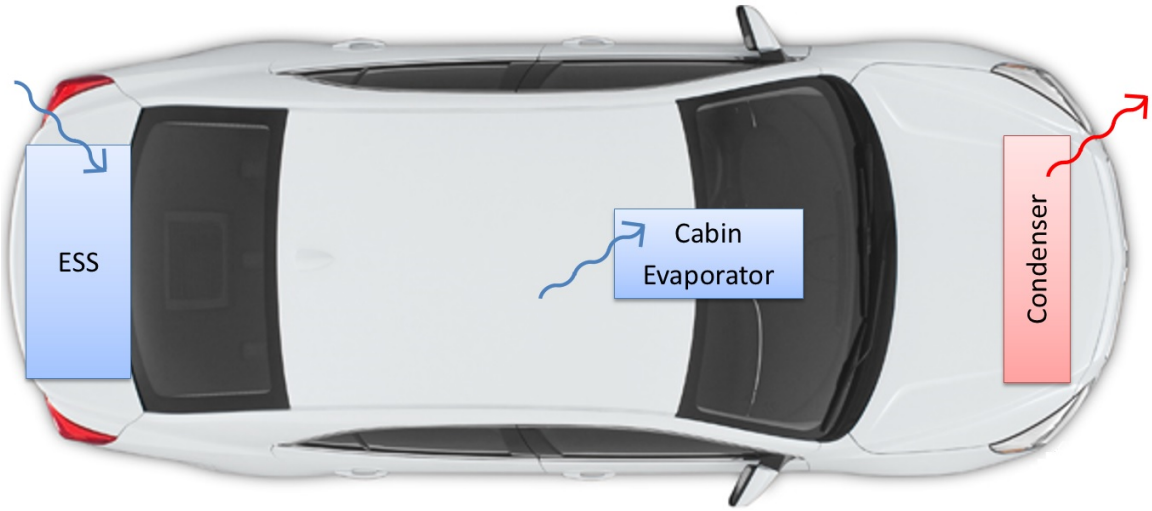

Figure 4.1. Diagram of vehicle with significant thermal components indicated.

not viable to be used for cooling purposes. Therefore, a high voltage electric AC compressor was used.

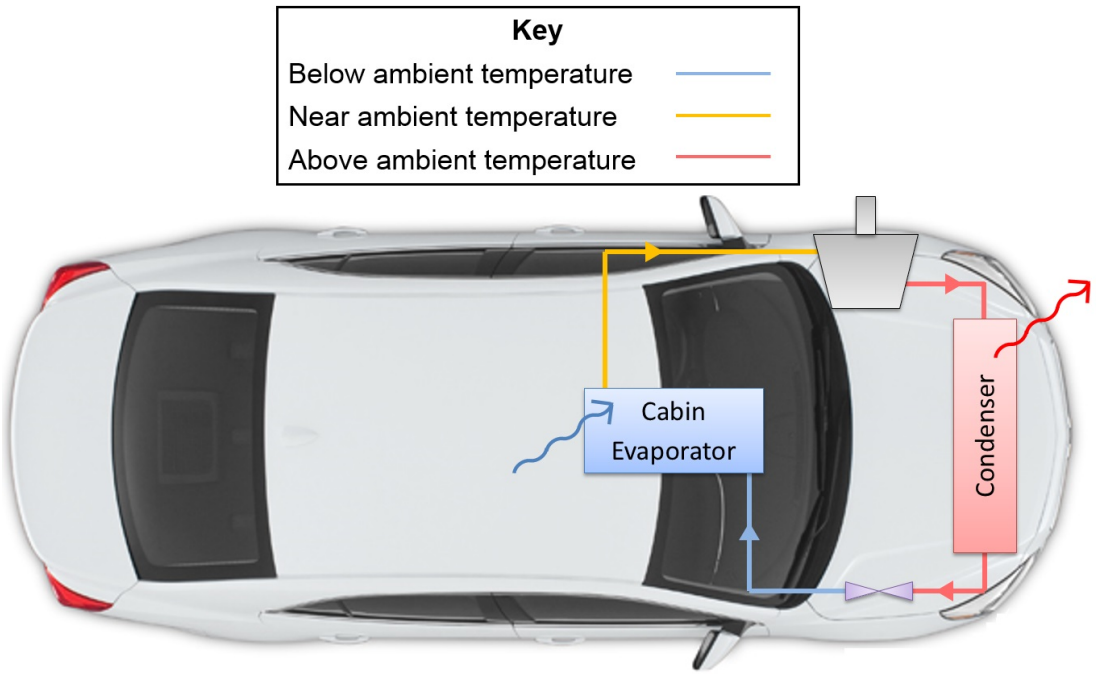

Figure 4.2. Diagram of vehicle with stock AC system indicated.

Figure 4.3 depicts the vehicle with the custom thermal loop created by the Purdue team. The high voltage AC compressor was placed in the rear of the vehicle so that the overall length of high voltage wiring between the ESS and compressor be decreased. Additionally, a liquid coolant loop (shown connecting the ESS, pump and heat exchanger) connected to a stacked plate heat exchanger was used in order to transfer thermal energy from the ESS to the refrigerant loop.

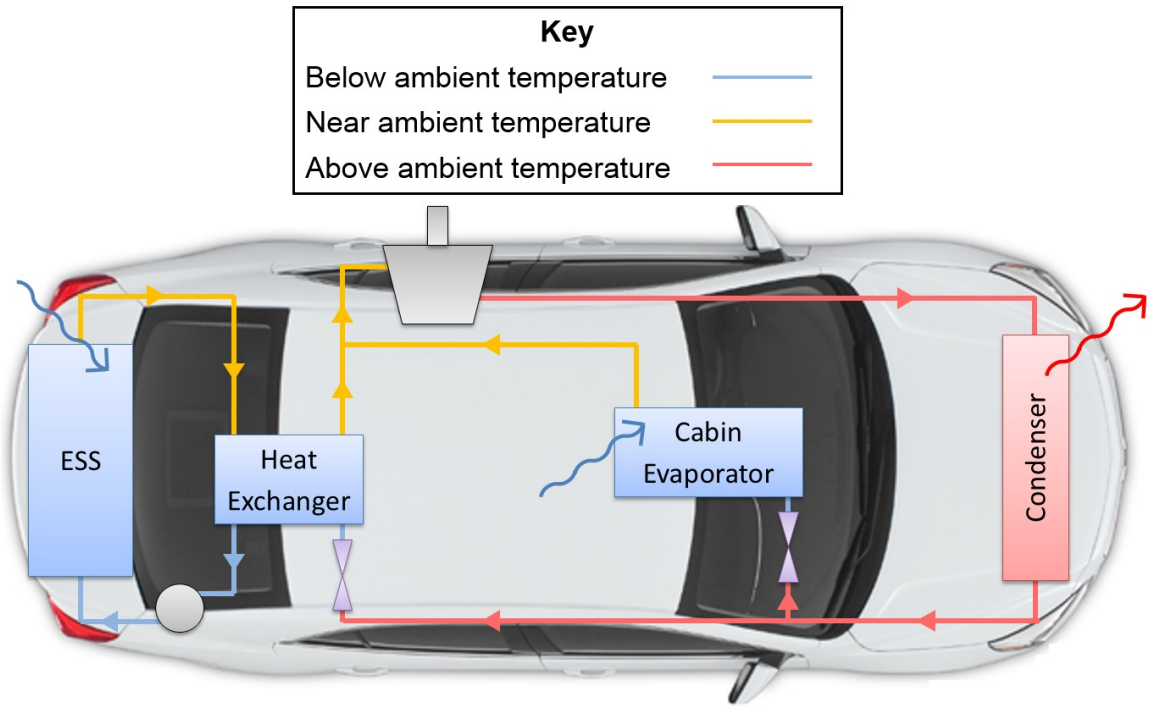

Figure 4.3. Diagram of vehicle with custom AC system indicated.

4.1.2 Battery Pack

Cooling Options

During the design phase of the ESS, there was much discussion concerning what method to use in order to absorb the heat generated by the battery modules. The

thermal-absorptive fluids proposed included cabin air, refrigerated air, ambient air-cooled liquid and refrigerated liquid. Overall, the refrigerated-liquid option was favored since it required less volume to package than air cooling (due to its use of tubing rather than air ducts), it had higher thermal transfer potential than air cooling (due to higher convection coefficients) and it was capable of reaching sub-ambient temperatures (due to refrigeration capability).

Thermal Transfer

Since the Lytron cold plates were press-fit into the aluminum structure, the thermal energy generated by the battery modules traveled from each module to the interior surface of the cold plate tubing via conduction sequences, a highly effective thermal transfer mode since all materials used (aluminum, copper, thermally conductive insulation pad) are very thermally conductive. Therefore, thermal transfer within the ESS was maximized via materials selection and fabrication techniques.

4.1.3 Heat Exchanger

The heat exchanger used in the thermal circuit shown in Figure 4.3 was a stock component from a 2013 Chevrolet Volt and contained a Thermal Expansion Valve (THX) and plate heat exchanger in one cohesive unit. Since the plate heat exchanger has two separate fluid loops, there are two fluids being used during operation: coolant and refrigerant. The coolant used for the Purdue vehicle was water, while the refrigerant used was R-134a.

Coolant Side

On the coolant side of the Heat Exchanger was a closed loop consisting of a pump and the Lytron cold plate embedded into the ESS. Therefore, it was possible to control the pump flow rate in the effort of removing more or less thermal energy from the

ESS, assuming that sufficient cold conditions were met on the refrigerant side of the heat exchanger.

Throughout the thermal circuit, there were two components which required power input: the ESS coolant pump and the high voltage AC compressor. Increasing the power supplied to either of these components would result in more heat removal from the ESS. However, the maximum power draw of the pump was significantly lower that the maximum power draw of the compressor. Therefore, operating the pump at maximum power was a more desirable method of increasing the ESS heat removal rate since it consumed less power than increasing the power of the compressor.

Refrigerant Side

On the refrigerant side of the heat exchanger, it was necessary that the refrigerant flow to the battery heat exchanger be independent from the flow to the climate control system. For instance, if there was a scenario where the cabin of the vehicle demanded AC cooling while the battery pack demanded none, the vehicle should have been capable of sending refrigerant only to the climate control evaporator. To accomplish this, the Purdue team incorporated a spring-loaded Evaporator Pressure Regulating Valve (EPRV) after the outlet of the refrigerant side of the battery heat exchanger.

Evaporator Pressure Regulating Valve

Several options of how to vary the flow rate between the cabin AC loop and the battery AC loop were proposed. The most common proposal was to incorporate two solenoid-actuated flow valves that could provide on/off flow control for each AC loop. However, these components were found to be expensive and cumbersome. Eventually, the team elected to use the EPRV since it was simple, small and durable enough to withstand the vibrations of the vehicle.

Figure 4.4 shows the custom Purdue thermal circuit used, with the addition of an Evaporator Pressure Regulating Valve (EPRV) after the heat exchanger used on

the ESS cooling loop. This component could increase or decrease the refrigerant flow across it based upon the temperature of the incoming refrigerant. Therefore, if the ESS required a high cooling rate, the ESS coolant pump could increase its flow rate, thus increasing the thermal rejection into refrigerant within the heat exchanger. This would increase the temperature of the refrigerant leaving the heat exchanger, thus allowing a higher flow rate of cold refrigerant across the ESS refrigerant loop of the thermal circuit.

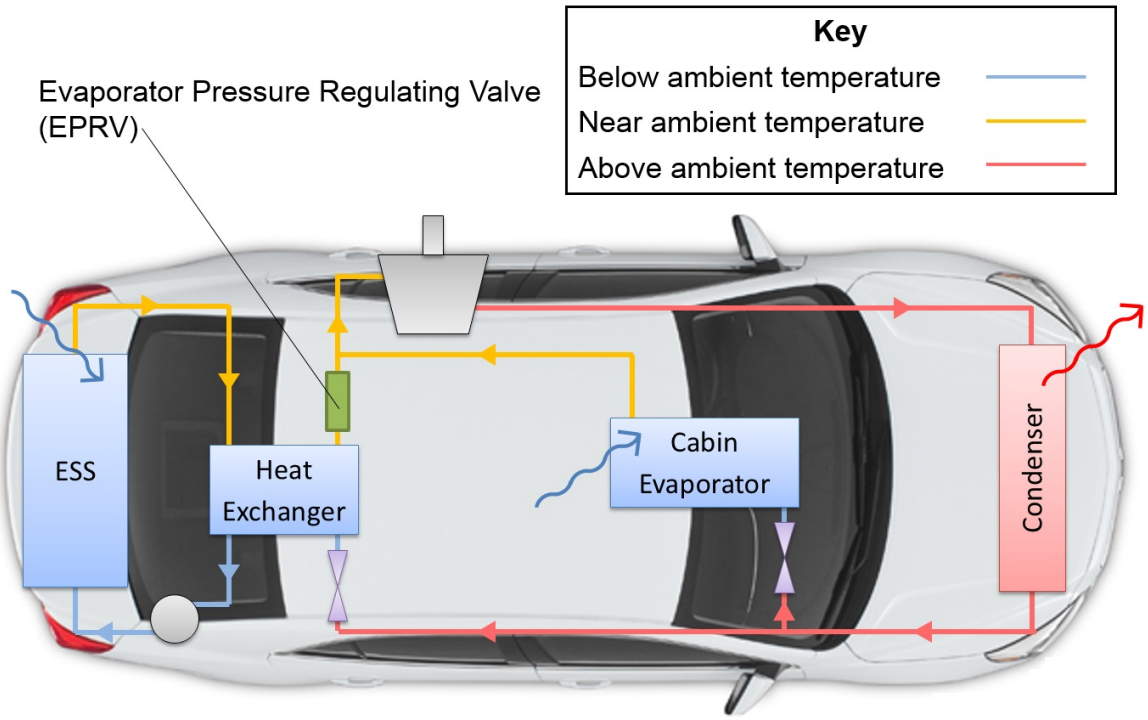

Figure 4.4. Diagram custom AC system with EPRV included.

Figure 4.5 shows how the pressure of the incoming refrigerant determines the flow rate across the valve. Therefore, since pressure of the refrigerant is proportional to the temperature, increasing the temperature of the incoming refrigerant was capable of controlling the flow rate. Additionally, since the battery modules had built-in thermocouples, the pump controller would measure the battery module temperature, and use this to vary the pump flow rate.

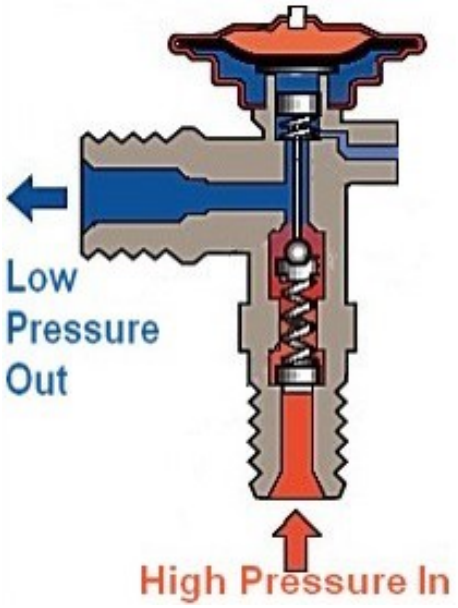

Figure 4.5. Sectioned diagram of the EPRV used.

4.1.4 Refrigerant Routing

Since some of the refrigerant components were located in the rear of the vehicle and others in the front, it was required to install refrigerant tubing that traveled from the front of the vehicle to the back. With this in mind, the tubing used was thermally conductive. Additionally, the expansion valve for the battery loop was located in the rear of the vehicle. Due to this, of the three refrigerant lines that traveled from the front of the vehicle to the back, two of them were kept above ambient temperature while the third was kept near ambient temperature. Therefore, the high temperature, conductive lines dissipated heat to the environment, thus increasing performance of the thermal circuit. Additionally, contact between the sub-ambient tubing and the environment was minimized, thus decreasing how much ambient thermal energy leaked into the cold refrigerant.

Figure 4.6 shows several of the refrigerant lines used to construct the refrigerant circuit on the Purdue vehicle. As mentioned previously, some sections of the refrigerant lines were desired to be thermally conductive. Therefore, these sections were

constructed from rigid aluminum tubing. However, the sections that were desired to be insulated were constructed of flexible rubber tubing. Therefore, a combination of flexible and rigid tubing allowed each component to move within a reasonable amount so that each connection could have been reached and serviced.

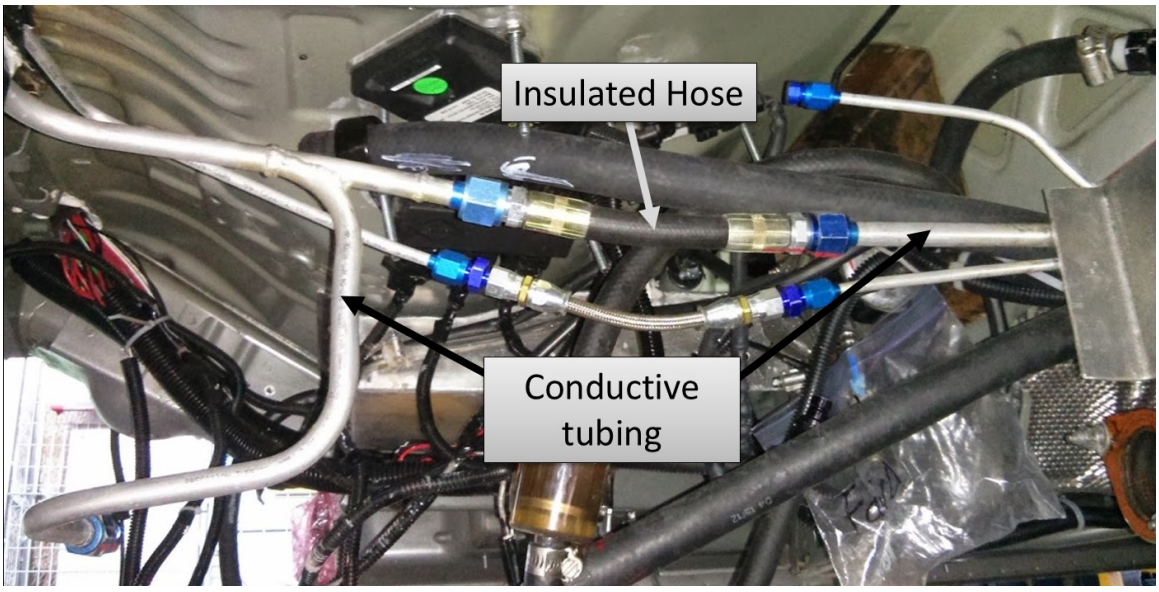

Figure 4.6. Image of refrigerant lines used on Purdue vehicle.

4.1.5 Refrigerant Line Connections

Since vehicle design process occurred during a relatively short period of time, it was assumed that the vehicle would be experiencing constant maintenance by the Purdue team. Additionally, it was assumed that some goals proposed initially may not be feasible during latter stages of the competition. Since the AC system of the vehicle spanned across the entire body of the vehicle, there would have been very steep maintenance challenges if the AC routing was not removable or flexible.

During Year 2 of the competition, the AC circuit was constructed via aluminum and inflexible rubber tubing. Many of the aluminum/aluminum connections were

welded, while many of the aluminum/rubber connections were crimped connections. Both methods are one-time connections and cannot be undone without destroying the connection. Eventually, the AC harness developed a leak which would have been a minor fix, however the component with the leak was very difficult to access and remove. Therefore, during year 3, the Purdue team elected to take a different approach to fabricating the AC circuit. The main difference was that the new design utilized 37° flared JIC fittings to connect flared aluminum tubing to flexible hose. The aluminum tubing was used as the female end of the fitting as seen in Figure 4.7 and the flexible hoses contained male JIC fittings similar to the one shown in Figure 4.8.

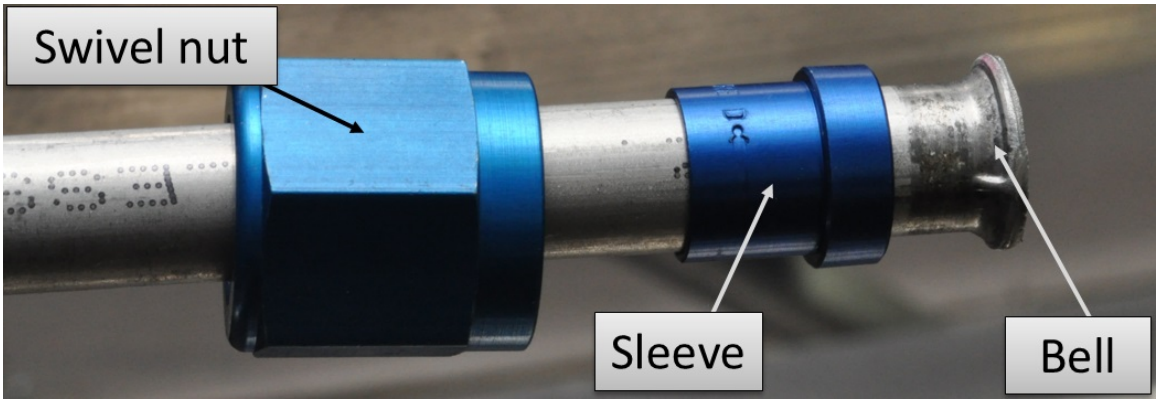

Figure 4.7. Concentrated view of flared aluminum tubing with a JIC nut and sleeve.

Figure 4.8. Example of a male JIC fitting.

To connect the two, the male flared fitting would fit inside the bell shape created on the aluminum tubing. Once in place, the blue swivel nut shown in Figure 4.7 would thread onto the male threads of the JIC fitting shown in Figure 4.8, thus creating a sealed connection between the two pieces as seen in Figure 4.9.

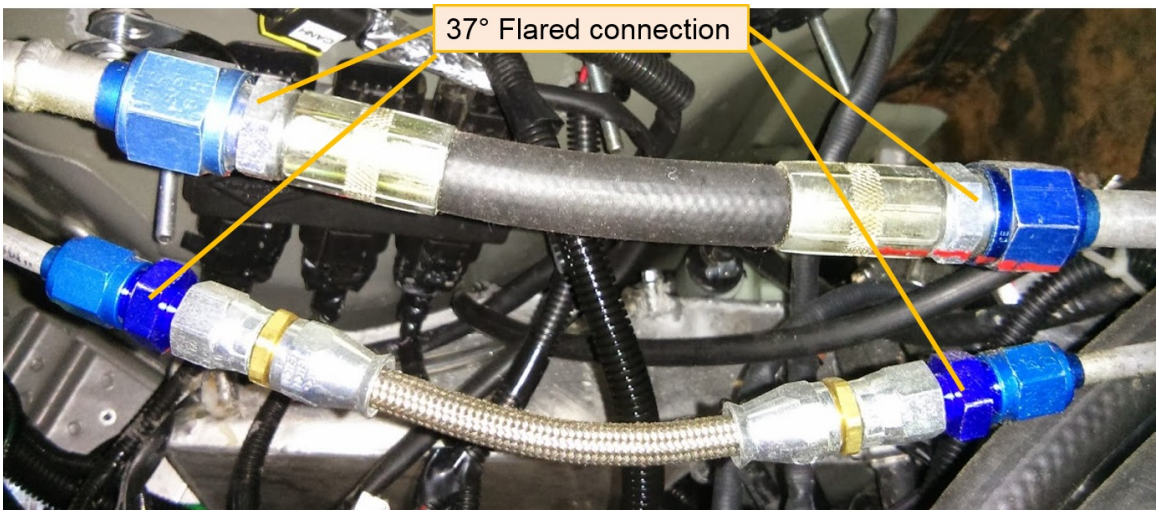

Figure 4.9. Example of a male JIC fitting.

By using these types of connections, the new AC harness consisted of rigid aluminum tubing as well as flexible, removable, hose. Thus, the aluminum sections were placed in less accessible places with their connections exposed in easy to reach areas. Therefore, the rigid tubing sections were packaged efficiently without causing maintenance issues if the hoses needed to be removed for any reason. Figure 4.10 shows a CAD image of the vehicle structure as well as the refrigerant lines used within the vehicle. Figure 4.11 shows a CAD image of the refrigerant lines, compressor and plate heat exhanger used. The lines indicated by red highlights are flexible hose while the lines indicated by black highlights are rigid tubing.

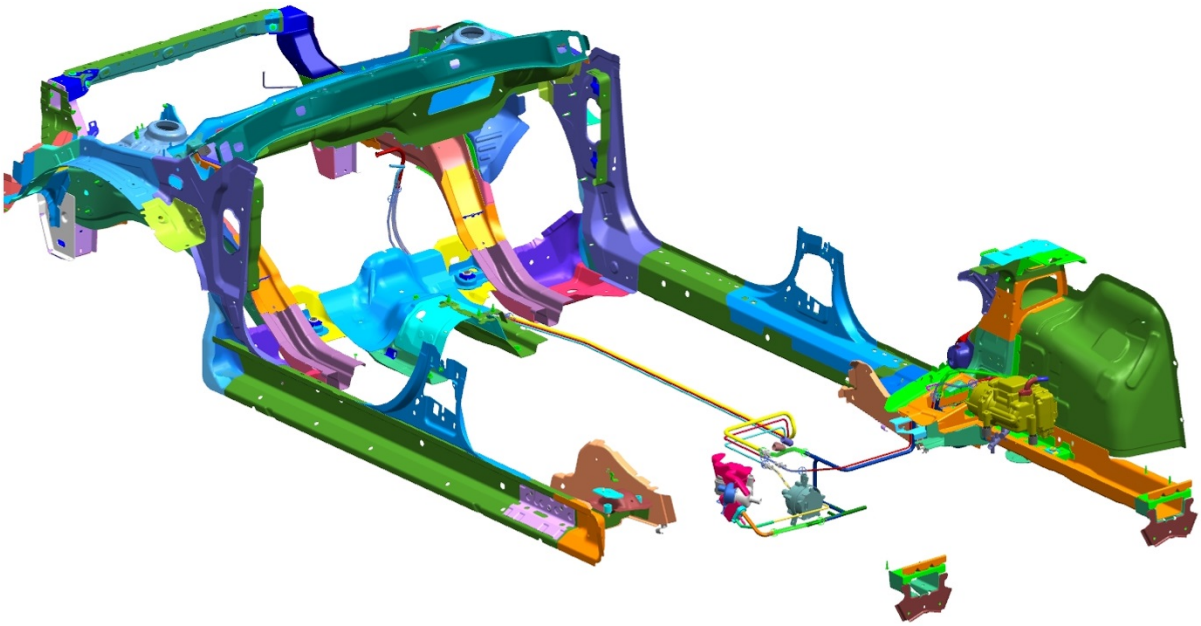

Figure 4.10. CAD assembly of vehicle body and AC harness.

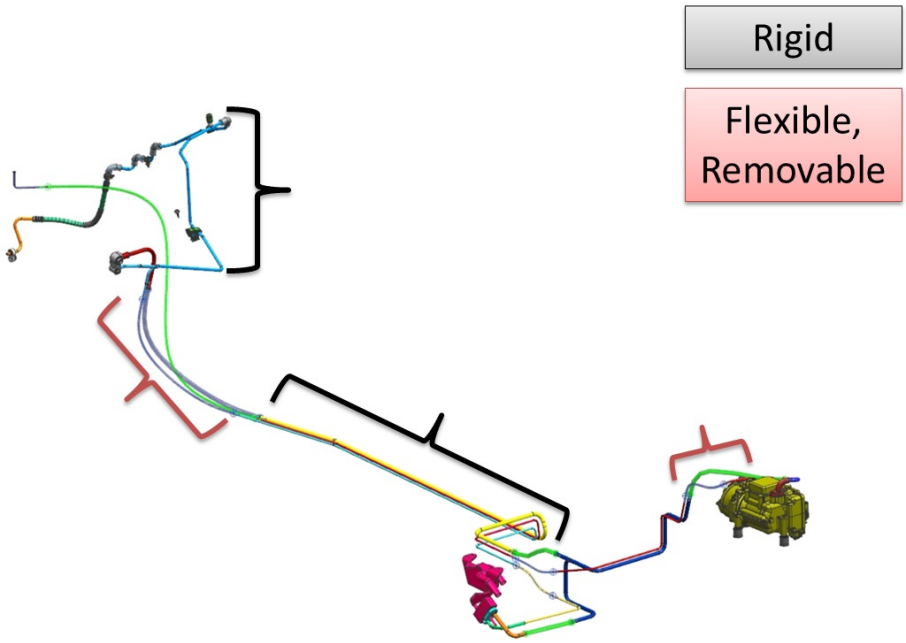

Figure 4.11. CAD assembly of AC harness.

The removability of the JIC connections was especially useful during the Year 3 competition when the Purdue team elected to remove the battery chilling unit. Since the AC harness was built in a removable, modular fashion, it was very easy to remove the necessary components, plug their respective connections, then operate using only the climate control loop as desired. If the Purdue team had used the AC harness built in year 2, this effort would have been impossible during the competition.

Mass Production Design

Since the EcoCar2 competition desired that teams create vehicles similar to those created via mass production, it was desired that the custom refrigerant circuit reflect one created via mass production. This initially seemed problematic since mass production AC harnesses are created using crimped connections. However, Figure 4.12 shows how the custom AC connections mimicked mass production connections. Since the only difference between the stock and custom AC harnesses were the connections between rubber and aluminum, the custom harness was very successful in replicating a mass production AC harness while still remaining accessible and serviceable.

Figure 4.13 shows how the Purdue team was able to use these plumbing techniques to successfully install the HVAC compressor. By having a combination of flexible hose and rigid tubing as sieen in Figure 4.13, it was possible to vibrationally isolate the compressor, a component that vibrates significantly during operation.

Once the team had a robust AC harness as well as components that were capable of controlling how the system operated, it was then necessary to determine what data was required of the AC circuit so that sensors could be placed in their necessary positions along the circuit. It is important to note that fewer sensors equated to greater weight saving of the vehicle. Therefore, only the most critical sensors were desired to be onboard the vehicle during operation.

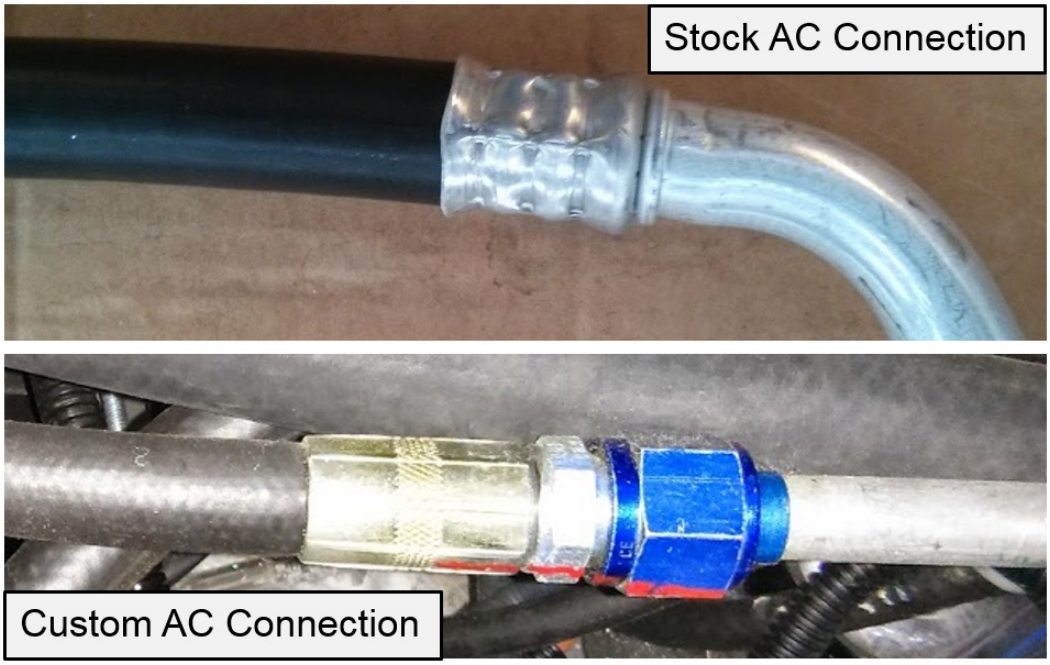

Figure 4.12. Comparison between stock and custom AC connection.

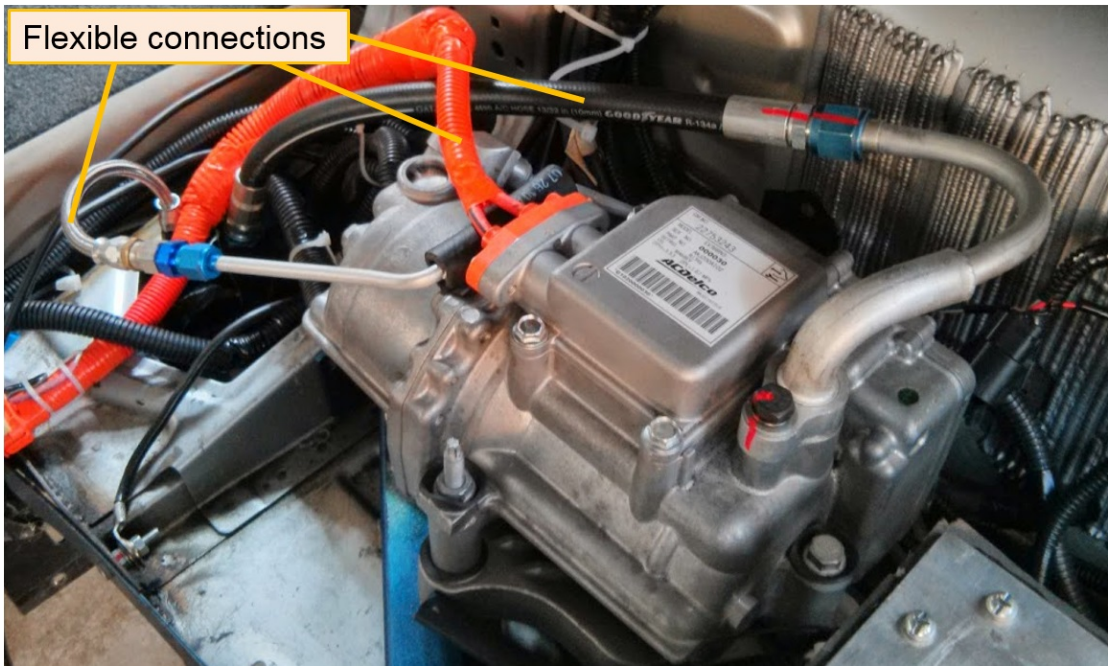

Figure 4.13. Image of HVAC compressor installed within Purdue vehicle.

4.1.6 Sensor Placement

Prior to any sensors being placed into the circuit by the Purdue team, there were already several values of data that were accessible. Specifically, the Battery Module temperatures, compressor work input, coolant pump work input and post-condenser pressure were available via the electrical network of the vehicle. The battery temperatures were measured within each module and recorded by the Battery Control Module. Since the compressor was driven via HV current, interpreting the amount of current sent to the compressor via HV junction box would yield an estimate for the amount of work input by the compressor. Concerning the coolant pump, it was more important to know the flow rate of the pump since the power draw of the pump was very low. Again, measuring the current sent to the pump would yield an estimate for both the flow rate and work input of the pump. Since the condenser used was the stock condenser of the 2013 Malibu's AC climate control system, a pressure sensor was built into the output of the condenser and was available for use. Shown in Figure 4.14 is a diagram of the thermal circuit with these signals included.

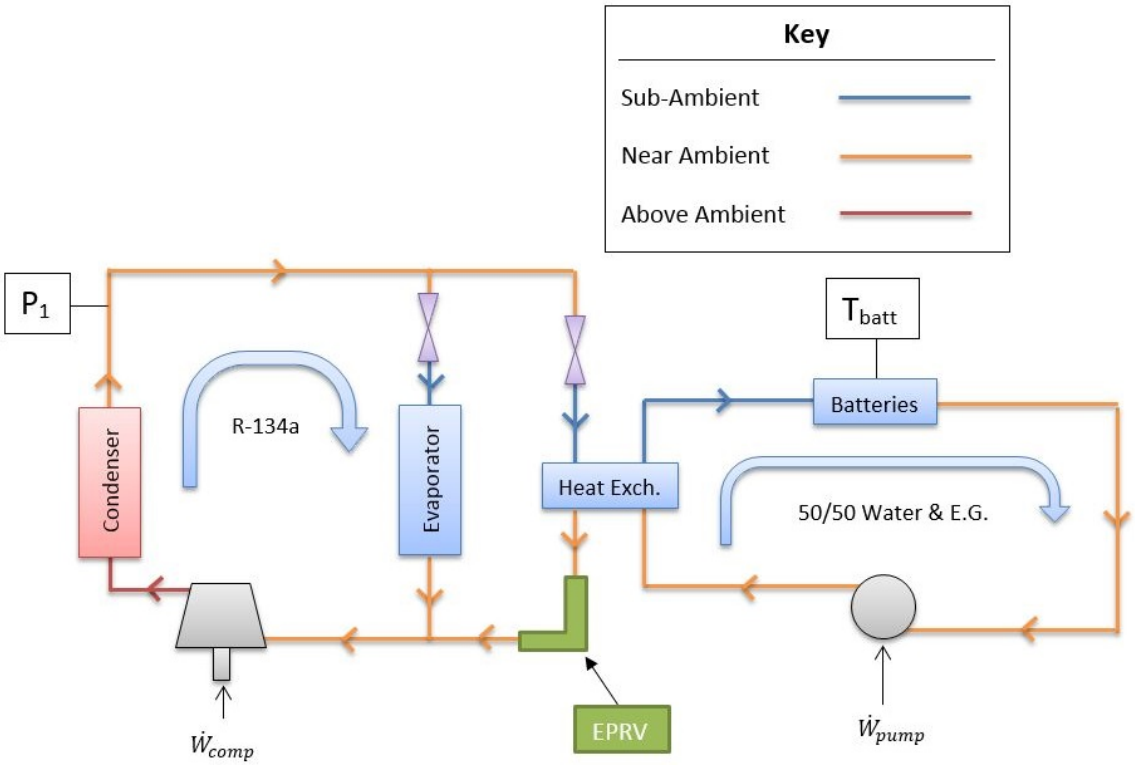

Figure 4.14. Diagram of AC routing system as packaged within the vehicle.

One critical signal that is not included in Figure 4.14 is the suction pressure of the compressor. The pressure difference between condenser output and compressor input would yield an estimate towards the total amount of thermal load provided by both the climate control system and the ESS. Therefore, adding a pressure sensor on the suction end of the compressor was desired, but not implemented on the Purdue vehicle due to time and resource restrictions.

4.1.7 Calibration

A direct way of measuring pressure losses within the system would be to include pressure sensors at the inlet and outlet of each major AC component. However, having these pressure sensors onboard the vehicle during operation was highly unlikely due

to the weight and cost of components. Due to the many reusable connections of the AC harness, it was possible to measure the pressure losses during operation of the AC system while the vehicle was immobile. Once known, many of these losses could have been accounted for within the algorithms used to control the AC components, thus allowing the AC circuit shown in Figure 4.15 to be constructed, which requires only two pressure sensors to be onboard the vehicle.

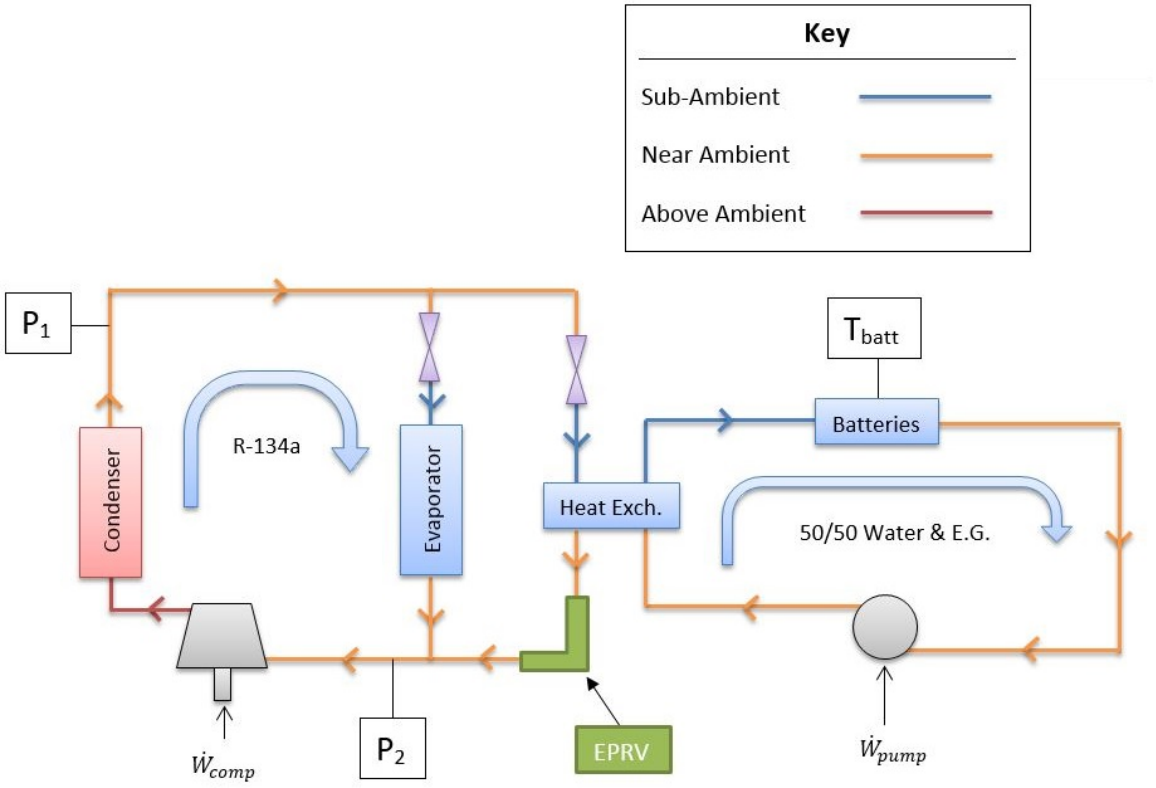

Figure 4.15. Diagram of AC routing system desired to be within the vehicle.

Additional calibrations to the AC system include adjustments to the EPRV spring rate as well as determinations of the heat exchange coefficients of both the ESS and the ESS Chiller. By adjusting the spring rate of the EPRV, the total amount of refrigerant flowing through the ESS chiller could have been minimized. By knowing the heat exchange coefficients, more accurate algorithms could be made to represent the system

within the vehicle's onboard controller. Both of the aforementioned calibrations would yield more efficient operation of the system.

Overall, a thermal circuit similar to the one shown in Figure 4.15, if constructed with the JIC fittings described previously, has the potential for being a robust, easily maintained AC circuit capable of all thermal goals desired by the vehicle with the addition of being ready for calibration and optimization through bench testing and control iteration.

5. SUMMARY

5.1 Conclusions

This work summarizes the procedures taken to design, analyze, fabricate, install and test a custom electric drivetrain for a Parallel-Through-the-Road Plug-in Hybrid Electric Vehicle (PTTR PHEV). By using CAD, logic and engineering analysis, the Purdue EcoCar2 team was successful in creating and operating the electric drivetrain of their vehicle for both the Year 2 and Year 3 compeitions of EcoCar2: Plugging Into the Future. Significant design challenges included the rear suspension cradle, Energy Storage System and High-Voltage AC circuit.

To summarize much of the modification work that was done to the base vehicle, Figure 5.1 indicates many umodified portions of the base vehicle, shown in gray. Figure 5.2 shows the same unmodified gray portions of the base vehicle. However, shown in color in Figure 5.2 are modified portions of the vehicle. Specifically, components shown in green are non-stock, purchased components which were custom-fitted into the base vehicle by the Purdue team such as the battery modules, diesel engine and suspension linkages. Shown in red are custom components which were designed, analyzed, fabricated and installed by the Purdue team such as the rear suspension cradle and the ESS structure.

Figure 5.3 shows the same assembly and color code as Figure 5.2, however the significant subsystems mentioned in this report are labeled.

The rear suspension cradle design utilized direct load paths as well as the rigid metal casing of the rear traction motor in order to exceed the safety and rigity of the stock cradle while still maintaining the correct mounting positions for the motor and suspension linkages. The cradle was designed and FEA analyzed using CAD software

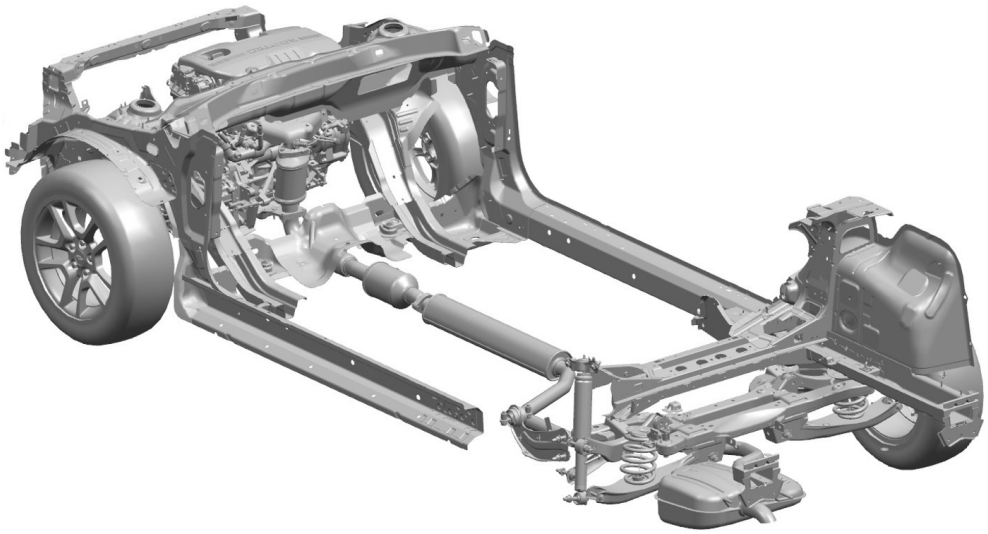

Figure 5.1. Unmodified portions of the base vehicle shown in gray.

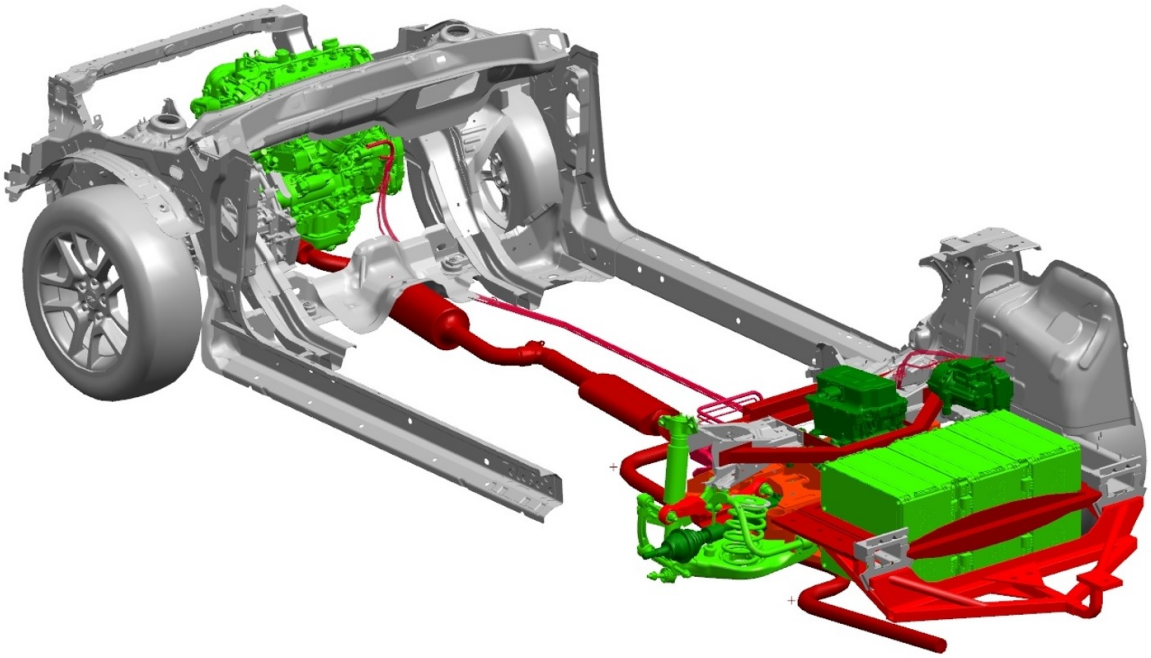

Figure 5.2. Unmodified portions of the base vehicle shown in gray, modified portions shown in color.

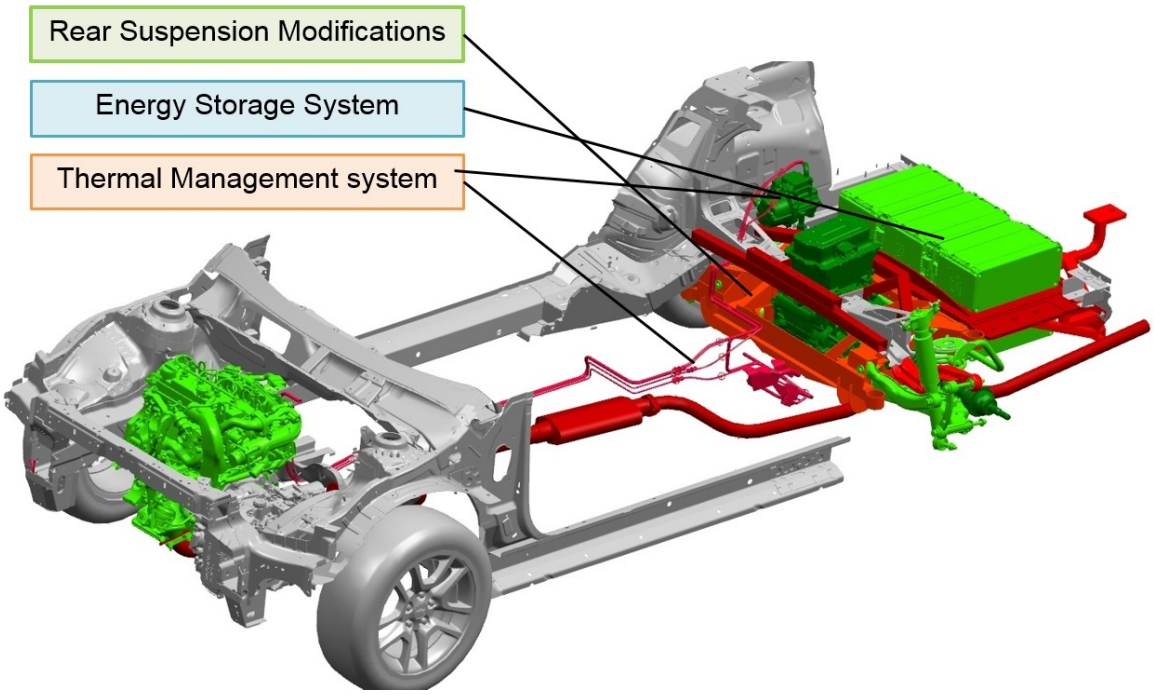

Figure 5.3. Unmodified portions of the base vehicle shown in gray, significant modified portions labeled and shown in color.

in order to confirm or deny any speculations made during the design process. After assurances in the design were made, the cradle was fabricated, installed and used.

The Energy Storage System design allowed the battery modules and respective power electronics to operate safely and robustly. The aluminum structure was both structurally sound as well as thermally conductive, allowing for a robust cooling system to be added in place. Similar to the suspension cradle, CAD and FEA analysis were used in order to ensure safe and robust operation of the ESS. Intergrity of the pack was ensured, fabrication was performed and the ESS operated as intended.

The High Voltage Thermal Management System of the vehicle utilized a design that accomplished a baseline goal set by the competition while still allowing room for easy maintenance and growth. The design utilized fittings and hardware that made the system robust enough to operate safely, included sufficient sensors and hardware

to accomplish all thermal goals set by the team yet avoided cumbersome results that would have made the vehicle too heavy to operate.

5.2 Competition Results

Of the 15 international Universities to compete in EcoCar2: Plugging into the Future, Purdue was one of 6 teams which were first time competitiors in the series of Advanced Vehicle Technology Competitions (AVTCs) managed by Argonne National Laboratory. At the year 3 competition in Milford, MI, the Purdue team placed 4th overall, 1st in braking distance and 2nd in Well-to-Wheel Greenhouse Gas Emissions. Additionally, the Purdue vehicle was able to surpass the base vehicle in both 0-60mph acceleration and 50-70mph acceleration, while still meeting the cargo and passenger capacity requirements set by the competition as seen in Figure 5.4.

	Production 2013 Malibu	Competition Requirement	Vehicle Technical Specifications (Y3 Final)	Y3 Competition Actual Results
Acceleration 0–60 mph	8.2 sec	11.5 sec	9 sec	7.7 sec
Acceleration 50–70 mph (Passing)	8.0 sec	10 sec	7 sec	3.9 sec
Braking 60–0 mph	143.4 ft (43.7 m)	180 ft (54.8 m)	171.5 ft (52.3 m)	128.7 ft
Highway Gradability @ 20 min	10+% @ 60 mph	3.5% @ 60 mph	11.76 % @ 60mph	Pass
Cargo Capacity	16.3 ft^3	7 ft^3	9 ft^3	7 ft^3
Passenger Capacity	5	2	5	5
Mass	1539 kg	<2250 kg	2200 kg	2077 kg

Figure 5.4. Year 3 competition final results.

5.3 Lessons Learned

Throughout the EcoCar2 competition, the Purdue team learned much of how a modern PHEV is created. Additionally, there were distinct differences between how a mass-production vehicle should be created versus a research-intended vehicle should be created. The Purdue team succeeded in creating a vehicle that was able to perform as a research-intended vehicle while still reflecting many design procedures used in creating mass-production vehicles.

The rear suspension cradle worked successfully, however it seemed to be over-engineered concerning stress factors of safety. Specifically, when calculating the factors of safety versus the material properties, the design saw FOS results between 1.9 and 4.5. However, when comparing FOS results to the stock design, the custom cradle FOS ratios relative to the stock FOS ratios ranged between 2.5 and 7. The large upper value of 7 (when compared to the stock design) indicates that the FEA analysis used may have been too conservative. This conservative approach was successful since the cradle maintained integrity while also preventing the vehicle from becoming overweight. However, it seems logical that there could have been significant reduction in material used while still performing safely and robustly.

Much like the rear suspension cradle, the aluminum structure of the ESS appeared to be over-engineered concerning both structural integrity as well as thermal performance. Specifically, if higher level fabrication techniques and knowledge of fasteners were known to the team during the design phase of the ESS, much less material could have been used to make the battery box. Also, it was advised that the team use three Lytron cold plates despite calcluation that suggested that one would be capable of the necessary power output, given that it transfers the energy successfully. Additionally, it was advised that the three plates would be needed in order to distribute the cold fluid more evenly across the aluminum structure. However, after observing the thermal loads of the battery modules, it seems logical that one cold plate could

have been used as long as it was press-fit into an aluminum structure similar to the method described in this paper.

When creating the Thermal Management System, it was highly beneficial to utilize design strategies that contained reusable fasteners. This was a great advantage within the competition environment and allowed the system to be flexible and robust. By using a modular approach to design, the team was able to accomplish increasingly difficult goals in a sequence, thus allowing the team to achieve baseline goals first, then stretch goals later on. Even if certain goals were not accomplished during the competition, the same design could be used for later projects that build upon the previous work.

5.4 Looking Forward

Future work will involve maintaining and refining the vehicle built during Eco-Car2. There was much intention to do control algorithm validation and subsystem optimization. However, there was very little time to perform these tasks since the vehicle was not fully operational until very late in the competition. Although the competition is now over, the vehicle still remains available at the Purdue facility for the very same control testing and optimization that was originally desired. However, if testing is desired to be performed, all subsystems must continue to be maintained in order to prevent failure of operation. If it is desired that the vehicle hardware be updated, there are several changes that would benefit operation of the vehicle.

Shown in Figure 5.5 is the stock rear suspension assembly with the suspension linkage geometry outlined. When the custom suspension cradle was created, it was assumed that the inboard pivot loactions were fixed. However, it would be a beneficial modification if the inboard bearing locations of the upper camber links were a slotted connection oriented laterally. Therefore, if the nominal ride hieght of the vehicle were to change, the inboard bearing locations would be capable of moving inboard

or outboard in order to correctly align the wheels such that rolling resistance of the tires can be minimized.

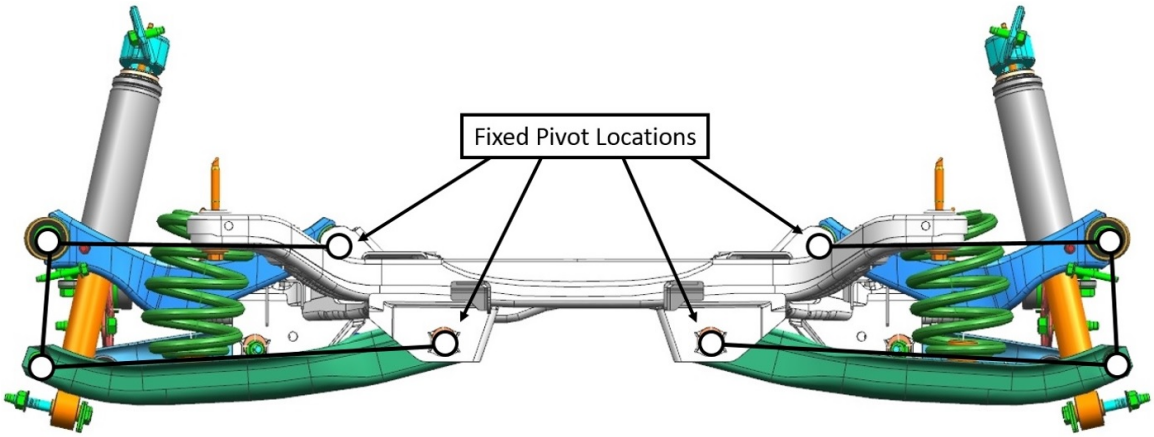

Figure 5.5. Stock rear suspension with linkage geometry highlighted.

Shown in Figure 5.6 is an image of the liquid cooling plates used in the ESS. As is indicated by the image, the height of each plate is approximately 0.375 inches. Since each plate was press-fit into the ESS main aluminum plate, the thickness of the main aluminum plate was required to be greater than or equal to the height of the liquid cooling plates. Therefore, if the ESS were remade, much material can be removed from the assembly if thinner liquid cooling plates are used.

Concerning the thermal management system, further calibration and bench testing can be performed to better understand the pressure losses across all refrigerant lines used. This data would allow more assumptions to be made in the control algortihms for the thermal loop, thus allowing highly sophisticated control without the need for abundant pressure sensors onboard the vehicle. Additionally, bench testing to determine the heat exchange coefficients of the ESS and heat exchanger would be highly beneficial for use within the control algorithms mentioned previously.

Although the vehicle performed well in the competition, there is still much research work that may be done using the same hardware and subsystems currently on the

Figure 5.6. Image of the liquid cooling plates used within the ESS.

vehicle. The vehicle performed successfully in dynamic operation, which gives great confidence that it can operate in stationary, dynamometer testing, which would still be capable of producing significant amounts of useful testing data. If it is desired to reconstruct some of the subsystems mentioned previously, dynamic operation would improve. However, it is imperative that more testing data be aquired as this is more critical to increasing the effectiveness of the vehicle. Therefore, the most effective use of the vehicle in the future would include bench testing and data aquisition so that the efficiency and power consumption of all systems be known.

LIST OF REFERENCES

LIST OF REFERENCES

[1] EcoCar2: Plugging into the future. *About EcoCAR 2*, 2014 (Last Modified November 21, 2014). `http://www.ecocar2.org/about-ecocar2`.

[2] Advanced Vehicle Technology Argonne National Laboratory. *Year One Event Rules*. Chicago Illinois, rev: h edition, 2012.

[3] Advanced Vehicle Technology Argonne National Laboratory. *Year Two Event Rules*. Chicago Illinois, rev: e edition, 2013.

[4] Advanced Vehicle Technology Argonne National Laboratory. *Year Three Event Rules*. Chicago Illinois, rev: g edition, 2014.

[5] Advanced Vehicle Technology Argonne National Laboratory. *Non-Year-Specific Rules*. Chicago Illinois, rev: n edition, 2014.

[6] E. Fallas, V. Freyermuth and A. Rousseau. Comparison of powertrain configuration for plug-in hevs from a fuel economy perspective. Technical report, SAE Technical Paper, 2008.

[7] P. Sharer, Y. Wu, M. Wang and A. Rousseau. Well-to-wheels results of energy use, greenhouse gas emissions, and criteria air pollutant emissions of selected vehicle/fuel systems. Technical report, SAE Technical Paper, 2006.

[8] Y. Qian, A. Vora. Purdue university ecocar2: Project initiation approval. Technical report, EcoCar2 Year 1 Competition, 2012.

[9] K. Oswald, A. Fogarty. Designing a rear suspension cradle for usage in a parallel-through-the-road plug-in hybrid electric vehicle. Technical report, SAE Technical Paper, 2014.